NACA RM E50J26

NACA

RESEARCH MEMORANDUM

FORCE AND PRESSURE CHARACTERISTICS FOR A SERIES OF NOSE INLETS AT MACH NUMBERS FROM 1.59 TO 1.99

I - CONICAL SPIKE ALL-EXTERNAL COMPRESSION INLET WITH SUBSONIC COWL LIP

By Fred T. Esenwein and Alfred S. Valerino

Lewis Flight Propulsion Laboratory
Cleveland, Ohio

NATIONAL ADVISORY COMMITTEE
FOR AERONAUTICS

WASHINGTON

January 19, 1951
Declassified July 17, 1958

2034

NATIONAL ADVISORY COMMITTEE FOR AERONAUTICS

RESEARCH MEMORANDUM

FORCE AND PRESSURE CHARACTERISTICS FOR A SERIES OF NOSE INLETS AT MACH NUMBERS FROM 1.59 TO 1.99

I - CONICAL SPIKE ALL-EXTERNAL COMPRESSION INLET WITH SUBSONIC COWL LIP

By Fred T. Esenwein and Alfred S. Valerino

SUMMARY

An experimental investigation to determine the force and pressure characteristics of a typical nose-inlet ram-jet configuration was conducted in the NACA Lewis 8- by 6-foot supersonic tunnel. The model consisted of a conical spike all-external compression inlet attached to an annular subsonic diffuser. Internal-and external-pressure distributions, pressure recovery, and lift, drag, and pitching moment were measured for a range of mass flows at angles of attack from 0° to 10° for free-stream Mach numbers of 1.59, 1.79, and 1.99. The investigation was conducted at a Reynolds number of approximately 2.13×10^{6} based on model inlet diameter.

Results of the investigation indicate that a rapid increase in total drag with decreasing mass flow was associated with the large increase in additive drag. The increment of external drag due to angle of attack was found to be essentially independent of mass flow and free-stream Mach number.

At critical mass flow, the external-lift-curve slope increased slightly with angle of attack and Mach number, whereas the pitching moment increased almost linearly with angle of attack and was independent of Mach number. At low angles of attack, the lift and pitching moment remained nearly independent of mass-flow spillage. At 10° angle of attack, however, the lift decreased with decreasing mass flow but the pitching moment remained nearly constant.

2034

In general, the decrease in pressure recovery with angles of attack up to 10° was of the order of 1 percent and no shock instability was noted except for very low mass flows at 6° and 10° angles of attack for Mach number 1.99.

Comparison of the experimental results with available theories revealed that the additive-drag and friction-drag coefficients were predicted satisfactorily at zero angle of attack for the range of mass flows and free-stream Mach numbers investigated. Prediction of the pressure drag, however, was limited to the condition of zero mass spillage.

INTRODUCTION

As part of a program to determine the aerodynamic characteristics of ram-jet engines, an investigation of four axially symmetric spike-type supersonic nose-inlets was conducted in the NACA Lewis 8- by 6-foot supersonic tunnel. In order to simulate a portion of a complete ram-jet engine, each inlet was attached to a fixed afterbody that formed the subsonic diffuser.

The purposes of this investigation were: (1) to obtain pressure, force, and moment data; and (2) to compare the experimental results with theory where possible.

Results obtained from the investigation of a conical-spike all-external compression inlet with a subsonic cowl lip are presented. The investigation was conducted through a range of mass flows and angles of attack from 0° to 10° at Mach numbers of 1.59, 1.79, and 1.99. The Reynolds number based on the inlet diameter varied from 2.11 to 2.15×10^6 for the range of the investigation.

SYMBOLS

The following symbols are used in this report:

C_D drag coefficient, D/q_0S_m

C_f friction-drag coefficient based on wetted area

C_L lift coefficient, L/q_0S_m

C_M pitching-moment coefficient about base of model, $G/q_0S_m l$

C_p pressure coefficient, $p-p_0/q_0$

2034

D	drag
d	diameter at area of maximum cross section, 8.125 inches
G	pitching moment about base of model
L	lift
l	length of model, 58.76 inches
M	Mach number
m	mass flow
P	total pressure
p	static pressure
q	dynamic pressure, $\gamma pM^2/2$
Re	Reynolds number
S	area
S_c	inlet capture area defined by cowl lip, 0.1750 square foot
S_m	maximum cross-sectional area, 0.3601 square foot
U	velocity
u	velocity in boundary layer
v_x	axial perturbation velocity
x,r,θ	cylindrical coordinates
y	distance from model surface
α	angle of attack
γ	ratio of specific heats, 1.40
δ	boundary-layer thickness

2034

Subscripts:

a	additive drag
f	friction
l	local condition in boundary layer
p	pressure
δ	conditions at outer edge of boundary layer
0	free stream
1	cowl lip
2	station at x = 7.558 inches
3	entrance to combustion chamber
5	minimum area at plug

APPARATUS AND PROCEDURE

Two identical models of the ram-jet configuration were investigated; one was used for force measurements, the other was used to obtain pressure data. The instrumentation conduits and the boundary-layer rake shown in figure 1 were not present on the force model.

The main components of the ram-jet configuration shown in figure 2(a) consisted of a conical-spike all-external compression inlet (fig. 2(b)) followed by an annular subsonic diffuser formed by the outer shell and the central inner body. Four support struts located 45° from the vertical center line were used to attach the outer shell to the center body. The over-all length of the model was 58.76 inches and the maximum body diameter was 8.125 inches.

The inlet was so designed that the angle formed between the center line of the model and a line joining the tip of the spike and the cowl lip was equal to the angle of the oblique shock generated by the 50° cone at a Mach number of 1.79. The cowl, which was designed for operation with the normal shock located slightly ahead of the cowl lip, had a rounded subsonic leading edge (fig. 2(b)). Coordinates for the center body and outer shell are presented in table I.

2034

The mean geometric flow-area ratio (fig. 3) represents the ratio of the area based on the average normal to the surfaces of the annulus to the maximum cross-sectional area in the combustion chamber. The region of nearly constant area at the inlet was provided to permit stabilization of the boundary layer behind the normal shock prior to deceleration of the flow in the subsonic diffuser. The small decrease in flow area from $x/d = 0$ to 0.25 resulted from the design of the subsonic cowl lip.

The force model was rigidly connected to a three-component strain-gage balance located inside the center body and the balance was attached to the tunnel sting-strut combination.

Instrumentation of the pressure model included static orifices as indicated in table II and a $1\frac{1}{2}$-inch boundary-layer rake located on the outer surface of the model ($\theta = 0^\circ$) at station 51 (fig. 2(a)). For one of the runs at a Mach number of 1.79, two total-head rakes were located inside the model immediately in front of the support struts at $\theta = 135^\circ$ and 315°.

Six similar radial static and total-pressure rakes, equally spaced with respect to the vertical center line, were attached to the sting at the entrance of the combustion chamber for both the force and pressure models. A sting-mounted, hydraulically actuated plug was provided at the exit of the model to vary the flow conditions through the engine and a pendulum-type angle-of-attitude indicator with an accuracy of 0.1° was located inside the center body to measure the angle of attack.

All pressures were measured on multiple-tube manometer boards and were photographically recorded. The total pressures in the boundary layer were measured using mercury as the working fluid; all other pressures were measured using tetrabromoethylene.

Both models were investigated through a range of mass flows at angles of attack from 0° to 10° for the free-stream Mach numbers of 1.59, 1.79, and 1.99. An additional run was made with the pressure model rotated 180° to obtain a more complete survey of the pressure distributions at Mach number 1.79.

For presentation of the data herein, the mass flow is expressed in terms of m_3/m_0, defined as the ratio of the flow passing through the engine to the flow in a free-stream tube of cross-sectional area S_c (fig. 4). The mass flow passing through the engine was computed for choking at the minimum geometric area of the plug using the measured total pressure at the combustion-chamber inlet and was corrected by the factor 0.97, which was determined for the shock-swallowed condition.

2034

RESULTS AND DISCUSSION

The presentation and the discussion of results are divided into two major sections covering the external and internal-flow characteristics. Evaluation of the effects produced by variations in mass flow, angle of attack, and free-stream Mach number are made in terms of the flow characteristics of the model.

External-Flow Characteristics

Zero angle of attack. - The total drag, which includes the pressure and the friction drag over the outer shell and the additive drag along the entering streamline, is presented in coefficient form in figure 5. At a constant mass-flow ratio, the mass-flow spillage had an increasingly adverse effect on the total drag as the free-stream Mach number varied from 1.59 to 1.99. At critical mass flow, the increase in drag with decreasing free-stream Mach number, as shown in figure 6, resulted from the increase in mass-flow spillage due to choking internally near the leading edge of the support struts.

Representative pressure distributions over the external surface of the model at zero angle of attack are shown in figure 7 for the three Mach numbers. These data indicate that the external static pressure over the cowl decreased with increasing mass spillage due to the rapid expansion produced by the increased curvature of the entering streamline. Additional pressure data are tabulated in table III.

The large variations in the external pressures over the cowl did not extend to more than approximately 1 diameter downstream of the cowl lip. For maximum mass flow at each free-stream Mach number, external pressures equal to or less than the stream static pressure were approached at approximately $x/d = 0.5$. Consequently, a greater part of the surface pressure drag occurred over the forward portion of the cowl.

The decrease in the external-pressure coefficient at $x/d = 4.31$ resulted from expansion of the flow produced by the change in contour of the outer shell. Variations in the pressure distributions at $x/d = 1.5$ at Mach number 1.79 and $x/d = 3.25$ at Mach number 1.99 have been determined to result from weak tunnel disturbances.

Comparison of the experimental pressure distributions at Mach number 1.99 with linearized potential theory ($C_p = -2\ v_x/U_0$) shows excellent agreement at a mass-flow ratio of 1.00 (fig. 7(c)). Although

2034

no valid comparison can be made at Mach numbers 1.59 and 1.79, the theoretical pressure distributions are included on figures 7(a) and 7(b) to represent the limiting pressures that would be attained at a mass-flow ratio of 1.00.

Typical schlieren photographs of the shock configuration at the inlet are presented in figure 8 for zero angle of attack. Enlargements of these photographs showed a small region of separated flow at the cowl lip with large mass spillage. Although the flow separation is not apparent in figure 8, the region of expansion and the compression shock subsequent to the separation of the flow can be readily identified.

The pressure-drag coefficient $C_{D,p}$ evaluated from a graphical integration of the pressures measured over the external surface of the model, decreased linearly with decreasing mass-flow ratio, as shown in figure 9. At mass-flow ratios below approximately 0.7, the pressure drag became negative due to the negative pressures over the cowl.

Reasonably good agreement is obtained between the theoretical pressure-drag coefficient and the experimental results for the shock-swallowed condition at Mach number 1.99. Extrapolation of the data for Mach numbers 1.59 and 1.79 to a mass-flow ratio of 1.00 would indicate that good agreement with theory could be expected at these conditions.

Typical boundary-layer profiles measured adjacent to the surface of the model at station 51 are presented in figure 10 in terms of the local Mach number. The Rayleigh equation was used to evaluate the boundary-layer data at zero angle of attack by assuming that the static pressure in the flow field was equal to the value measured at the model surface and that the total temperature was constant throughout the flow field.

The variations in the profiles with mass-flow spillage and free-stream Mach number were found to be associated with the detached bow wave ahead of the cowl lip and the data were analyzed using the method presented in reference 1. As a result of this analysis, the boundary-layer thickness δ was determined to extend to the point at which the slope of the profile rapidly increased, as indicated in figure 10.

The nondimensional-velocity profiles were calculated using the boundary-layer thickness δ, which was determined by the method in reference 1, and are presented in figure 11. For the range of mass flows and free-stream Mach numbers of this investigation, the velocity profiles are in agreement with the 1/7 power law, which is usually applied to flat-plate data without pressure gradients. Calculations of the effect of the pressure gradient on the boundary layer indicated that

2034

inasmuch as the gradient occurred only over the cowl in the region of thin boundary layer the effect would be of the order of 1.5 percent of the experimental friction-drag coefficient.

The experimental values of friction-drag coefficients, evaluated from a graphical integration of the decrement of momentum in the boundary layer, are presented in figure 12. Examination of the schlieren photographs indicated that the transition point in the boundary layer occurred at approximately $x/d = 0.6$ and that small variations in the friction-drag coefficient probably resulted from the movement of the transition point along the model.

A comparison of the average values of the experimental friction-drag coefficients with the theoretical values, obtained from the equations given by von Kármán (reference 2) for turbulent compressible flow over a smooth flat plate, is presented in figure 13. Although the small region of laminar boundary layer over the cowl and possible three-dimensional effects have been neglected in this comparison, good agreement is obtained.

The experimental additive-drag coefficients were evaluated at zero angle of attack from a momentum balance between the free-stream flow station 0 and flow station 2. The results presented in figure 14 indicate a very rapid increase in additive drag with decreasing mass flow with the rate of change being essentially independent of free-stream Mach number.

Good agreement is obtained between the theory based on one-dimensional flow considerations as presented in reference 3 and the experimental results for the three free-stream Mach numbers. Inasmuch as the oblique shock fell slightly ahead of the cowl lip at Mach number 1.59, the ordinate of the theoretical curve at a mass-flow ratio of 0.93 represents the supersonic additive drag at the maximum mass flow as determined from conical-flow theory for the shock-swallowed condition.

The drag components are summarized and compared with the total drag measured with the force model in figure 15. For this comparison, the friction drag was modified to include the increment of drag due to friction over the surface of the model from station 51 to 56 using the average friction coefficient obtained from the boundary-layer measurements. Good agreement was obtained at Mach numbers 1.79 and 1.99. At Mach number 1.59, however, the force-model drag was approximately 15 percent higher at critical mass flow than that obtained from the pressure model.

For critical mass flow, the additive drag at Mach number 1.59 was greater than the sum of the pressure and friction drags, whereas at Mach numbers 1.79 and 1.99 the friction drag was the largest component.

2034

The decrease in pressure drag with decreasing mass flow was relatively unimportant because the increase in additive drag was much greater and the net effect was a rapid increase in total drag. For a mass-flow ratio of 1.0 at a Mach number of 1.99, the additive drag was zero and the pressure drag became a significant part of the total drag.

Angle of attack. - The effect of angle of attack on the total-drag coefficient is presented in figure 16. For a constant mass flow, the axial force due to the external flow was found to be nearly independent of angle of attack; the increase in drag with angle of attack therefore resulted from the component of the normal force. All increments of drag were essentially independent of mass flow except at 10° angle of attack for Mach number 1.99 where slight shock instability occurred.

Included in the external lift presented in figure 17 is the component of the force along the entering stream tube, which is inherent in the definition of the external forces. At low angles of attack for the three Mach numbers, the lift did not vary greatly with mass-flow spillage. At 10° angle of attack, however, the lift decreased with decreasing mass flow. The external pitching moment, evaluated by assuming that the turning of the flow occurred at the cowl lip, was almost independent of mass-flow spillage at all angles of attack, as shown in figure 18. For the complete range of the investigation, the center of pressure location presented in figure 19 varied from 5.4 to 4.4 diameters ahead of the base.

The variation of the drag increment, the lift, and the pitching moment with angle of attack for critical mass flow is presented in figure 20. The increase in drag increment was essentially independent of free-stream Mach number. The lift-curve slope increased slightly with angle of attack and Mach number whereas the pitching moment increased almost linearly with angle of attack and was independent of Mach number.

In order to provide a simple comparison, theoretical curves were calculated by the semiempirical method of reference 4, modified to apply to an open-nosed body, and are included in figure 20. End effects were neglected for the calculations. Comparison of the experimental results with the modified semiempirical method indicates that the increment of drag and the external lift are underestimated but that the pitching moment is in agreement with experimental values for low angles of attack. Inasmuch as the decrease in critical mass flow at 10° angle of attack resulted in an increase in drag, the discrepancy between the experimental increment of drag and the theoretical value at this condition is somewhat exaggerated.

2034

Variation of the external-pressure distribution with angle of attack for a constant mass-flow ratio at Mach number 1.79 is shown in figure 21. As the angle of attack increased, the loading increased in the region of the cowl. It is of interest to note that the major contribution to the lift resulted from the increase in static pressure over the lower surface of the model ($\theta = 0^\circ$). Beyond 2 diameters downstream of the cowl lip, the external pressures over the upper surface ($\theta = 180^\circ$), which were practically unaffected by increasing angles of attack up to 10°, may indicate separation of the cross flow (reference 5).

Comparison of the angle-of-attack contribution to the circumferential pressure distribution with three-dimensional linearized potential theory at Mach number 1.79 indicated progressively better agreement as the distance downstream of the cowl lip was increased. For zero mass spillage at Mach number 1.99, better agreement was obtained between the experimental results obtained near the cowl lip and two-dimensional theory.

Variations of the total pressure in the boundary layer over the bottom ($\theta = 0^\circ$) and the top ($\theta = 180^\circ$) surfaces of the model at station 51 are presented in figure 22 for Mach number 1.79 in terms of the ratio of the local measured total pressure to the free-stream total pressure. With increasing angle of attack, a thinning of the boundary layer occurred over the bottom surface of the model. Over the top surface, however, a slight increase in boundary-layer thickness was noted for small angles of attack. At higher angles of attack, the boundary-layer thickness decreased appreciably and it is presumed that the boundary-layer air shifted to form a pair of lobes along the sides of the model similar to the boundary-layer shift reported for the RM-10 model in reference 5.

Internal-Flow Characteristics

Zero angle of attack. - The variation of total-pressure recovery and combustion-chamber Mach number with mass-flow ratio is presented in figure 23. The total pressure P_3 was determined from the corrected mass flow and the measured static pressure in the combustion chamber. The combustion-chamber Mach number was calculated based on isentropic expansion of the flow from the annular area at the rake to the cross-sectional area of the combustion chamber with the sting removed.

At Mach number 1.59, the total-pressure recovery remained nearly independent of mass flow in the subcritical region and the shock configuration was stable throughout the range of mass flow. Although the total-pressure recovery decreased with decreasing mass flow at Mach numbers 1.79 and 1.99, no shock instability occurred at zero angle of attack.

2034

A breakdown of total-pressure losses into inlet and subsonic diffuser losses, as shown in figure 24, indicates a decrease in subsonic diffuser losses and an increase in inlet losses for decreasing mass flow. The decrease in total-pressure recovery with decreasing mass flow for Mach numbers 1.79 and 1.99 resulted from a more rapid increase in inlet losses than the corresponding decrease in subsonic diffuser losses. At maximum pressure recovery near the critical mass flow for the three free-stream Mach numbers, the subsonic diffuser losses were approximately equal to the inlet losses.

Comparison of the experimental inlet recovery with a calculated shock recovery is presented in figure 25. In order to provide an independent method of estimating the shock recovery, the location of the normal shock ahead of the cowl lip for mass-flow ratios less than 1 was predicted by the method presented in reference 6. An over-all total-pressure recovery was then computed by weighing the separate recoveries of the flow passing through both the oblique and normal shocks and the flow passing through only the normal shock. Inasmuch as the friction effects over the internal surfaces were neglected, the agreement between the calculated values and the experimental results is fair and within the accuracy of the computations.

The subsonic diffuser characteristics shown in figure 26 indicate that the increase in total-pressure recovery P_3/P_2 with decreasing mass flow was independent of Mach number except in the region of critical mass flow. At maximum total-pressure recovery for Mach number 1.79, subsequent investigation revealed that approximately 4 percent of the loss in total pressure in the subsonic diffuser resulted from wake effects produced by the support struts.

The diffuser performance has also been expressed in terms of a loss coefficient $\Delta P/q_2$ and an effectiveness parameter $(\Delta p/\Delta p_{ideal})$. Although no Mach number effect was indicated in terms of the pressure recovery, the total-pressure loss expressed in terms of the available dynamic pressure showed an increase with Mach number as well as with mass flow. Attempts to correlate these data as a function of either Reynolds number or Mach number at the entrance to the subsonic diffuser were unsuccessful, and it is believed that the variation with Mach number may result from differences in the initial boundary layer (reference 7).

Typical Mach number profiles at the entrance to the combustion chamber for several mass flows at Mach number 1.79 are presented in figure 27. The largest variations in Mach number across the annular passage occurred at mass flows near maximum pressure recovery. The variations in the profiles measured by the various rakes were found to result from the wake effects produced by the support struts.

2034

Angle of attack. - The effect of angle of attack on the total-pressure recovery is shown in figure 28. A decrease of approximately 1 percent in total-pressure recovery was measured as the angle of attack was increased to 10°. These results indicate a somewhat smaller decrement in pressure recovery with angle of attack than reported in reference 8.

The critical mass flow was essentially unaffected by changes in angle of attack up to and including 6°. At 10° angle of attack, however, a decrease in the critical mass-flow ratio from 0.915 at zero angle of attack to 0.865 was measured for Mach number 1.79. A similar decrease occurred at Mach numbers 1.59 and 1.99.

The abrupt decrease in pressure recovery for low mass flows ($m_3/m_0 \approx 0.46$) at Mach number 1.99 for 6° and 10° angles of attack resulted from boundary-layer separation over the upper surface of the spike and slight instability of the shock configuration. No appreciable decrease in pressure recovery resulted from the separation at high angles of attack for Mach numbers 1.79 and 1.99 when no instability occurred in the shock configuration (fig. 29).

The effect of angle of attack on the inlet and subsonic diffuser losses is presented for Mach number 1.79 in figure 30. These data indicate that the components of the total-pressure loss are essentially independent of angle of attack.

The basic cause of the reduction in critical mass flow at 10° angle of attack can be found from a study of the variation in internal pressure distribution with angle of attack at Mach number 1.79 presented in figure 31. For a constant mass flow, a slight decrease in pressure occurs over the bottom surface of the spike ($\theta = 0°$) near the cowl lip at 10° angle of attack but the remainder of the static pressures show no significant trend. Over the top surface ($\theta = 180°$), however, the decrease in static pressure in the region of $x/d = 1.0$ at 10° angle of attack indicates that the flow tends to choke between the upper support struts. It is believed that the cross-flow effects over the spike may result in increased mass flow in the upper portion of the annulus and consequently produces premature choking between the struts. Additional internal pressure data are tabulated in table III.

The variation of total-pressure distributions at the entrance to the combustion chamber was very pronounced with angle of attack (fig. 32). As the angle of attack was varied from 0° to 10°, the peak of the profile shifted toward the upper surface of the annulus, indicating an increase in mass flow in this region. In the lower portion of the combustion chamber, the profile tended to become flat with a reversal in curvature

near the wall. Comparison of the total-pressure ratio in this region with the pressure ratio at the wall indicates separation of the flow along this surface of the combustion chamber.

SUMMARY OF RESULTS

The force and pressure characteristics of a typical ram-jet configuration utilizing a conical spike all-external compression inlet were investigated in the NACA Lewis 8-by 6-foot supersonic tunnel at a Reynolds number of approximately 2.13×10^6 based on the inlet diameter. For the range of mass flows and angles of attack investigated at Mach numbers 1.59, 1.79, and 1.99, the following results were obtained:

1. At zero angle of attack, the external-pressure distribution for zero mass spillage was adequately predicted by linearized potential theory.

2. The boundary-layer velocity profiles measured over the external surface at the rear of the model were in good agreement with the 1/7 power law. The skin-friction coefficients were essentially independent of mass flow and were predicted by two-dimensional compressible turbulent-flow theory.

3. The rapid increase in total drag with decreasing mass flow resulted from the large increase in additive drag. The variation of additive drag with mass flow was predicted at zero angle of attack from one-dimensional-flow considerations.

4. For a constant mass flow, the axial force due to the external flow was nearly independent of angle of attack indicating that the increase in drag with angle of attack resulted from the component of the normal force.

5. The external lift was essentially independent of mass flow at low angles of attack. At critical mass flow, the lift-curve slope increased with Mach number and was linear at angles of attack below 6°. The pitching moment was independent of mass flow and Mach number and increased almost linearly with angle of attack. The resulting center of pressure, which was located approximately 2 diameters downstream of the cowl lip, moved slightly rearward with angle of attack and Mach number.

6. At critical mass flow, the increment of drag and the lift were underestimated but the pitching moment was predicted with reasonable accuracy by a semiempirical method, which was modified to apply to an open-nosed body.

2034

Lewis Flight Propulsion Laboratory,
National Advisory Committee for Aeronautics,
Cleveland, Ohio.

REFERENCES

1. Luidens, Roger W., and Madden, Robert T.: Interpretation of Boundary-Layer Pressure-Rake Data in Flow with a Detached Shock. NACA RM E50I29a, 1950.

2. de Kármán, Th.: The Problem of Resistance in Compressible Fluids. Quinto Convegno "Volta", Reale Accademia d'Italia (Roma), Sett. 30-Ott. 6, 1935, pp. 3-57.

3. Dailey, C. L., and McFarland, H. W.: Development of Ramjet Components. Prog. Rep. 9961-8, Univ. Southern Calif. Aero. Lab., USC, Feb. 7, 1950. (Bi-Monthly Prog. Rep. Dec. 1949 - Jan. 1950 under Navy Contract NOa(s) 9961.)

4. Allen, H. Julian: Estimation of the Forces and Moments Acting on Inclined Bodies of Revolution of High Fineness Ratio. NACA RM A9I26, 1949.

5. Luidens, Roger W., and Simon, Paul C.: Aerodynamic Characteristics of NACA RM-10 Missile in 8- by 6-Foot Supersonic Wind Tunnel at Mach Numbers from 1.49 to 1.98. I - Presentation and Analysis of Pressure Measurements (Stabilizing Fins Removed). NACA RM E50D10, 1950.

6. Moeckel, W. E.: Approximate Method for Predicting Form and Location of Detached Shock Waves Ahead of Plane or Axially Symmetric Bodies. NACA TN 1921, 1949.

7. Copp, Martin R., and Klevatt, Paul L.: Investigation of High-Subsonic Performance Characteristics of a 12° 21-Inch Conical Diffuser, Including the Effects of Change in Inlet-Boundary-Layer Thickness. NACA RM L9H10, 1950.

8. Moeckel, W. E., Connors, J. F., and Schroeder, A. H.: Investigation of Shock Diffusers at Mach Number 1.85. I - Projecting Single-Shock Cones. NACA RM E6K27, 1947.

2034

TABLE I - TABLE OF COORDINATES FOR NACA 8-INCH RAM-JET CONFIGURATION

(a) Center-body coordinates.

Station	Diameter (in.)
0.500	3.000
1.000	3.330
1.500	3.600
2.000	3.820
2.500	3.983
3.000	4.1125
3.500	4.220
4.000	4.303
4.500	4.371
5.000	4.430
6.000	4.524
7.000	4.580
7.750	4.600
7.875	4.600
10.000	4.585
12.000	4.545
14.000	4.486
16.000	4.415
18.000	4.327
20.000	4.220
22.000	4.084
24.000	3.922
26.000	3.715
30.031	3.343

(b) Outer-shell coordinates.

Station	Diameter (in.)	
	External	Internal
0.100	5.730	5.598
.200	5.791	5.604
.300	5.844	5.622
.400	5.887	5.648
.500	5.927	5.678
1.000	6.100	5.845
2.000	6.360	6.110
3.000	6.550	6.300
4.000	6.666	6.416
5.000	6.750	6.500
9.875	6.998	6.748
22.000	7.616	7.366
30.000	8.024	7.774
32.000	8.125	7.875
56.000	8.125	7.875



TABLE II - LOCATION OF STATIC-PRESSURE ORIFICES FOR PRESSURE MODEL

(a) Location of static tubes along shell contour.

Station		
External[a]		Internal[b]
0.50	11.00	0.50
1.00	12.00	1.00
1.50	14.00	1.50
2.00	16.00	2.00
2.50	18.00	2.50
3.00	21.00	3.00
4.00	24.00	4.00
5.00	27.00	5.00
6.00	31.00	6.00
7.00	35.00	7.00
8.00	40.00	8.00
9.00	45.00	9.00
10.00		

[a]Two rows of orifices, one at $\theta = 180^{\circ}$ and one at $\theta = 270^{\circ}$

[b]$\theta = 0^{\circ}$

(b) Location of static tubes ($\theta = 0^{\circ}$).

Station	
Spike	Island
-1.50	8.00
-1.00	9.00
-0.50	10.00
0	11.00
0.50	12.00
1.00	14.00
1.50	16.00
2.00	18.00
2.50	21.00
3.00	24.00
4.00	27.00
5.00	31.00
6.00	37.00
7.00	



2034

TABLE III - EXTERNAL AND INTERNAL PRESSURE COEFFICIENTS OF NACA 8-INCH RAM-JET CONFIGURATION FOR FOUR ANGLES OF ATTACK

(a) Free-stream Mach number of 1.59.

NACA

Station	$\alpha = 0°$; $m_3/m_0 = 0.805$				$\alpha = 0°$; $m_3/m_0 = 0.735$				$\alpha = 0°$; $m_3/m_0 = 0.663$				$\alpha = 0°$; $m_3/m_0 = 0.601$				$\alpha = 0°$; $m_3/m_0 = 0.484$			
	Longitudinal distribution of C_p																			
	Outer shell			Center body	Outer shell			Center body	Outer shell			Center body	Outer shell			Center body	Outer shell			Center body
	External		Internal		External		Internal		External		Internal		External		Internal		External		Internal	
θ→	180°	270°	0°	0°	180°	270°	0°	0°	180°	270°	0°	0°	180°	270°	0°	0°	180°	270°	0°	0°
-1.5				0.515				0.514				0.635				0.987				1.091
-1.0				.582				.901				1.013				1.075				1.151
-.5				.890				.989				1.071				1.127				1.206
0				.932				1.021				1.105				1.166				1.261
.5	0.164	0.155	0.882	.890	0.092	0.079	1.058	1.012	0.014	-0.005	1.190	1.118	-0.047	-0.079	1.277	1.196	-0.156	-0.207	1.398	1.308
1.0	.122	.121	.865	.818	.074	.071	1.053	.996	.021	.018	1.183	1.127	-.028	-.025	1.268	1.215	-.104	-.112	1.381	1.338
1.5	.076	.078	.855	.788	.044	.054	1.053	.994	.006	.015	1.183	1.133	-.028	-.022	1.268	1.225	-.084	-.084	1.380	1.351
2.0	.043	.052	.858	.753	.020	.033	1.056	.977	-.006	.003	1.187	1.124	-.028	-.025	1.269	1.220	-.071	-.074	1.381	1.349
2.5	.025	.027	.878	.795	.009	.014	1.066	1.003	-.012	-.010	1.194	1.142	-.029	-.031	1.275	1.235	-.066	-.069	1.383	1.359
3.0	.021	.013	.854	.806	.007	.004	1.049	1.013	-.008	-.015	1.182	1.150	-.018	-.032	1.266	1.241	-.052	-.063	1.377	1.363
4.0	-.015	-.027	.834	.803	-.027	-.034	1.043	1.018	-.039	-.047	1.176	1.159	-.051	-.060	1.263	1.248	-.074	-.084	1.375	1.365
5.0	-.030	-.036	.767	.760	-.039	-.044	1.017	1.012	-.048	-.054	1.161	1.159	-.058	-.064	1.250	1.248	-.076	-.079	1.367	1.365
6.0	-.032	-.038	.623	.626	-.039	-.046	.995	.991	-.046	-.052	1.148	1.143	-.054	-.061	1.242	1.240	-.068	-.072	1.362	1.360
7.0	-.022	-.030	.510	.506	-.029	-.038	1.002	1.003	-.035	-.044	1.151	1.151	-.042	-.050	1.245	1.245	-.054	-.058	1.363	1.363
8.0	-.030	-.033	.659	.678	-.035	-.039	1.030	1.030	-.040	-.044	1.169	1.167	-.047	-.050	1.257	1.257	-.057	-.058	1.372	1.370
9.0	-.027	-.030	.707	.716	-.029	-.035	1.021	1.028	-.035	-.040	1.167	1.171	-.041	-.045	1.254	1.259	-.049	-.051	1.368	1.372
10.0	-.020	-.017		.620	-.024	-.021		1.022	-.030	-.025		1.171	-.034	-.031		1.259	-.041	-.037		1.372
11.0	-.014	-.014		.442	-.019	-.019		1.043	-.022	-.023		1.184	-.026	-.027		1.269	-.033	-.032		1.378
12.0	-.013	-.014		.278	-.016	-.019		1.082	-.020	-.022		1.209	-.023	-.025		1.287	-.031	-.031		1.388
14.0	-.012	-.009		.474	-.014	-.013		1.159	-.017	-.017		1.262	-.021	-.020		1.328	-.026	-.022		1.411
16.0	-.015	-.013		.778	-.017	-.017		1.221	-.020	-.021		1.306	-.022	-.022		1.360	-.026	-.025		1.432
18.0	-.010	-.013		.917	-.012	-.016		1.270	-.014	-.018		1.342	-.016	-.022		1.388	-.021	-.024		1.448
21.0	-.010	-.017		1.064	-.013	-.021		1.335	-.014	-.022		1.394	-.016	-.024		1.429	-.019	-.025		1.474
24.0	-.007	-.014		1.170	-.009	-.016		1.388	-.011	-.018		1.435	-.013	-.020		1.463	-.015	-.022		1.497
27.0	-.014	-.018		1.233	-.016	-.019		1.427	-.017	-.022		1.466	-.018	-.022		1.488	-.021	-.025		1.513
31.0	-.017	-.023		1.275	-.019	-.025		1.453	-.020	-.025		1.483	-.022	-.027		1.502	-.022	-.027		1.523
35.0	-.048	-.044			-.050	-.046			-.052	-.046			-.053	-.048			-.053	-.048		
37.0				1.304				1.481				1.504				1.517				1.532
40.0	-.028	-.029			-.029	-.031			-.030	-.031			-.032	-.031			-.032	-.033		
45.0	-.021	-.025			-.023	-.027			-.023	-.027			-.024	-.027			-.025	-.029		
	Circumferential distribution of C_p																			
Station	Outer shell, external				Outer shell, external				Outer shell, external				Outer shell, external				Outer shell, external			
θ→	198°	216°	234°	252°	198°	216°	234°	252°	198°	216°	234°	252°	198°	216°	234°	252°	198°	216°	234°	252°
0.5	0.177	0.176	0.172	0.161	0.100	0.097	0.092	0.085	0.014	0.012	0.005	-0.001	-0.063	-0.067	-0.073	-0.076	-0.187	-0.192	-0.195	-0.203
14.0	-.015	-.020	-.017	-.017	-.019	-.024	-.023	-.014	-.022	-.027	-.024	-.017	-.026	-.031	-.028	-.021	-.031	-.034	-.033	-.024
43.0	-.027	-.025	-.027	-.028	-.029	-.026	-.029	-.029	-.029	-.028	-.029	-.029	-.031	-.028	-.031	-.031	-.031	-.030	-.031	-.031

TABLE III - EXTERNAL AND INTERNAL PRESSURE COEFFICIENTS OF NACA 8-INCH RAM-JET CONFIGURATION FOR FOUR ANGLES OF ATTACK - Continued

(a) Continued. - Free-stream Mach number of 1.59.



Station	$\alpha = 0^\circ$; $m_3/m_0 = 0.329$				$\alpha = 3^\circ$; $m_3/m_0 = 0.804$				$\alpha = 3^\circ$; $m_3/m_0 = 0.740$				$\alpha = 3^\circ$; $m_3/m_0 = 0.652$				$\alpha = 3^\circ$; $m_3/m_0 = 0.592$			
	Longitudinal distribution of C_p																			
	Outer shell			Center body	Outer shell			Center body	Outer shell			Center body	Outer shell			Center body	Outer shell			Center body
	External		Internal		External		Internal		External		Internal		External		Internal		External		Internal	
$\theta \longrightarrow$	180°	270°	0°	0°	180°	270°	0°	0°	180°	270°	0°	0°	180°	270°	0°	0°	180°	270°	0°	0°
-1.5				1.184				0.584				0.583				0.729				1.008
-1.0				1.248				.657				.769				1.030				1.096
-.5				1.305				.880				.961				1.079				1.133
0				1.369				.909				.976				1.095				1.158
.5	-0.331	-0.422	1.504	1.423	0.021	0.157	0.751	.826	-0.020	0.103	0.921	.928	-0.099	0.041	1.130	1.089	-0.154	-0.076	1.229	1.171
1.0	-.214	-.231	1.487	1.454	.004	.124	.783	.723	-.028	.090	.950	.891	-.089	.030	1.145	1.094	-.132	-.017	1.236	1.189
1.5	-.166	-.169	1.483	1.466	-.012	.083	.798	.722	-.036	.060	.966	.898	-.082	.021	1.156	1.105	-.111	-.012	1.245	1.202
2.0	-.133	-.139	1.482	1.469	-.018	.056	.824	.707	-.038	.041	.987	.892	-.074	.013	1.169	1.104	-.096	-.013	1.253	1.202
2.5	-.122	-.124	1.483	1.472	-.028	.036	.854	.769	-.045	.024	1.002	.932	-.071	.005	1.179	1.130	-.090	-.017	1.263	1.223
3.0	-.096	-.103	1.480	1.474	-.031	.030	.838	.789	-.047	.018	1.991	.948	-.065	-.002	1.171	1.141	-.085	-.019	1.256	1.233
4.0	-.108	-.113	1.480	1.475	-.065	-.024	.826	.793	-.079	-.031	1.989	.961	-.089	-.044	1.172	1.154	-.103	-.054	1.258	1.243
5.0	-.097	-.105	1.477	1.475	-.070	-.040	.759	.753	-.079	0.046	1.965	.958	-.091	-.054	1.161	1.156	-.101	-.061	1.250	1.246
6.0	-.085	-.089	1.474	1.474	-.064	-.044	.619	.619	-.071	-.049	1.943	.939	-.079	-.054	1.151	1.148	-.087	-.061	1.243	1.241
7.0	-.066	-.069	1.475	1.475	-.049	-.038	.507	.510	-.053	-.041	1.958	.958	-.061	-.046	1.157	1.157	-.067	-.046	1.248	1.248
8.0	-.066	-.067	1.478	1.478	-.049	-.040	.663	.684	-.053	-.044	1.996	.995	-.058	-.049	1.178	1.177	-.062	-.054	1.263	1.261
9.0	-.057	-.059	1.477	1.478	-.041	-.040	.701	.710	-.045	-.044		1.002	-.048	-.048	1.177	1.182	-.054	-.052	1.263	1.267
10.0	-.047	-.044		1.480	-.034	-.026		.613	-.038	-.030		1.002	-.040	-.033		1.184	-.044	-.038		1.269
11.0	-.039	-.038		1.480	-.026	-.024		.435	-.030	-.029		1.025	-.030	-.031		1.205	-.034	-.035		1.281
12.0	-.034	-.036		1.483	-.022	-.026		.273	-.024	-.029		1.067	-.025	-.031		1.220	-.029	-.035		1.299
14.0	-.029	-.026		1.493	-.018	-.021		.478	-.020	-.025		1.147	-.021	-.026		1.270	-.023	-.029		1.335
16.0	-.028	-.029		1.503	-.018	-.023		.769	-.020	-.026		1.073	-.020	-.028		1.313	-.022	-.029		1.367
18.0	-.022	-.026		1.509	-.013	-.023		.906	-.014	-.025		1.259	-.014	-.026		1.347	-.015	-.029		1.393
21.0	-.021	-.028		1.528	-.013	-.027		1.048	-.016	-.029		1.326	-.014	-.029		1.396	-.015	-.031		1.431
24.0	-.016	-.022		1.531	-.013	-.023		1.155	-.017	-.025		1.384	-.013	-.025		1.437	-.014	-.026		1.465
27.0	-.020	-.025		1.536	-.018	-.027		1.220	-.020	-.029		1.423	-.019	-.029		1.467	-.020	-.029		1.490
31.0	-.022	-.028		1.542	-.022	-.032		1.263	-.023	-.034		1.452	-.022	-.033		1.486	-.023	-.034		1.503
35.0	-.053	-.048			-.051	-.053			-.054	-.055			-.052	-.053			-.053	-.054		
37.0				1.546				1.292				1.480				1.507				1.518
40.0	-.031	-.032			-.029	-.038			-.030	-.039			-.029	-.038			-.029	-.038		
45.0	-.031	-.028			-.021	-.034			-.022	-.036			-.021	-.034			-.021	-.035		

Station	Circumferential distribution of C_p																			
	Outer shell, external				Outer shell, external				Outer shell, external				Outer shell, external				Outer shell, external			
$\theta \longrightarrow$	198°	216°	234°	252°	198°	216°	234°	252°	198°	216°	234°	252°	198°	216°	234°	252°	198°	216°	234°	252°
0.5	-0.383	-0.400	-0.408	-0.416	0.024	0.049	0.079	0.112	-0.022	-0.002	-0.025	-0.058	-0.112	-0.096	-0.071	-0.043	-0.175	-0.171	-0.138	-0.114
14.0	-.034	-.037	-.037	-.029	-.023	-.029	-.029	-.023	-.027	-.032	-.030	-.027	-.027	-.033	-.032	-.028	-.029	-.034	-.034	-.030
43.0	-.031	-.029	-.030	-.031	-.029	-.029	-.032	-.035	-.029	-.029	-.034	-.036	-.028	-.028	-.031	-.034	-.029	-.029	-.032	-.035

TABLE III - EXTERNAL AND INTERNAL PRESSURE COEFFICIENTS OF NACA 8-INCH RAM-JET CONFIGURATION FOR FOUR ANGLES OF ATTACK - Continued

(a) Continued. - Free-stream Mach number of 1.59.

Station	$\alpha = 3°$; $m_3/m_0 = 0.436$				$\alpha = 3°$; $m_3/m_0 = 0.336$				$\alpha = 6°$; $m_3/m_0 = 0.800$				$\alpha = 6°$; $m_3/m_0 = 0.715$				$\alpha = 6°$; $m_3/m_0 = 0.596$			
	Longitudinal distribution of C_p																			
	Outer shell			Center body	Outer shell			Center body	Outer shell			Center body	Outer shell			Center body	Outer shell			Center body
	External		Internal		External		Internal		External		Internal		External		Internal		External		Internal	
$\theta \rightarrow$	180°	270°	0°	0°	180°	270°	0°	0°	180°	270°	0°	0°	180°	270°	0°	0°	180°	270°	0°	0°
-1.5				1.117				1.201				1.667				0.680				0.987
-1.0				1.170				1.252				.760				.922				1.104
-0.5				1.210				1.300				.864				1.006				1.131
0				1.251				1.351				.889				1.005				1.139
0.5	-0.242	-0.198	1.359	1.287	-0.346	-0.375	1.473	1.401	-0.094	-0.174	0.492	.763	-0.145	0.075	0.919	.947	-0.251	-0.071	1.165	1.135
1.0	-.205	-.105	1.354	1.317	-.309	-.215	1.463	1.431	-.023	-.169	.639	.494	-.140	.093	.981	.926	-.231	-.007	1.194	1.147
1.5	-.171	-.077	1.364	1.331	-.251	-.159	1.463	1.445	-.096	-.118	.778	.700	-.130	.078	1.021	.950	-.203	.004	1.213	1.168
2.0	-.146	-.064	1.369	1.333	-.211	-.129	1.465	1.450	-.096	-.071	.809	.795	-.122	.061	1.045	.960	-.180	.005	1.231	1.175
2.5	-.123	-.058	1.367	1.346	-.183	-.106	1.467	1.455	-.099	-.050	.843	.762	-.120	.037	1.065	1.002	-.168	-.005	1.242	1.201
3.0	-.120	-.052	1.367	1.351	-.165	-.095	1.466	1.458	-.098	-.030	.830	.785	-.112	.021	1.060	1.022	-.154	-.009	1.240	1.214
4.0	-.123	-.072	1.363	1.357	-.160	-.190	1.467	1.462	-.116	-.030	.819	.786	-.126	-.038	1.063	1.040	-.157	-.055	1.246	1.229
5.0	-.120	-.077	1.359	1.359	-.145	-.092	1.465	1.463	-.106	-.048	.752	.745	-.117	-.055	1.048	1.042	-.142	-.069	1.239	1.235
6.0	-.103	-.074	1.363	1.357	-.120	-.086	1.463	1.462	-.082	-.057	.614	.616	-.095	-.061	1.035	1.031	-.116	-.073	1.235	1.232
7.0	-.080	-.062	1.371	1.363	-.494	-.074	1.465	1.465	-.059	-.051	.505	.509	-.068	-.055	1.045	1.045	-.085	-.068	1.240	1.240
8.0	-.071	-.061	1.372	1.371	-.079	-.066	1.467	1.468	-.056	-.061	.682	.696	-.060	-.064	1.075	1.073	-.071	-.080	1.257	1.255
9.0	-.060	-.059		1.374	-.066	-.066	1.467	1.470	-.046	-.063	.688	.696	-.048	-.067	1.075	1.080	-.058	-.077	1.257	1.261
10.0	-.050	-.046		1.376	-.056	-.053		1.471	-.038	-.064		.600	-.040	-.058		1.081	-.047	-.068		1.263
11.0	-.039	-.043		1.383	-.045	-.048		1.474	-.028	-.055		.423	-.029	-.058		1.010	-.035	-.068		1.276
12.0	-.034	-.041		1.393	-.036	-.047		1.478	-.021	-.057		.265	-.023	-.059		1.033	-.030	-.069		1.292
14.0	-.027	-.035		1.413	-.029	-.038		1.488	-.016	-.055		.597	-.017	-.058		1.197	-.022	-.066		1.329
16.0	-.026	-.035		1.433	-.025	-.038		1.496	-.015	-.053		.811	-.016	-.055		1.251	-.020	-.063		1.361
18.0	-.019	-.031		1.449	-.020	-.035		1.504	-.010	-.051		.928	-.011	-.052		1.292	-.014	-.058		1.387
21.0	-.019	-.033		1.472	-.020	-.035		1.515	-.011	-.054		1.061	-.011	-.054		1.353	-.014	-.058		1.425
24.0	-.016	-.029		1.495	-.017	-.029		1.526	-.011	-.047		1.163	-.011	-.046		1.403	-.014	-.051		1.458
27.0	-.021	-.031		1.510	-.022	-.032		1.533	-.018	-.051		1.226	-.017	-.051		1.439	-.021	-.054		1.482
31.0	-.025	-.037		1.521	-.025	-.037		1.537	-.021	-.056		1.268	-.020	-.055		1.464	-.024	-.059		1.497
35.0	-.054	-.055			-.054	-.056			-.051	-.076			-.049	-.074			-.053	-.078		
37.0				1.528				1.542				1.297				1.491				1.513
40.0	-.031	-.040			-.030	.041			-.025	-.062			-.023	-.060			-.027	-.063		
45.0	-.023	-.037			-.022	.037			-.019	-.059			-.017	-.058			-.020	-.062		

Station	Circumferential distribution of C_p																			
	Outer shell, external				Outer shell, external				Outer shell, external				Outer shell, external				Outer shell, external			
$\theta \rightarrow$	198°	216°	234°	252°	198°	216°	234°	252°	198°	216°	234°	252°	198°	216°	234°	252°	198°	216°	234°	252°
0.5	-0.278	-0.268	-0.246	-0.226	-0.447	-0.447	-0.442	-0.408	-0.010	-0.059	-0.003	-0.080	-0.152	-0.033	-0.079	-0.009	-0.283	-0.243	-0.206	-0.149
14.0	-.232	-.038	-.039	-.035	-.035	-.040	-.042	-.031	-.025	-.039	-.047	-.054	-.027	-.039	-.047	-.054	-.030	-.045	-.055	-.063
43.0	-.030	-.030	-.035	-.038	-.029	-.029	-.034	-.037	-.030	-.034	-.042	-.053	-.029	-.033	-.040	-.051	-.032	-.035	-.042	-.054

TABLE III - EXTERNAL AND INTERNAL PRESSURE COEFFICIENTS OF NACA 8-INCH RAM-JET CONFIGURATION FOR FOUR ANGLES OF ATTACK - Continued

(a) Concluded. - Free-stream Mach number of 1.59.



Station	$\alpha = 6^\circ$; $m_3/m_0 = 0.338$				$\alpha = 10^\circ$; $m_3/m_0 = 0.759$				$\alpha = 10^\circ$; $m_3/m_0 = 0.686$				$\alpha = 10^\circ$; $m_3/m_0 = 0.574$				$\alpha = 10^\circ$; $m_3/m_0 = 0.330$			
	Longitudinal distribution of C_p																			
	Outer shell			Center body	Outer shell			Center body	Outer shell			Center body	Outer shell			Center body	Outer shell			Center body
	External		Internal		External		Internal		External		Internal		External		Internal		External		Internal	
$\theta \rightarrow$	180°	270°	0°	0°	180°	270°	0°	0°	180°	270°	0°	0°	180°	270°	0°	0°	180°	270°	0°	0°
-1.5				1.229				0.787				0.806				1.016				1.251
-1.0				1.265				.875				.950				1.117				1.273
-0.5				1.306				.924				1.008				1.136				1.293
0				1.348				.908				.978				1.119				1.317
0.5	-0.386	-0.335	1.452	1.389	-0.170	0.281	0.288	.740	-0.243	0.106	0.743	.863	-0.295	-0.042	1.067	1.090	-0.347	-0.312	1.387	1.343
1.0	-.406	-.204	1.451	1.420	-.204	.186	.383	.421	-.259	.166	.911	.834	-.322	.029	1.145	1.096	-.475	-.184	1.400	1.369
1.5	-.334	-.149	1.455	1.436	-.200	.125	.355	.136	-.246	.101	.970	.892	-.293	.070	1.180	1.129	-.441	-.120	1.412	1.389
2.0	-.286	-.115	1.459	1.443	-.192	.079	.265	.188	-.232	.062	1.008	.918	-.267	.040	1.204	1.133	-.378	-.087	1.424	1.398
2.5	-.243	-.096	1.464	1.451	-.186	.046	.762	.630	-.222	.031	1.037	.972	-.253	.012	1.222	1.178	-.351	-.064	1.431	1.412
3.0	-.234	-.083	1.464	1.455	-.181	.026	.823	.764	-.201	.012	1.037	.998	-.234	-.006	1.222	1.197	-.324	-.070	1.433	1.420
4.0	-.211	-.098	1.467	1.462	-.177	-.038	.810	.784	-.188	-.047	1.050	1.026	-.221	-.060	1.234	1.219	-.285	-.090	1.439	1.431
5.0	-.188	-.100	1.466	1.464	-.125	-.064	.739	.733	-.154	-.070	1.039	1.032	-.184	-.081	1.231	1.227	-.244	-.106	1.439	1.436
6.0	-.153	-.096	1.466	1.464	-.094	-.079	.607	.608	-.104	-.085	1.029	1.022	-.126	-.094	1.229	1.226	-.179	-.116	1.439	1.438
7.0	-.113	-.088	1.469	1.467	-.071	-.081	.499	.504	-.075	-.085	1.040	1.040	-.095	-.094	1.237	1.237	-.112	-.114	1.442	1.442
8.0	-.090	-.085	1.472	1.472	-.061	-.093	.671	.677	-.064	-.092	1.070	1.068	-.066	-.101	1.253	1.252	-.079	-.114	1.446	1.444
9.0	-.070	-.088	1.472	1.474	-.046	-.098	.664	.674	-.051	-.107	1.070	1.075	-.052	-.114	1.254	1.257	-.058	-.127	1.444	1.444
10.0	-.054	-.082		1.475	-.037	-.105		.575	-.040	-.110		1.078	-.040	-.115		1.261	-.042	-.132		1.444
11.0	-.039	-.080		1.478	-.026	-.112		.401	-.028	-.115		1.098	-.029	-.122		1.272	-.029	-.137		1.449
12.0	-.031	-.082		1.482	-.018	-.120		.244	-.021	-.124		1.129	-.022	-.129		1.288	-.023	-.146		1.456
14.0	-.023	-.078		1.492	-.011	-.129		.715	-.014	-.133		1.194	-.015	-.138		1.325	-.016	-.154		1.467
16.0	-.021	-.072		1.500	-.011	-.136		.861	-.012	-.141		1.245	-.012	-.146		1.358	-.013	-.163		1.479
18.0	-.015	-.065		1.507	-.005	-.136		.950	-.007	-.141		1.286	-.007	-.149		1.383	-.008	-.169		1.490
21.0	-.016	-.063		1.519	-.005	-.123		1.060	-.007	-.126		1.345	-.007	-.129		1.422	-.008	-.145		1.505
24.0	-.016	-.055		1.529	-.004	-.108		1.153	-.005	-.110		1.397	-.006	-.111		1.456	-.008	-.114		1.518
27.0	-.023	-.056		1.536	-.013	-.113		1.214	-.014	-.113		1.433	-.014	-.114		1.480	-.016	-.117		1.525
31.0	-.025	-.046		1.541	-.014	-.110		1.255	-.014	-.112		1.459	-.014	-.111		1.498	-.018	-.114		1.532
35.0	-.054	-.078			-.054	-.129			-.054	-.129			-.055	-.128			-.056	-.130		
37.0				1.545				1.284				1.484				1.512				1.534
40.0	-.028	-.063			-.020	-.112			-.020	-.112			-.020	-.114			-.023	-.114		
45.0	-.021	-.060			-.020	-.110			-.020	-.110			-.020	-.109			-.023	-.110		

Station	Circumferential distribution of C_p																			
	Outer shell, external				Outer shell, external				Outer shell, external				Outer shell, external				Outer shell, external			
$\theta \rightarrow$	198°	216°	234°	252°	198°	216°	234°	252°	198°	216°	234°	252°	198°	216°	234°	252°	198°	216°	234°	252°
0.5	-0.470	-0.472	-0.461	-0.402	-.0.197	-0.153	-0.079	-0.042	-0.294	-0.249	-0.165	-0.054	-0.374	-0.335	-0.268	-0.175	-0.483	-0.479	-0.471	-0.410
14.0	-.034	-.047	-.062	-.073	-.029	-.055	-.088	-.133	-.031	-.057	-.091	-.140	-.032	-.059	-.094	-.150	-.034	-.064	-.107	-.177
43.0	-.033	-.037	-.042	-.055	-.043	-.058	-.059	-.078	-.043	-.058	-.061	-.078	-.043	-.056	-.060	-.077	-.044	-.059	-.062	-.078

TABLE III - EXTERNAL AND INTERNAL PRESSURE COEFFICIENTS OF NACA 8-INCH RAM-JET CONFIGURATION FOR FOUR ANGLES OF ATTACK - Continued

(b) Free-stream Mach number of 1.79.

NACA

Longitudinal distribution of C_p.

Station	$\alpha = 0°$; $m_3/m_0 = 0.915$				$\alpha = 0°$; $m_3/m_0 = 0.903$				$\alpha = 0°$; $m_3/m_0 = 0.842$				$\alpha = 0°$; $m_3/m_0 = 0.796$				$\alpha = 0°$; $m_3/m_0 = 0.667$			
	Outer shell			Center body	Outer shell			Center body	Outer shell			Center body	Outer shell			Center body	Outer shell			Center body
	External		Internal		External		Internal		External		Internal		External		Internal		External		Internal	
θ →	180°	270°	0°	0°	180°	270°	0°	0°	180°	270°	0°	0°	180°	270°	0°	0°	180°	270°	0°	0°
-1.5				0.459				0.456				0.458				0.458				0.458
-1.0				.503				.500				.501				.505				1.045
-0.5				.503				.501				.554				1.034				1.252
0				.555				.944				1.172				1.211				1.286
0.5	0.269		1.036	1.059	0.238	0.212	1.107	1.087	0.176	0.151	1.211	1.153	0.097	0.075	1.289	1.207	-0.003	-0.028	1.410	1.317
1.0	.171	0.167	1.017	.959	.158	.153	1.093	1.028	.128	.124	1.203	1.138	.088	.081	1.282	1.211	.034	.022	1.403	1.341
1.5	.118	.116	1.005	.931	.109	.107	1.088	1.017	.092	.090	1.203	1.151	.065	.065	1.282	1.220	.028	.021	1.403	1.358
2.0	.083	.082	1.008	.892	.076	.076	1.093	.992	.064	.061	1.206	1.136	.044	.043	1.286	1.209	.020	.012	1.404	1.352
2.5	.059	.055	1.025	.919	.053	.050	1.105	1.033	.042	.039	1.214	1.156	.027	.024	1.292	1.236	.010	.002	1.409	1.372
3.0	.043	.040	1.006	.956	.038	.035	1.090	1.044	.028	.025	1.203	1.166	.017	.013	1.280	1.245	.007	-.003	1.403	1.378
4.0	-.006	-.010	.987	.955	-.011	-.013	1.078	1.049	-.017	-.019	1.197	1.174	-.026	-.029	1.277	1.253	-.032	-.041	1.400	1.388
5.0	-.025	-.023	.919	.915	-.028	-.026	1.040	1.028	-.034	-.031	1.185	1.170	-.039	-.038	1.267	1.253	-.045	-.047	1.393	1.390
6.0	-.024	-.026	.771	.771	-.028	-.028	1.004	.998	-.034	-.034	1.155	1.151	-.037	-.039	1.246	1.241	-.042	-.046	1.385	1.383
7.0	-.014	-.018	.654	.657	-.021	-.023	1.020	1.021	-.026	-.026	1.162	1.165	-.027	-.030	1.251	1.250	.032	-.037	1.388	1.388
8.0	-.018	-.018	.741	.768	-.021	-.021	1.064	1.066	-.026	-.024	1.189	1.191	-.029	-.029	1.270	1.269	-.034	-.035	1.399	1.399
9.0	-.012	-.018	.853	.865	-.017	-.021	1.049	1.058	-.021	-.024	1.180	1.201	-.022	-.029	1.265	1.269	-.026	-.032	1.399	1.403
10.0	-.003	-.004		.774	-.007	-.007		1.038	-.010	-.012		1.192	-.012	-.015		1.267	-.017	-.019		1.403
11.0	.013	-.001		.587	.008	-.004		1.071	.003	-.008		1.199	.005	-.011		1.283	-.002	-.014		1.414
12.0	.012	.004		.422	.008	.002		1.133	.003	-.002		1.238	-.002	-.004		1.311	-.008	-.008		1.430
14.0	-.008	.002		.895	-.009	-.001		1.239	-.012	-.004		1.313	-.018	-.008		1.370	-.020	-.010		1.465
16.0	-.021	-.010		1.060	-.023	-.012		1.316	-.024	-.014		1.375	-.029	-.018		1.417	-.032	-.019		1.495
18.0	.002	-.010		1.167	.001	-.011		1.378	-.002	-.013		1.422	-.005	-.016		1.453	-.007	-.016		1.516
21.0	.001	-.003		1.292	-.001	-.006		1.459	-.003	-.008		1.487	-.005	-.010		1.506	-.007	-.011		1.551
24.0	.004	-.006		1.391	-.009	-.007		1.528	-.003	-.008		1.542	-.002	-.010		1.551	-.002	-.011		1.580
27.0	-.004	-.001		1.455	-.006	-.002		1.574	-.007	-.004		1.582	-.009	-.004		1.586	-.002	-.005		1.604
31.0	-.004	-.001		1.497	-.006	-.003		1.607	-.007	-.004		1.608	-.008	-.006		1.606	-.008	-.006		1.617
35.0	-.028	-.025			-.028	-.026			-.030	-.026			-.029	-.026			-.030	-.026		
37.0				1.530				1.644				1.644				1.640				1.639
40.0	-.016	-.016			-.018	-.004			-.018	-.018			-.018	-.018			-.019	-.019		
45.0	-.016	-.016			-.018	-.004			-.018	-.018			-.018	-.018			-.018	-.019		

Circumferential distribution of C_p.

Station	Outer shell, external				Outer shell, external				Outer shell, external				Outer shell, external				Outer shell, external			
θ →	198°	216°	234°	252°	198°	216°	234°	252°	198°	216°	234°	252°	198°	216°	234°	252°	198°	216°	234°	252°
0.5	0.268	0.269	0.266	0.251	0.237	0.238	0.232	0.222	0.175	0.175	0.168	0.159	0.093	0.091	0.086	0.081	-0.008	-0.009	-0.014	-0.020
14.0	-.009	-.009	-.020	.001	-.013	-.011	-.023	-.004	-.017	-.013	-.022	-.008	-.018	-.018	-.023	-.012	-.024	-.022	-.019	-.013
43.0	-.018	-.016	-.008	-.018	-.018	-.018	-.018	-.018	-.019	-.018	-.018	-.019	-.020	-.018	-.018	-.018	-.019	-.018	-.019	-.019

TABLE III - EXTERNAL AND INTERNAL PRESSURE COEFFICIENTS OF NACA 8-INCH RAM-JET CONFIGURATION FOR FOUR ANGLES OF ATTACK - Continued
(b) Continued. - Free-stream Mach number of 1.79.



Station	$\alpha = 0^\circ$; $m_3/m_0 = 0.544$				$\alpha = 3^\circ$; $m_3/m_0 = 0.914$				$\alpha = 3^\circ$; $m_3/m_0 = 0.864$				$\alpha = 3^\circ$; $m_3/m_0 = 0.783$				$\alpha = 3^\circ$; $m_3/m_0 = 0.661$			
	Longitudinal distribution of C_p																			
	Outer shell			Center body	Outer shell			Center body	Outer shell			Center body	Outer shell			Center body	Outer shell			Center body
	External		Internal		External		Internal		External		Internal		External		Internal		External		Internal	
$\theta \rightarrow$	180°	270°	0°	0°	180°	270°	0°	0°	180°	270°	0°	0°	180°	270°	0°	0°	180°	270°	0°	0°
-1.5				0.722				0.534				0.540				0.534				0.535
-1.0				1.264				.580				.610				.580				1.110
-0.5				1.313				.591				.599				.769				1.252
0				1.366				.541				1.013				1.185				1.274
0.5	-0.120	-0.140	1.508	1.412	0.140	0.247	0.893	.994	0.085	0.195	1.044	1.047	-0.007	0.096	1.210	1.164	-0.116	-0.026	1.361	1.288
1.0	-.044	-.056	1.495	1.449	.081	.178	.920	.845	.055	.155	1.069	.998	.003	.103	1.227	1.162	-.066	-.023	1.367	1.312
1.5	-.037	-.035	1.495	1.466	.042	.121	.941	.857	.024	.106	1.088	1.012	-.009	.074	1.240	1.180	-.056	-.023	1.376	1.332
2.0	-.018	-.028	1.496	1.461	.015	.085	.970	.842	.003	.074	1.109	1.005	-.020	.051	1.255	1.176	-.054	-.013	1.385	1.332
2.5	-.020	-.028	1.498	1.477	-.003	.057	1.000	.917	-.014	.048	1.126	1.055	-.030	.031	1.265	1.214	-.058	-.003	1.392	1.358
3.0	-.017	-.027	1.495	1.481	-.016	.039	.992	.940	-.024	.031	1.119	1.073	-.034	.017	1.260	1.227	-.057	-.003	1.390	1.367
4.0	-.047	-.055	1.493	1.488	-.053	-.009	.981	.948	-.061	-.016	1.121	1.092	-.065	-.025	1.265	1.245	-.081	-.040	1.394	1.382
5.0	-.056	-.057	1.490	1.490	-.063	-.022	.913	.910	-.068	-.028	1.097	1.090	-.071	-.035	1.255	1.250	-.083	-.047	1.390	1.389
6.0	-.051	-.054	1.486	1.487	-.058	-.027	.768	.767	-.063	-.033	1.076	1.069	-.065	-.038	1.248	1.243	-.075	-.048	1.387	1.385
7.0	-.039	-.044	1.488	1.491	-.046	-.022	.653	.658	-.051	-.026	1.094	1.092	-.051	-.032	1.258	1.258	-.059	-.040	1.394	1.395
8.0	-.039	-.040	1.496	1.496	-.039	-.024	.811	.845	-.044	-.028	1.134	1.134	-.046	-.033	1.282	1.284	-.054	-.040	1.411	1.411
9.0	-.031	-.037	1.496	1.500	-.027	-.024	.840	.852	-.029	-.028	1.138	1.144	-.028	-.033	1.286	1.291	-.036	-.039	1.414	1.418
10.0	-.020	-.023		1.501	-.017	-.011		.758	-.020	-.013		1.145	-.019	-.019		1.296	-.025	-.025		1.423
11.0	-.004	-.018		1.506	-.018	-.005		.573	-.015	-.009		1.170	-.020	-.013		1.313	-.027	-.020		1.432
12.0	-.009	-.011		1.515	-.013	-.007		.412	-.015	-.011		1.212	-.024	-.015		1.337	-.029	-.020		1.446
14.0	-.023	-.013		1.537	-.022	-.012		.267	-.027	-.015		1.291	-.032	-.018		1.388	-.036	-.023		1.478
16.0	-.034	-.022		1.556	-.024	-.019		.802	-.027	-.023		1.351	-.028	-.025		1.431	-.030	-.030		1.505
18.0	-.008	-.018		1.571	.001	-.019		.956	-.003	-.021		1.398	-.005	-.023		1.463	-.008	-.026		1.525
21.0	-.007	-.013		1.593	-.002	-.013		1.123	-.003	-.015		1.465	-.005	-.018		1.508	-.008	-.021		1.554
24.0	-.002	-.011		1.613	.003	-.016		1.244	0	-.018		1.521	-.003	-.018		1.533	-.005	-.020		1.578
27.0	-.009	-.005		1.629	-.007	-.009		1.325	-.009	-.013		1.567	-.009	-.011		1.518	-.012	-.013		1.599
31.0	-.008	-.005		1.638	-.007	-.009		1.376	-.008	-.011		1.597	-.008	-.018		1.600	-.010	-.013		1.611
35.0	-.028	-.026			-.030	-.034			-.030	-.034			-.030	-.035			-.033	-.036		
37.0				1.651				1.412				1.637				1.634				1.633
40.0	-.018	-.019			-.017	-.026			-.019	-.026			-.018	-.026			-.020	-.027		
45.0	-.016	-.017			-.016	-.026			-.016	-.026			-.017	-.026			-.018	-.027		

Station	Circumferential distribution of C_p																			
	Outer shell, external				Outer shell, external				Outer shell, external				Outer shell, external				Outer shell, external			
$\theta \rightarrow$	198°	216°	234°	252°	198°	216°	234°	252°	198°	216°	234°	252°	198°	216°	234°	252°	198°	216°	234°	252°
0.5	-0.125	-0.127	-0.129	-0.135	0.144	0.162	0.185	0.213	0.088	0.105	0.129	0.158	-0.003	0.010	0.033	0.060	-0.113	-0.102	-0.080	-0.059
14.0	-.024	-.024	-.020	-.015	-.024	-.027	-.019	-.018	-.028	-.030	-.018	-.022	-.033	-.034	-.018	-.024	-.038	-.038	-.019	-.028
43.0	-.018	-.016	-.018	-.018	-.019	-.018	-.022	-.024	-.020	-.020	-.024	-.025	-.020	-.020	-.024	-.025	-.021	-.021	-.023	-.026

2034

TABLE III - EXTERNAL AND INTERNAL PRESSURE COEFFICIENTS OF NACA 8-INCH RAM-JET CONFIGURATION FOR FOUR ANGLES OF ATTACK - Continued

(b) Continued. - Free-stream Mach number of 1.79.

NACA

Station	$\alpha = 3°$; $m_3/m_0 = 0.446$				$\alpha = 6°$; $m_3/m_0 = 0.911$				$\alpha = 6°$; $m_3/m_0 = 0.869$				$\alpha = 6°$; $m_3/m_0 = 0.784$				$\alpha = 6°$; $m_3/m_0 = 0.669$			
	Longitudinal distribution of C_p																			
	Outer shell			Center body	Outer shell			Center body	Outer shell			Center body	Outer shell			Center body	Outer shell			Center body
	External		Internal		External		Internal		External		Internal		External		Internal		External		Internal	
$\theta \rightarrow$	180°	270°	0°	0°	180°	270°	0°	0°	180°	270°	0°	0°	180°	270°	0°	0°	180°	270°	0°	0°
-1.5				1.238				0.612				0.613				0.612				1.614
-1.0				1.299				.668				.669				.669				1.133
-.5				1.346				.684				.686				1.050				1.245
0				1.398				.644				.968				1.161				1.259
.5	-0.309	-0.207	1.524	1.445	0.013	0.261	0.658	.921	-0.032	0.200	0.926	.983	-0.115	0.102	1.135	1.125	-0.195	-0.008	1.302	1.258
1.0	-.186	-.107	1.517	1.483	-.006	.187	.713	.633	-.034	.163	1.014	.926	-.086	.109	1.185	1.122	-.144	.038	1.329	1.278
1.5	-.145	-.072	1.520	1.500	-.030	.129	.918	.697	-.050	.118	1.061	.973	-.085	.084	1.218	1.152	-.128	.038	1.350	1.306
2.0	-.121	-.057	1.524	1.502	-.047	.090	.961	.848	-.060	.081	1.092	.987	-.085	.058	1.240	1.160	-.119	.028	1.366	1.311
2.5	-.113	-.050	1.527	1.529	-.057	.061	.991	.913	-.070	.052	1.118	1.049	-.090	.036	1.258	1.205	-.118	.013	1.377	1.345
3.0	-.102	-.045	1.527	1.520	-.058	.042	.981	.933	-.072	.033	1.116	1.072	-.088	.021	1.258	1.225	-.111	.004	1.379	1.357
4.0	-.113	-.067	1.530	1.527	-.088	-.011	.967	.938	-.098	-.016	1.121	1.094	-.108	-.025	1.266	1.248	-.124	-.037	1.386	1.377
5.0	-.106	-.067	1.530	1.531	-.090	-.026	.908	.898	-.097	-.032	1.101	1.095	-.105	-.040	1.259	1.257	-.118	-.048	1.386	1.386
6.0	-.092	-.065	1.530	1.531	-.079	-.033	.762	.761	-.084	-.039	1.085	1.077	-.091	-.045	1.254	1.251	-.101	-.053	1.386	1.386
7.0	-.074	-.055	1.534	1.537	-.058	-.033	.648	.656	-.061	-.037	1.102	1.101	-.066	-.042	1.266	1.267	-.074	-.048	1.393	1.396
8.0	-.065	-.051	1.542	1.542	-.040	-.038	.817	.850	-.045	-.042	1.142	1.142	-.049	-.045	1.290	1.290	-.053	-.052	1.410	1.411
9.0	-.045	-.048	1.546	1.431	-.035	-.041	.826	.838	-.039	-.044	1.150	1.154	-.044	-.048	1.294	1.299	-.048	-.054	1.413	1.418
10.0	-.034	-.035		1.549	-.034	-.031		.744	-.037	-.033		1.159	-.042	-.037		1.303	-.045	-.042		1.422
11.0	-.034	-.027		1.554	-.031	-.031		.561	-.034	-.033		1.185	-.039	-.037		1.319	-.041	-.043		1.432
12.0	-.035	-.029		1.559	-.033	-.038		.402	-.034	-.041		1.222	-.039	-.045		1.341	-.041	-.049		1.444
14.0	-.040	-.029		1.571	-.034	-.045		.262	-.036	-.048		1.294	-.039	-.051		1.390	-.040	-.054		1.475
16.0	-.033	-.035		1.581	-.008	-.052		.700	-.010	-.-54		1.350	-.012	-.057		1.429	-.140	-.061		1.500
18.0	-.011	-.031		1.590	-.002	-.053		.865	-.004	-.054		1.393	-.005	-.056		1.460	-.008	-.058		1.521
21.0	-.011	-.024		1.603	-.002	-.041		1.037	-.004	-.044		1.452	-.005	-.045		1.501	-.007	-.048		1.548
24.0	-.008	-.024		1.615	-.001	-.043		1.165	-.003	-.046		1.502	-.004	-.047		1.536	-.004	-.048		1.574
27.0	-.013	-.017		1.625	-.008	-.036		1.255	-.009	-.038		1.547	-.010	-.038		1.564	-.011	-.039		1.593
31.0	-.012	-.016		1.630	-.007	-.032		1.312	-.008	-.033		1.578	-.008	-.034		1.584	-.008	-.034		1.603
35.0	-.034	-.037			-.031	-.058			-.032	-.059			-.033	-.060			-.033	-.061		
37.0				1.637				1.353				1.622				1.620				1.625
40.0	-.021	-.028			-.016	-.051			-.018	-.052			-.018	-.051			-.018	-.053		
45.0	-.019	-.028			-.014	-.051			-.015	-.052			-.015	-.051			-.015	-.053		
	Circumferential distribution of C_p																			
Station	Outer shell, external				Outer shell, external				Outer shell, external				Outer shell, external				Outer shell, external			
$\theta \rightarrow$	198°	216°	234°	252°	198°	216°	234°	252°	198°	216°	234°	252°	198°	216°	234°	252°	198°	216°	234°	252°
0.5	-0.307	-0.294	-0.267	-0.237	0.023	0.070	0.113	0.178	-0.028	0.003	0.051	0.117	-0.108	-0.082	-0.037	0.022	-0.188	-0.164	-0.126	-0.078
40.0	-.043	-.043	-.015	-.034	-.039	-.047	-.018	-.054	-.041	-.048	-.018	-.056	-.044	-.051	-.013	-.059	-.046	-.053	-.014	-.051
43.0	-.022	-.022	-.026	-.027	-.023	-.026	-.033	-.045	-.024	-.028	-.033	-.046	-.024	-.028	-.033	-.045	-.024	-.028	-.033	-.046

TABLE III - EXTERNAL AND INTERNAL PRESSURE COEFFICIENTS OF NACA 8-INCH RAM-JET CONFIGURATION FOR FOUR ANGLES OF ATTACK - Continued

(b) Concluded. - Free-stream Mach number of 1.79.

NACA

Station	$\alpha = 6°$; $m_3/m_0 = 0.410$				$\alpha = 10°$; $m_3/m_0 = 0.867$				$\alpha = 10°$; $m_3/m_0 = 0.793$				$\alpha = 10°$; $m_3/m_0 = 0.631$				$\alpha = 10°$; $m_3/m_0 = 0.383$			
	Longitudinal distribution of C_p																			
	Outer shell			Center body	Outer shell			Center body	Outer shell			Center body	Outer shell			Center body	Outer shell			Center body
	External		Internal		External		Internal		External		Internal		External		Internal		External		Internal	
$\theta \rightarrow$	180°	270°	0°	0°	180°	270°	0°	0°	180°	270°	0°	0°	180°	270°	0°	0°	180°	270°	0°	0°
-1.5				1.276				0.723				0.722				0.774				1.237
-1.0				1.332				.817				.815				1.017				1.302
-0.5				1.375				.801				.800				1.144				1.336
0				1.420				.798				1.004				1.153				1.366
0.5	-0.351	-0.231	1.530	1.466	-0.140	0.298	0.445	.847	-0.180	0.178	0.805	.923	-0.246	0.029	1.091	1.115	-0.349	-0.183	1.437	1.396
1.0	-.288	-.125	1.529	1.502	-.120	.194	.523	.537	-.154	.180	.986	.894	-.236	.067	1.164	1.121	-.320	-.087	1.456	1.429
1.5	-.237	-.086	1.535	1.520	-.128	.142	.478	.257	-.153	.123	1.057	.978	-.229	.070	1.219	1.161	-.298	-.048	1.473	1.453
2.0	-.204	-.064	1.541	1.525	-.132	.098	.904	.603	-.149	.080	1.106	1.012	-.219	.058	1.248	1.181	-.270	-.032	1.487	1.463
2.5	-.189	-.054	1.548	1.535	-.137	.065	.991	.908	-.148	.051	1.142	1.080	-.214	.035	1.272	1.229	-.257	-.022	1.497	1.482
3.0	-.172	-.048	1.548	1.541	-.137	.043	1.007	.976	-.142	.032	1.151	1.112	-.203	.017	1.274	1.252	-.240	-.022	1.499	1.492
4.0	-.167	-.070	1.553	1.550	-.147	-.015	1.012	.988	-.151	-.023	1.171	1.149	-.199	.004	1.291	1.279	-.224	-.058	1.509	1.507
5.0	-.151	-.073	1.555	1.555	-.123	-.037	.986	.983	-.132	-.043	1.170	1.166	-.174	-.051	1.287	1.291	-.194	-.069	1.509	1.513
6.0	-.127	-.073	1.555	1.555	-.078	-.051	.964	.959	-.095	-.056	1.170	1.164	-.128	-.063	1.282	1.286	-.151	-.078	1.511	1.514
7.0	-.045	-.065	1.560	1.560	-.064	-.052	.996	.996	-.073	-.058	1.194	1.192	-.093	-.063	1.296	1.295	-.112	-.077	1.519	1.521
8.0	-.070	-.067	1.565	1.565	-.063	-.061	1.060	1.061	-.069	-.065	1.227	1.233	-.078	-.068	1.303	1.305	-.090	-.080	1.523	1.527
9.0	-.060	-.067	1.569	1.571	-.055	-.068	1.093	1.099	-.060	-.070	1.252	1.257	-.067	-.078	1.294	1.301	-.073	-.091	1.524	1.528
10.0	-.053	-.055		1.574	-.048	-.068		1.122	-.053	-.073		1.270	-.058	-.080		1.296	-.063	-.092		1.530
11.0	-.048	-.057		1.577	-.041	-.079		1.151	-.047	-.082		1.291	-.050	-.088		1.309	-.053	-.099		1.533
12.0	-.047	-.062		1.581	-.038	-.090		1.187	-.042	-.093		1.317	-.045	-.099		1.330	-.047	-.110		1.540
14.0	-.044	-.065		1.589	-.011	-.102		1.252	-.015	-.106		1.366	-.013	-.111		1.380	-.020	-.121		1.553
16.0	-.013	-.070		1.597	-.004	-.118		1.303	-.007	-.120		1.406	-.009	-.126		1.420	-.013	-.135		1.564
18.0	-.012	-.067		1.604	.001	-.130		1.344	-.002	-.132		1.435	-.003	-.138		1.450	-.007	-.145		1.574
21.0	-.010	-.055		1.613	.001	-.125		1.397	-.002	-.125		1.474	-.004	-.135		1.494	-.007	-.142		1.589
24.0	-.009	-.053		1.621	.005	-.113		1.447	.003	-.115		1.506	.001	-.123		1.532	-.003	-.126		1.603
27.0	-.015	-.043		1.629	0	-.107		1.488	-.002	-.108		1.533	.007	-.113		1.559	-.008	-.113		1.614
31.0	-.012	-.038		1.633	.002	-.084		1.519	-.002	-.086		1.555	-.003	-.088		1.572	-.007	-.087		1.620
35.0	-.035	-.062			-.030	-.108			-.032	-.108			-.034	-.111			-.036	-.091		
37.0				1.638				1.561				1.598				1.590				1.625
40.0	-.019	-.054			-.010	-.103			-.012	-.103			-.014	-.106			-.015	-.104		
45.0	-.018	-.054			-.014	-.101			-.015	-.101			-.017	-.103			-.024	-.102		
	Circumferential distribution of C_p																			
Station	Outer shell, external				Outer shell, external				Outer shell, external				Outer shell, external				Outer shell, external			
$\theta \rightarrow$	198°	216°	234°	252°	198°	216°	234°	252°	198°	216°	234°	252°	198°	216°	234°	252°	198°	216°	234°	252°
0.5	-0.349	-0.344	-0.331	-0.292	-0.128	-0.081	0.011	0.139	-0.170	-0.130	-0.066	-0.033	-0.240	-0.210	-0.161	-0.086	-0.347	-0.328	-0.304	-0.259
14.0	-.051	-.060	-.018	-.073	-.029	-.058	-.014	-.134	-.031	-.059	-.015	-.137	-.035	-.064	-.015	-.146	-.036	-.068	-.013	-.155
43.0	-.026	-.030	-.035	-.046	-.033	-.051	-.052	-.068	-.036	-.051	-.053	-.068	-.036	-.051	-.052	-.068	-.033	-.024	-.183	-.087

TABLE III - EXTERNAL AND INTERNAL PRESSURE COEFFICIENTS OF NACA 8-INCH RAM-JET CONFIGURATION FOR FOUR ANGLES OF ATTACK - Continued

(c) Free-stream Mach number of 1.79 with model rotated 180°.

NACA

Station	$\alpha = 0°$; $m_3/m_0 = 0.915$				$\alpha = 0°$; $m_3/m_0 = 0.870$				$\alpha = 0°$; $m_3/m_0 = 0.800$				$\alpha = 0°$; $m_3/m_0 = 0.651$				$\alpha = 0°$; $m_3/m_0 = 0.401$			
	Longitudinal distribution of C_p.																			
	Outer shell			Center body	Outer shell			Center body	Outer shell			Center body	Outer shell			Center body	Outer shell			Center body
	External		Internal		External		Internal		External		Internal		External		Internal		External		Internal	
θ →	0°	90°	180°	180°	0°	90°	180°	180°	0°	90°	180°	180°	0°	90°	180°	180°	0°	90°	180°	180°
-1.5				0.489				0.490				0.490				0.492				1.262
-1.0				.540				.540				.541				1.156				1.330
-0.5				.535				.536				1.067				1.282				1.397
0				.636				1.082				1.227				1.323				1.464
0.5	0.271		1.052	1.057	0.215		1.172	1.126	0.121		1.304	1.227	-0.027		1.452	1.356	-0.251		1.606	1.524
1.0	.180	0.200	1.033	.980	.156	0.176	1.163	1.096	.108	0.126	1.299	1.235	.023	0.030	1.443	1.387	-.120	-0.119	1.605	1.561
1.5	.118	.141	1.023	.947	.105	.125	1.160	1.086	.073	.097	1.300	1.243	.021	.036	1.444	1.402	-.085	-.075	1.591	1.575
2.0	.090	.102	1.027	.924	.078	.091	1.164	1.074	.057	.070	1.302	1.236	.016	.027	1.446	1.401	-.064	-.057	1.591	1.576
2.5	.044	.075	1.045	.964	.033	.064	1.175	1.106	.017	.049	1.308	1.259	-.011	.016	1.500	1.418	-.069	-.046	1.592	1.583
3.0	.054	.059	1.023	.976	.047	.051	1.160	1.116	.032	.050	1.299	1.268	.004	.010	1.443	1.424	-.046	-.040	1.591	1.586
4.0	.002	.003	1.004	.955	-.004	-.003	1.151	1.113	-.015	-.011	1.295	1.270	-.033	-.027	1.443	1.428	-.065	-.061	1.591	1.586
5.0	-.015	-.009	.932	.930	-.021	-.015	1.118	1.111	-.030	-.021	1.277	1.276	-.041	-.034	1.435	1.434	-.066	-.059	1.588	1.589
6.0	-.015	-.015	.782	.787	-.019	-.020	1.089	1.084	-.026	-.024	1.263	1.262	-.038	-.034	1.428	1.428	-.058	-.054	1.585	1.588
7.0		-.009	.674	.677		-.015	1.096	1.096		-.017	1.267	1.268		-.027	1.429	1.431		-.042	1.586	1.589
8.0	-.011	-.012	.868	.878	-.021	-.015	1.127	1.126	-.023	-.019	1.284	1.285	-.031	-.027	1.440	1.441	-.044	-.040	1.591	1.591
9.0	.005	-.007	.860	.870	.008	-.010	1.114	1.121	.004	-.014	1.277	1.285	.001	-.020	1.438	1.443	-.009	-.032	1.589	1.592
10.0		-.003		.785		-.006		1.113		-.009		1.282		-.015		1.444		-.025		1.593
11.0	-.003	-.004		.598	-.006	-.008		1.140	-.010	-.010		1.297	-.016	-.015		1.452	-.026	-.025		1.596
12.0	-.003	-.002		.434	-.004	-.005		1.169	-.010	-.006		1.325	-.015	-.012		1.468	-.023	-.020		1.601
14.0	-.003	.003		.797	-.004	0		1.281	-.008	0		1.383	-.014	-.007		1.500	-.021	-.013		1.611
16.0	-.001	.003		1.013	-.002	0		1.351	-.005	0		1.431	-.009	-.005		1.527	-.016	-.012		1.621
18.0	.005	.003		1.130	.003	.002		1.406	.002	.001		1.468	-.002	-.003		1.549	-.007	-.009		1.628
21.0	.021	.003		1.263	.006	0		1.484	.004	0		1.521	.002	-.003		1.568	-.003	-.008		1.640
24.0	.012	.017		1.366	.010	.004		1.547	.008	.004		1.568	.006	.002		1.608	.002	-.003		1.651
27.0	.005	.006		1.432	.004	.004		1.590	.003	.005		1.601	.001	.003		1.631	-.002	-.001		1.664
31.0	.006	.029		1.477	.005	.029		1.622	.006	.013		1.622	.005	.010		1.643	.002	.009		1.670
35.0	.016	-.001			-.017	-.002			-.015	-.001			-.015	.001			-.018	-.018		
37.0				1.511				1.658				1.654				1.662				
40.0	-.009	-.009			-.009	-.009			-.009	-.011			-.008	-.007			-.010	-.010		
45.0	-.012	-.006			-.012	-.007			-.011	-.009			-.012	-.007			-.013	-.010		

Station	Circumferential distribution of C_p.																			
	Outer shell, external				Outer shell, external				Outer shell, external				Outer shell, external				Outer shell, external			
θ →	18°	36°	54°	72°	18°	36°	54°	72°	18°	36°	54°	72°	18°	36°	54°	72°	18°	36°	54°	72°
0.5	0.275	0.283	0.286	0.278	0.218	0.224	0.226	0.221	0.127	0.129	0.129	0.122	-0.026	-0.023	-0.021	-0.024	-0.249	-0.243	-0.240	-0.241
14.0	-.003	-.005	-.006	.005	-.006	-.006	-.009	.002	-.008	-.008	-.010	0	-.014	-.015	-.018	-.006	-.022	-.022	-.024	-.013
43.0	-.011	-.009	-.012	-.012	-.012	-.010	-.012	-.013	-.010	-.010	-.011	-.012	-.010	-.010	-.012	-.012	-.013	-.012	-.013	-.015

TABLE III - EXTERNAL AND INTERNAL PRESSURE COEFFICIENTS OF NACA 8-INCH RAM-JET CONFIGURATION FOR FOUR ANGLES OF ATTACK - Continued

(c) Continued. - Free-stream Mach number of 1.79 with model rotated 180°.

Station	$\alpha = 3°$; $m_3/m_0 = 0.914$				$\alpha = 3°$; $m_3/m_0 = 0.869$				$\alpha = 3°$; $m_3/m_0 = 0.793$				$\alpha = 3°$; $m_3/m_0 = 0.527$				$\alpha = 3°$; $m_3/m_0 = 0.384$			
	Longitudinal distribution of C_p																			
	Outer shell			Center body	Outer shell			Center body	Outer shell			Center body	Outer shell			Center body	Outer shell			Center body
	External		Internal		External		Internal		External		Internal		External		Internal		External		Internal	
θ →	0°	90°	180°	180°	0°	90°	180°	180°	0°	90°	180°	180°	0°	90°	180°	180°	0°	90°	180°	180°
-1.5				0.421				0.422				0.417				0.892				1.282
-1.0				.466				.467				.464				1.262				1.316
-0.5				.458				.460				1.024				1.326				1.393
0				.849				1.091				1.242				1.393				1.469
0.5	0.403		1.163	1.108	0.360		1.279	1.193	0.276		1.369	1.266	0.006		1.556	1.450	-0.121		1.625	1.531
1.0	.276	0.195	1.116	1.068	.256	0.173	1.241	1.175	.222	0.127	1.344	1.275	.073	-0.010	1.536	1.487	-.018	-0.114	1.608	1.570
1.5	.202	.141	1.086	1.022	.189	.125	1.225	1.158	.170	.097	1.332	1.275	.072	-.011	1.531	1.500	.010	-.071	1.603	1.583
2.0	.165	.104	1.073	.977	.154	.092	1.216	1.134	.135	.072	1.327	1.262	.066	-.005	1.528	1.497	.022	-.054	1.600	1.582
2.5	.107	.076	1.080	1.002	.098	.065	1.217	1.153	.084	.050	1.325	1.278	.036	-.010	1.528	1.506	.003	-.045	1.600	1.587
3.0	.117	.060	1.051	1.004	.108	.052	1.196	1.155	.095	.038	1.312	1.281	.051	-.010	1.523	1.509	.024	-.039	1.597	1.590
4.0	.054	.007	1.024	.979	.048	-.002	1.179	1.143	.037	-.011	1.300	1.275	.007	-.041	1.506	1.508	-.010	-.059	1.594	1.588
5.0	.029	-.010	.947	.942	.026	-.016	1.141	1.136	.016	-.023	1.276	1.274	-.007	-.047	1.511	1.511	-.021	-.059	1.590	1.588
6.0	.022	-.015	.789	.797	.019	-.020	1.105	1.102	.011	-.026	1.254	1.254	-.009	-.045	1.504	1.503	-.019	-.056	1.586	1.585
7.0		-.010	.683	.676		-.016	1.104	1.105		-.021	1.251	1.253		-.039	1.501	1.503		-.047	1.583	1.583
8.0	.018	-.015	.881	.885	.015	-.020	1.126	1.125	.009	-.024	1.258	1.259	-.006	-.039	1.503	1.504	-.014	-.045	1.583	1.582
9.0	.035	-.010	.872	.881	.039	-.015	1.093	1.102	.034	-.019	1.236	1.245	.026	-.032	1.494	1.500	.021	-.039	1.580	1.580
10.0		-.010		.790		-.014		1.075		-.016		1.231		-.028		1.496		-.035		1.578
11.0	.022	-.010		.608	.019	-.015		1.100	.014	-.018		1.244	.002	-.028		1.499	-.003	-.034		1.574
12.0	.020	-.008		.441	.018	-.011		1.157	.012	-.015		1.276		.025		1.509	-.003	-.029		1.579
14.0	.017	-.003		.754	.014	-.007		1.261	.009	-.011		1.346	.001	-.019		1.534	-.003	-.022		1.593
16.0	.012	-.006		1.006	.010	-.008		1.332	.005	-.011		1.403	-.002	-.019		1.556	-.006	-.022		1.605
18.0	.016	-.003		1.129	.014	-.007		1.397	.011	-.009		1.447	.004	-.016		1.575	.001	-.019		1.615
21.0	.016	-.005		1.264	.015	-.008		1.476	.012	-.009		1.511	.006	-.015		1.602	.003	-.017		1.630
24.0	.020	-.003		1.366	.019	-.004		1.541	.016	-.006		1.560	.011	-.010		1.625	.009	-.012		1.643
27.0	.013	-.001		1.429	.013	-.003		1.584	.009	-.004		1.595	.006	-.009		1.643	.004	-.010		1.652
31.0	.014	.008		1.476	.012	.009		1.615	.010	.003		1.617	.008	.004		1.649	.005	.003		1.655
35.0	-.010	-.002			-.014	-.007			-.014	-.009			-.015	-.010			-.016	-.011		
37.0				1.510				1.650				1.648				1.662				1.662
40.0	-.003	-.011			-.004	-.017			-.004	-.019			-.007	-.019			-.009	-.020		
45.0	-.006	-.008			-.009	-.015			-.009	-.016			-.011	-.016			-.012	-.017		

Station	Circumferential distribution of C_p																			
	Outer shell, external				Outer shell, external				Outer shell, external				Outer shell, external				Outer shell, external			
θ →	18°	36°	54°	72°	18°	36°	54°	72°	18°	36°	54°	72°	18°	36°	54°	72°	18°	36°	54°	72°
0.5	0.396	0.391	0.369	0.322	0.357	0.345	0.315	0.264	0.264	0.251	0.219	0.173	-0.001	-0.013	-0.036	-0.072	-0.126	-0.135	-0.155	-0.185
14.0	.015	.009	-.002	.005	.011	.006	-.004	.002	.007	.002	-.009	-.003	-.002	-.007	-.016	-.011	-.006	-.011	-.022	-.016
43.0	-.005	-.008	-.013	-.017	-.007	-.011	-.015	-.020	-.009	-.011	-.016	-.021	-.010	-.012	-.017	-.020	-.011	-.014	-.019	-.022

TABLE III - EXTERNAL AND INTERNAL PRESSURE COEFFICIENTS OF NACA 8-INCH RAM-JET CONFIGURATION FOR FOUR ANGLES OF ATTACK - Continued

(c) Continued. - Free-stream Mach number of 1.79 with model rotated 180°.

Station	$\alpha = 6°$; $m_3/m_0 = 0.911$				$\alpha = 6°$; $m_3/m_0 = 0.869$				$\alpha = 6°$; $m_3/m_0 = 0.785$				$\alpha = 6°$; $m_3/m_0 = 0.534$				$\alpha = 6°$; $m_3/m_0 = 0.388$			
	Longitudinal distribution of C_p																			
	Outer shell			Center body	Outer shell			Center body	Outer shell			Center body	Outer shell			Center body	Outer shell			Center body
	External		Internal		External		Internal		External		Internal		External		Internal		External		Internal	
$\theta \rightarrow$	0°	90°	180°	180°	0°	90°	180°	180°	0°	90°	180°	180°	0°	90°	180°	180°	0°	90°	180°	180°
-1.5				0.351				0.351				0.352				0.823				1.227
-1.0				.394				.393				.712				1.211				1.309
-0.5				.388				.850				.904				1.321				1.396
0				.870				.934				1.142				1.400				1.483
0.5	0.525		1.237	1.074	0.502		1.363	1.202	0.427		1.449	1.331	0.158		1.580	1.464	-0.007		1.648	1.551
1.0	.369	0.201	1.178	1.168	.362	0.176	1.307	1.280	.321	0.118	1.410	1.358	.199	-0.027	1.555	1.503	.100	-0.114	1.628	1.589
1.5	.281	.139	1.143	1.096	.282	.126	1.287	1.241	.247	.091	1.390	1.346	.176	-.003	1.545	1.515	.112	-.071	1.621	1.601
2.0	.239	.102	1.119	1.037	.100	.092	1.268	1.202	.213	.071	1.377	1.326	.157	.001	1.539	1.509	.113	-.049	1.616	1.597
2.5	.172	.072	1.114	1.040	.170	.063	1.260	1.202	.152	.052	1.369	1.327	.112	-.002	1.535	1.515	.080	-.041	1.614	1.602
3.0	.180	.059	1.074	1.033	.175	.050	1.230	1.196	.163	.038	1.352	1.323	.124	-.003	1.528	1.515	.097	-.034	1.610	1.602
4.0	.106	.001	1.037	.992	.101	-.004	1.204	1.170	.094	-.015	1.332	1.309	.066	-.041	1.520	1.510	.049	-.059	1.604	1.598
5.0	.075	-.015	.954	.949	.071	-.021	1.157	1.152	.065	-.029	1.302	1.299	.043	-.049	1.508	1.508	.030	-.061	1.597	1.597
6.0	.065	-.024	.791	.802	.062	-.028	1.110	1.110	.057	-.036	1.272	1.272	.038	-.053	1.495	1.496	.027	-.063	1.592	1.590
7.0		-.022	.682	.674		-.026	1.098	1.103		-.033	1.258	1.259		-.047	1.486	1.489		-.056	1.587	1.587
8.0	.052	-.031	.881	.885	.051	-.033	1.108	1.106	.045	-.038	1.253	1.251	.031	-.053	1.481	1.481	.021	-.061	1.582	1.580
9.0	.068	-.032	.877	.885	.071	-.033	1.042	1.054	.070	-.039	1.206	1.213	.060	-.051	1.463	1.468	.053	-.058	1.573	1.573
10.0		-.032		.794		-.033		.980		-.038		1.177		-.051		1.456		-.056		1.568
11.0	.053	-.036		.610	.051	-.038		1.009	.048	-.041		1.189	.035	-.051		1.457	.028	-.058		1.563
12.0	.048	-.036		.442	.046	-.038		1.088	.044	-.041		1.230	.033	-.051		1.471	.026	-.056		1.568
14.0	.043	-.034		.684	.039	-.036		1.216	.038	-.041		1.315	.028	-.049		1.503	.023	-.054		1.585
16.0	.035	-.037		.991	.033	-.039		1.305	.031	-.042		1.382	.023	-.051		1.533	.081	-.055		1.599
18.0	.035	-.037		1.121	.033	-.039		1.372	.032	-.041		1.434	.024	-.047		1.556	.021	-.051		1.612
21.0	.033	-.037		1.259	.031	-.038		1.460	.030	-.041		1.506	.023	-.045		1.592	.019	-.047		1.631
24.0	.034	-.032		1.358	.032	-.033		1.529	.032	-.034		1.562	.026	-.037		1.621	.023	-.039		1.645
27.0	.027	-.031		1.422	.025	-.031		1.570	.026	-.032		1.594	.021	-.034		1.638	.018	-.036		1.656
31.0	.025	-.016		1.468	.026	-.017		1.600	.023	-.017		1.613	.020	-.020		1.644	.018	-.019		1.658
35.0	-.003	-.029			-.002	-.032			-.003	-.032			-.005	-.031			-.007	-.031		
37.0				1.503				1.637				1.642				1.658				1.665
40.0	.006	-.042			.006	-.042			.005	-.044			.003	-.045			.003	-.042		
45.0	0	-.040			.001	-.039			0	-.038			-.002	-.040			-.003	-.038		
	Circumferential distribution of C_p																			
Station	Outer shell, external				Outer shell, external				Outer shell, external				Outer shell, external				Outer shell, external			
$\theta \rightarrow$	18°	36°	54°	72°	18°	36°	54°	72°	18°	36°	54°	72°	18°	36°	54°	72°	18°	36°	54°	72°
0.5	0.516	0.497	0.448	0.373	0.485	0.466	0.420	0.319	0.416	0.378	0.306	0.210	0.140	0.102	0.045	-0.032	-0.021	-0.051	-0.096	-0.164
14.0	.036	.021	-.018	-.014	.034	.019	-.006	-.015	.032	.016	-.009	-.017	.023	.008	-.018	-.027	.016	.001	-.024	-.033
43.0	0	-.014	-.028	-.042	.001	-.013	-.028	-.043	0	-.014	-.029	-.044	-.003	-.015	-.031	-.045	-.003	-.016	-.030	-.044

TABLE III - EXTERNAL AND INTERNAL PRESSURE COEFFICIENTS OF NACA 8-INCH RAM-JET CONFIGURATION FOR FOUR ANGLES OF ATTACK - Continued

(c) Concluded. - Free-stream Mach number of 1.79 with model rotated 180°.

NACA

Station	$\alpha = 10°$; $m_3/m_0 = 0.867$				$\alpha = 10°$; $m_3/m_0 = 0.782$				$\alpha = 10°$; $m_3/m_0 = 0.644$				$\alpha = 10°$; $m_3/m_0 = 0.510$				$\alpha = 10°$; $m_3/m_0 = 0.371$			
	Longitudinal distribution of C_p																			
	Outer shell			Center body	Outer shell			Center body	Outer shell			Center body	Outer shell			Center body	Outer shell			Center body
	External		Internal		External		Internal		External		Internal		External		Internal		External		Internal	
θ →	0°	90°	180°	180°	0°	90°	180°	180°	0°	90°	180°	180°	0°	90°	180°	180°	0°	90°	180°	180°
-1.5				0.268				0.460				0.843				0.915				1.089
-1.0				.314				.787				.910				1.042				1.285
-0.5				.616				.846				.980				1.193				1.382
0				.747				.928				1.067				1.315				1.481
0.5	0.670		1.226	.865	0.645		1.277	1.039	0.577		1.424	1.169	0.442		1.482	1.409	0.203		1.662	1.557
1.0	.484	0.215	1.152	1.122	.475	0.184	1.265	1.194	.444	0.084	1.456	1.286	.389	-0.002	1.490	1.474	.284	-0.101	1.654	1.599
1.5	.382	.151	1.121	1.137	.379	.136	1.324	1.310	.358	.090	1.371	1.368	.320	.022	1.504	1.507	.260	-.055	1.632	1.613
2.0	.333	.112	1.091	1.038	.331	.096	1.351	1.342	.307	.075	1.396	1.404	.276	.029	1.514	1.516	.235	-.029	1.624	1.610
2.5	.256	.082	1.081	1.012	.254	.064	1.359	1.342	.237	.049	1.409	1.414	.215	.020	1.520	1.516	.184	-.021	1.619	1.608
3.0	.262	.060	1.037	.998	.264	.045	1.335	1.344	.245	.031	1.409	1.416	.223	.012	1.519	1.517	.198	-.020	1.611	1.606
4.0	.178	-.003	1.007	.962	.182	-.012	1.310	1.297	.170	-.023	1.409	1.407	.153	-.036	1.517	1.514	.134	-.054	1.602	1.596
5.0	.142	-.026	.932	.928	.144	-.034	1.264	1.266	.133	-.042	1.396	1.400	.120	-.053	1.509	1.511	.105	-.067	1.590	1.590
6.0	.128	-.039	.772	.783	.128	-.046	1.221	1.226	.120	-.052	1.384	1.389	.109	-.063	1.499	1.504	.096	-.074	1.578	1.578
7.0		-.044	.658	.652		-.051	1.197	1.202		-.056	1.385	1.389		-.064	1.500	1.503		-.074	1.568	1.568
8.0	.108	-.056	.829	.840	.108	-.061	1.181	1.179	.102	-.067	1.393	1.395	.092	-.075	1.503	1.504	.082	-.083	1.559	1.556
9.0	.116	-.063	.865	.875	.125	-.069	1.096	1.107	.120	-.073	1.389	1.397	.114	-.081	1.499	1.504	.107	-.089	1.539	1.540
10.0		-.069		.784		-.074		1.024		-.079		1.400		-.085		1.506		-.093		1.529
11.0	.104	-.077		.599	.103	-.081		1.039	.099	-.085		1.410	.092	-.092		1.509	.083	-.098		1.527
12.0	.099	-.083		.432	.100	-.086		1.110	.094	-.091		1.426	.088	-.097		1.519	.080	-.102		1.537
14.0	.091	-.093		.476	.090	-.096		1.228	.086	-.101		1.458	.080	-.106		1.538	.074	-.110		1.559
16.0	.083	-.103		.954	.081	-.106		1.315	.079	-.111		1.486	.074	-.115		1.556	.067	-.120		1.578
18.0	.076	-.112		1.091	.076	-.115		1.382	.073	-.119		1.510	.068	-.124		1.571	.063	-.127		1.594
21.0	.073	-.120		1.226	.072	-.124		1.470	.069	-.129		1.544	.065	-.135		1.593	.062	-.137		1.618
24.0	.073	-.110		1.324	.072	-.113		1.536	.069	-.120		1.576	.066	-.124		1.615	.063	-.127		1.636
27.0	.063	-.098		1.383	.063	-.100		1.573	.060	-.103		1.599	.057	-.105		1.629	.056	-.103		1.646
31.0	.057	-.070		1.426	.055	-.070		1.593	.054	-.072		1.615	.052	-.073		1.639	.050	-.072		1.648
35.0	.024	-.082			.023	-.082			.022	-.091			.020	-.084			.020	-.083		
37.0				1.467				1.628				1.630				1.648				1.653
40.0	.028	-.099			.026	-.098			.025	-.099			.025	-.101			.023	-.100		
45.0	.023	-.093			.021	-.094			.020	-.094			.020	-.094			.020	-.093		
	Circumferential distribution of C_p																			
Station	Outer shell, external				Outer shell, external				Outer shell, external				Outer shell, external				Outer shell, external			
θ →	18°	36°	54°	72°	18°	36°	54°	72°	18°	36°	54°	72°	18°	36°	54°	72°	18°	36°	54°	72°
0.5	0.652	0.612	0.531	0.424	0.625	0.580	0.501	0.391	0.550	0.516	0.383	0.231	0.402	0.331	0.853	0.046	0.182	0.113	0.019	-0.120
14.0	.079	.045	-.003	-.042	.078	.044	-.004	-.044	.074	.040	-.008	-.047	.068	.035	-.015	-.054	.062	.028	-.021	-.059
43.0	.015	-.015	-.056	-.094	.015	-.017	-.058	-.095	.014	-.018	-.059	-.097	.012	-.019	-.059	-.097	.012	-.019	-.059	-.097

TABLE III - EXTERNAL AND INTERNAL PRESSURE COEFFICIENTS OF NACA 8-INCH RAM-JET CONFIGURATION FOR FOUR ANGLES OF ATTACK - Continued

(d) Free-stream Mach number of 1.99.

NACA

Station	$\alpha = 0°$; $m_3/m_0 = 1.00$				$\alpha = 0°$; $m_3/m_0 = 0.966$				$\alpha = 0°$; $m_3/m_0 = 0.885$				$\alpha = 0°$; $m_3/m_0 = 0.773$				$\alpha = 0°$; $m_3/m_0 = 0.559$			
	Longitudinal distribution of C_p.																			
	Outer shell			Center body	Outer shell			Center body	Outer shell			Center body	Outer shell			Center body	Outer shell			Center body
	External		Internal		External		Internal		External		Internal		External		Internal		External		Internal	
θ →	180°	270°	0°	0°	180°	270°	0°	0°	180°	270°	0°	0°	180°	180°	0°	0°	180°	180°	0°	0°
-1.5				0.448				0.444				0.444				0.444				
-1.0				.486				.480				.482				.499				1.194
-.5				.483				.480				.511				1.098				1.427
0				.461				.533				1.175				1.380				1.460
.5	0.293	0.281	0.577	.353	0.269	0.255	1.146	1.206	0.206	0.190	1.327	1.296	0.107	0.088	1.445	1.365		-0.086	1.591	1.498
1.0	.186	.189	.608	.399	.172	.173	1.156	1.146	.148	.145	1.325	1.257	.102	.098	1.441	1.376	-0.007	-.012	1.581	1.535
1.5	.133	.132	.523	.457	.121	.119	1.156	1.124	.104	.102	1.327	1.264	.078	.078	1.443	1.394	.006	.003	1.581	1.554
2.0	.099	.098	.551	.550	.094	.088	1.163	1.099	.079	.074	1.330	1.247	.061	.057	1.445	1.383	.013	.006	1.582	1.552
2.5	.073	.072	.668	.428	.068	.062	1.180	1.144	.056	.051	1.337	1.282	.043	.038	1.450	1.411	.006	.001	1.583	1.568
3.0	.065	.054	.589	.458	.053	.044	1.175	1.159	.043	.035	1.330	1.293	.035	.020	1.445	1.420	.005	-.009	1.586	1.575
4.0	.014	.011	.600	.511	.009	.003	1.170	1.173	0	-.003	1.327	1.306	-.005	-.011	1.445	1.433	-.024	-.031	1.587	1.583
5.0	.002	-.005	.543	.615	-.006	-.009	1.154	1.168	-.013	-.014	1.312	1.310	-.018	-.021	1.438	1.438	-.034	-.036	1.587	1.588
6.0	0	-.008	.620	.538	-.010	-.009	1.134	1.141	-.016	-.013	1.298	1.294	-.019	-.020	1.431	1.430	-.032	-.033	1.587	1.587
7.0	0	-.001	.633	.573	-.005	-.007	1.150	1.159	-.010	-.012	1.306	1.306	-.014	-.018	1.436	1.438	-.026	-.030	1.592	1.593
8.0	-.004	-.003	.505	.489	-.010	-.009	1.185	1.201	-.015	-.014	1.327	1.330	-.019	-.020	1.450	1.452	-.029	-.030	1.600	1.600
9.0	-.003	-.008	.533	.478	-.008	-.012	1.182	1.199	-.013	-.017	1.325	1.332	-.017	-.021	1.452	1.457	-.026	-.030	1.602	1.604
10.0	0	.002		.754	-.005	-.004		1.185	-.010	-.008		1.330	-.013	-.013		1.460	-.022	-.021		1.607
11.0	.003	-.001		.670	-.001	-.004		1.218	-.005	-.008		1.348	-.010	-.013		1.470	-.019	-.021		1.612
12.0	.003	0		.991	0	-.004		1.269	-.003	-.008		1.378	-.009	-.011		1.490	-.017	-.019		1.622
14.0	.005	-.001		1.163	.003	0		1.361	0	-.004		1.444	-.005	-.008		1.530	-.012	-.013		1.639
16.0	.005	.001		1.282	.003	-.002		1.431	0	-.004		1.494	-.004	-.008		1.564	-.011	-.013		1.657
18.0	.008	.003		1.374	.007	.001		1.487	.005	-.002		1.537	.001	-.005		1.593	-.004	-.011		1.672
21.0	.013	.005		1.492	.011	.003		1.566	.008	.003		1.598	.006	-.001		1.636	.001	-.006		1.696
24.0	.019	.016		1.585	.016	.013		1.630	.013	.011		1.652	.011	.008		1.676	.005	.003		1.716
27.0	-.009	.003		1.651	-.010	.001		1.678	-.011	0		1.692	.014	-.002		1.706	-.018	-.006		1.730
31.0	.003	-.006		1.696	.001	-.008		1.707	.001	-.008		1.714	-.001	-.008		1.772	-.004	-.008		1.738
35.0	-.020	-.018			-.021	-.020			-.022	-.020			-.023	-.022			-.024	-.023		
37.0				1.731				1.748				1.748				1.744				1.745
40.0	-.013	-.013			-.014	-.015			-.014	-.015			-.016	-.015			-.017	-.015		
45.0	-.008	-.011			-.009	-.012			-.009	-.013			-.011	-.013			-.012	-.014		

Station	Circumferential distribution of C_p.																			
	Outer shell, external				Outer shell, external				Outer shell, external				Outer shell, external				Outer shell, external			
θ →	198°	216°	234°	252°	198°	216°	234°	252°	198°	216°	234°	252°	198°	216°	234°	252°	198°	216°	234°	252°
0.5					0.269	0.273	0.271	0.262	0.206	0.206	0.204	0.198	0.102	0.100	0.099	0.093				
14.0	0.003	0.001	0	0.005	.003	-.003	-.001	.002	-.003	-.006	-.011	-.003	-.008	-.009	-.003	-.007	-0.014	-0.017	-0.007	-0.013
43.0	-.011	-.008	-.011	-.013	-.012	-.011	-.012	-.013	-.013	-.011	-.013	-.014	-.013	-.013	-.013	-.015	-.016	-.013	-.016	-.016

TABLE III - EXTERNAL AND INTERNAL PRESSURE COEFFICIENTS OF NACA 8-INCH RAM-JET CONFIGURATION FOR FOUR ANGLES OF ATTACK - Continued

(d) Continued. - Free-stream Mach number of 1.99.



Station	$\alpha = 0°$; $m_3/m_0 = 0.376$				$\alpha = 0°$; $m_3/m_0 = 0.992$				$\alpha = 3°$; $m_3/m_0 = 0.999$				$\alpha = 3°$; $m_3/m_0 = 0.934$				$\alpha = 3°$; $m_3/m_0 = 0.861$			
	Longitudinal distribution of C_p																			
	Outer shell			Center body	Outer shell			Center body	Outer shell			Center body	Outer shell			Center body	Outer shell			Center body
	External		Internal		External		Internal		External		Internal		External		Internal		External		Internal	
$\theta \rightarrow$	180°	270°	0°	0°	180°	270°	0°	0°	180°	270°	0°	0°	180°	270°	0°	0°	180°	270°	0°	0°
-1.5				1.209				0.440				0.521				0.520				0.521
-1.0				1.421				.479				.561				.561				.563
-.5				1.467				.478				.559				.559				.561
0				1.530				.681				.548				.561				1.230
.5	-0.228	-0.233	1.660	1.590	0.251	0.236	1.234	1.269	0.208	0.282	0.537	0.400	0.158	0.253	1.094	1.214	0.084	0.189	1.257	1.252
1.0	-.102	-.113	1.650	1.624	.164	.165	1.238	1.193	.142	.187	.563	.286	.094	.172	1.137	1.097	.062	.150	1.282	1.214
1.5	-.060	-.065	1.648	1.638	.117	.113	1.240	1.188	.071	.131	.487	.411	.055	.119	1.161	1.103	.034	.107	1.297	1.233
2.0	-.038	-.044	1.651	1.636	.100	.083	1.244	1.165	.046	.096	.575	.254	.032	.088	1.175	1.091	.018	.077	1.314	1.228
2.5	-.032	-.038	1.652	1.647	.063	.059	1.254	1.204	.025	.070	.441	.364	.012	.062	1.193	1.145	-.001	.055	1.325	1.272
3.0	-.024	-.039	1.653	1.648	.048	.043	1.248	1.218	.013	.051	.300	.444	.001	.045	1.200	1.173	-.011	.032	1.324	1.290
4.0	-.040	-.048	1.655	1.653	-.001	.002	1.244	1.232	-.025	.009	.487	.277	-.034	.007	1.214	1.197	-.041	-.001	1.330	1.312
5.0	-.047	-.049	1.656	1.657	-.011	-.011	1.229	1.232	-.036	-.008	.355	.493	-.045	-.008	1.202	1.201	-.051	-.012	1.324	1.321
6.0	-.042	-.042	1.657	1.657	-.013	-.010	1.211	1.210	-.037	-.012	.553	.507	-.045	-.010	1.190	1.183	-.049	-.015	1.317	1.315
7.0	-.033	-.037	1.658	1.660	-.008	-.008	1.221	1.225	-.030	-.010	.693	.720	-.037	-.011	1.207	1.206	-.039	-.017	1.330	1.330
8.0	-.037	-.037	1.662	1.662	-.012	-.011	1.251	1.257	-.028	-.014	.704	.704	-.035	-.013	1.245	1.247	-.040	-.019	1.357	1.359
9.0	-.032	.036	1.664	1.665	-.011	-.013	1.244	1.256	-.026	-.015	.863	.864	-.032	-.017	1.252	1.257	-.035	-.022	1.364	1.369
10.0	-.028	.027		1.666	-.008	-.005		1.249	-.021	-.010		.892	-.026	-.010		1.261	-.027	-.014		1.376
11.0	-.024	-.025		1.668	-.001	-.005		1.271	-.012	-.010		.979	-.018	-.011		1.286	-.020	-.014		1.392
12.0	-.022	-.023		1.672	.001	-.003		1.312	-.007	-.011		1.079	-.010	-.012		1.324	-.017	-.017		1.417
14.0	-.017	-.018		1.681	.002	-.001		1.389	-.003	-.012		1.223	-.006	-.011		1.392	-.011	-.012		1.467
16.0	-.014	-.018		1.687	.002	-.003		1.452	-.001	-.003		1.325	-.002	-.008		1.446	-.006	-.012		1.507
18.0	-.008	-.014		1.695	.006	0		1.503	.008	-.003		1.405	.004	-.008		1.491	0	-.010		1.541
21.0	-.001	-.008		1.704	.010	.003		1.573	.021	-.003		1.507	.019	-.005		1.556	.018	-.008		1.592
24.0	-.002	.002		1.713	.015	.013		1.633	.008	.008		1.594	.004	.007		1.613	.003	.004		1.637
27.0	-.020	-.008		1.720	-.011	0		1.678	-.013	-.005		1.655	-.015	-.005		1.661	-.017	-.008		1.675
31.0	-.005	-.012		1.723		-.008		1.705	.002	-.015		1.700	0	-.015		1.692	-.001	-.016		1.699
35.0	-.027	-.027			-.022	-.020			-.022	-.026			-.022	-.027			-.024	-.028		
37.0				1.726				1.743				1.738				1.735				1.733
40.0	-.018	-.015			-.015	-.015			-.012	-.023			-.012	-.023			-.014	-.023		
45.0	-.013	-.015			-.008	-.013			-.008	-.020			-.008	-.020			-.008	-.021		
	Circumferential distribution of C_p																			
Station	Outer shell, external				Outer shell, external				Outer shell, external				Outer shell, external				Outer shell, external			
$\theta \rightarrow$	198°	216°	234°	252°	198°	216°	234°	252°	198°	216°	234°	252°	198°	216°	234°	252°	198°	216°	234°	252°
0.5	-0.226	-0.225	-0.225	-0.229	0.250	0.254	0.250	0.244	0.211	0.225	0.243	0.261	0.162	0.181	0.201	0.225	0.087	0.104	0.127	0.154
14.0	-.018	-.020	-.010	-.017	-.001	-.004	-.001	-.001	-.007	-.011	-.007	-.008	-.010	-.013	-.006	-.012	-.013	-.017	-.005	-.015
43.0	-.017	-.015	-.017	-.017	-.013	-.010	-.013	-.013	-.013	-.013	.029	.035	-.012	-.013	-.017	-.045	-.012	-.014	-.017	-.051

TABLE III - EXTERNAL AND INTERNAL PRESSURE COEFFICIENTS OF NACA 8-INCH RAM-JET CONFIGURATION FOR FOUR ANGLES OF ATTACK - Continued

(d) Continued. - *Free-stream Mach number of 1.99.*

Station	$\alpha = 3^\circ$; $m_3/m_0 = 0.740$				$\alpha = 3^\circ$; $m_3/m_0 = 0.511$				$\alpha = 3^\circ$; $m_3/m_0 = 0.445$				$\alpha = 6^\circ$; $m_3/m_0 = 0.995$				$\alpha = 6^\circ$; $m_3/m_0 = 0.944$			
	Longitudinal distribution of C_p																			
	Outer shell			Center body	Outer shell			Center body	Outer shell			Center body	Outer shell			Center body	Outer shell			Center body
	External		Internal		External		Internal		External		Internal		External		Internal		External		Internal	
$\theta \rightarrow$	180°	270°	0°	0°	180°	270°	0°	0°	180°	270°	0°	0°	180°	270°	0°	0°	180°	270°	0°	0°
-1.5				0.521				0.621				1.031				0.601				0.601
-1.0				.564				1.374				1.410				.645				.646
-.5				1.243				1.416				1.438				.646				.646
0				1.364				1.444				1.235				.632				.634
0.5	-0.019	0.075	1.407	1.340	-0.168	-0.084	1.562	1.479	-0.247	-0.180	1.610	1.535	0.128	0.282	0.441	.494	0.074	0.270	0.792	.657
1.0	.008	.093	1.417	1.355	-.086	-.013	1.559	1.516	-.140	-.069	1.604	1.572	.051	.189	.507	.768	.028	.182	1.001	.922
1.5	0.002	.075	1.429	1.381	-.065	.005	1.565	1.541	-.103	-.038	1.608	1.594	.014	.134	.474	.352	-.003	.133	1.095	1.030
2.0	-.005	.056	1.438	1.377	-.051	.008	1.570	1.541	-.079	-.024	1.612	1.594	-.005	.097	.525	-.006	-.020	.098	1.136	1.046
2.5	-.017	.038	1.448	1.410	-.052	.003	1.577	1.560	-.075	-.021	1.617	1.608	-.022	.069	.386	.301	-.036	.071	1.155	1.118
3.0	-.020	.018	1.446	1.422	-.049	-.009	1.577	1.567	-.068	-.026	1.618	1.614	-.031	.050	.239	.386	-.046	.038	1.160	1.143
4.0	-.049	-.012	1.453	1.441	-.067	-.028	1.584	1.579	-.081	-.041	1.624	1.624	-.062	.005	.413	.226	-.073	.007	1.171	1.169
5.0	-.056	-.022	1.451	1.451	-.070	-.036	1.586	1.589	-.079	-.045	1.628	1.629	-.068	-.014	.792	.683	-.078	-.012	1.175	1.176
6.0	-.054	-.022	1.451	1.450	-.065	-.035	1.584	1.591	-.073	-.041	1.631	1.632	-.062	-.021	.845	.846	-.072	-.019	1.162	1.161
7.0	-.046	-.022	1.460	1.463	-.055	-.032	1.597	1.599	-.060	-.039	1.636	1.637	-.052	-.022	.830	.831	-.059	-.020	1.179	1.183
8.0	-.046	-.024	1.479	1.481	-.052	-.033	1.608	1.608	-.058	-.039	1.643	1.643	-.044	-.026	.950	.950	-.053	-.032	1.214	1.221
9.0	-.039	-.027	1.486	1.491	-.046	-.035	1.613	1.616	-.050	-.041	1.647	1.650	-.038	-.031	.999	1.005	-.042	-.031	1.218	1.228
10.0	-.032	-.019		1.498	-.038	-.026		1.621	-.043	-.031		1.653	-.029	-.029		1.031	-.032	-.027		1.228
11.0	-.025	-.019		1.510	-.031	-.027		1.627	-.036	-.031		1.657	-.022	-.033		1.085	-.022	-.031		1.256
12.0	-.022	-.020		1.525	-.027	-.027		1.633	-.031	-.031		1.662	-.017	-.031		1.152	-.017	-.032		1.297
14.0	-.015	-.017		1.556	-.019	-.023		1.647	-.024	-.027		1.671	-.004	-.033		1.264	-.006	-.036		1.374
16.0	-.010	-.017		1.583	-.014	-.022		1.661	-.017	-.026		1.680	-.005	-.036		1.348	-.001	-.038		1.436
18.0	-.003	-.012		1.604	-.007	-.018		1.671	-.010	-.022		1.686	.010	-.037		1.412	-.005	-.038		1.486
21.0	-.015	-.010		1.639	.011	-.014		1.690	.007	-.017		1.696	.020	-.034		1.498	.016	-.036		1.555
24.0	0	.002		1.671	-.004	-.003		1.707	-.007	-.006		1.708	.002	-.023		1.576	-.003	-.024		1.615
27.0	-.019	-.009		1.698	-.022	-.013		1.719	-.025	-.017		1.715	-.015	-.029		1.632	-.016	-.030		1.661
31.0	-.003	-.017		1.714	-.004	-.018		1.728	-.007	-.022		1.720	.003	-.041		1.671	0	-.041		1.695
35.0	-.025	-.030			-.027	-.031			-.029	-.034			-.024	-.051			-.024	-.052		
37.0				1.735				1.733				1.723				1.707				1.736
40.0	-.014	-.023			-.014	-.023			-.017	-.026			-.010	-.048			-.011	-.049		
45.0	-.009	-.020			-.011	-.021			-.012	-.024			-.007	-.046			-.007	-.045		

Station	Circumferential distribution of C_p																			
	Outer shell, external				Outer shell, external				Outer shell, external				Outer shell, external				Outer shell, external			
$\theta \rightarrow$	198°	216°	234°	252°	198°	216°	234°	252°	198°	216°	234°	252°	198°	216°	234°	252°	198°	216°	234°	252°
0.5	-0.015	-0.001	0.021	0.041	-0.163	-0.147	-0.127	-0.109	-0.243	-0.238	-0.224	-0.202	0.184	0.101	0.155	0.208	0.135	0.161	0.193	0.233
14.0	-.017	-.022	-.005	-.019	-.023	-.027	-.004	-.025	-.026	-.031	-.005	-.029	-.013	-.026	-.003	-.040	-.012	-.024	-.053	-.038
43.0	-.013	-.014	-.019	-.041	-.014	-.016	-.019	-.017	-.017	-.017	-.022	-.007	-.015	-.020	-.026	-.009	-.014	-.021	-.026	-.010

TABLE III - EXTERNAL AND INTERNAL PRESSURE COEFFICIENTS OF NACA 8-INCH RAM-JET CONFIGURATION FOR FOUR ANGLES OF ATTACK - Concluded

(d) Concluded. - Free-stream Mach number of 1.99.



Station	$\alpha = 6^\circ$; $m_3/m_0 = 0.733$				$\alpha = 6^\circ$; $m_3/m_0 = 0.374$				$\alpha = 10^\circ$; $m_3/m_0 = 0.956$				$\alpha = 10^\circ$; $m_3/m_0 = 0.902$				$\alpha = 10^\circ$; $m_3/m_0 = 0.710$			
	Longitudinal distribution of C_p																			
	Outer shell			Center body	Outer shell			Center body	Outer shell			Center body	Outer shell			Center body	Outer shell			Center body
	External		Internal		External		Internal		External		Internal		External		Internal		External		Internal	
$\theta \rightarrow$	180°	270°	0°	0°	180°	270°	0°	0°	180°	270°	0°	0°	180°	270°	0°	0°	180°	270°	0°	0°
-1.5				0.605				0.996				0.728				0.720				0.781
-1.0				.675				1.318				.791				.785				.875
-.5				1.075				1.370				.785				.785				.937
0				1.297				1.416				.745				.746				1.053
.5	-0.084	0.100	1.295	1.264	-0.251	-0.125	1.531	1.470	-0.001	0.291	0.326	0.594	-0.053	0.298	0.414	0.771	-0.142	0.135	0.946	1.055
1.0	-.068	.106	1.333	1.272	-.212	-.050	1.532	1.494	-.044	.201	.436	.713	-.062	.213	.692	.647	-.154	.130	1.046	.981
1.5	-.070	.083	1.361	1.307	-.187	-.026	1.541	1.520	-.072	.142	.533	.264	-.080	.155	.893	.580	-.162	.110	1.122	1.055
2.0	-.069	.064	1.379	1.312	-.157	-.014	1.550	1.522	-.082	.104	.768	.578	-.086	.116	1.008	.865	-.157	.098	1.175	1.091
2.5	-.075	.045	1.395	1.356	-.150	-.012	1.556	1.542	-.096	.072	.754	.568	-.098	.082	1.084	1.050	-.162	.065	1.210	1.161
3.0	-.076	.024	1.398	1.375	-.137	-.019	1.554	1.551	-.099	.051	.737	.624	-.100	.058	1.133	1.115	-.158	.041	1.224	1.197
4.0	-.095	-.009	1.413	1.402	-.135	-.036	1.564	1.563	-.110	.002	.918	.856	-.116	.007	1.172	1.154	-.162	-.002	1.250	1.238
5.0	-.095	-.022	1.413	1.417	-.123	-.045	1.559	1.566	-.104	-.018	1.008	1.007	-.110	-.016	1.175	1.173	-.151	-.020	1.247	1.254
6.0	-.084	-.026	1.416	1.417	-.108	-.045	1.554	1.563	-.090	-.026	1.024	1.024	-.092	-.025	1.181	1.175	-.127	-.030	1.237	1.245
7.0	-.069	-.029	1.432	1.433	-.088	-.045	1.560	1.564	-.076	-.035	1.050	1.053	-.068	-.035	1.208	1.207	-.094	-.039	1.249	1.251
8.0	-.061	-.034	1.452	1.456	-.075	-.050	1.554	1.560	-.053	-.049	1.100	1.100	-.055	-.047	1.253	1.255	-.072	-.052	1.254	1.266
9.0	-.051	-.039	1.461	1.469	-.061	-.055	1.546	1.552	-.034	-.058	1.122	1.129	-.041	-.057	1.282	1.288	-.055	-.061	1.224	1.245
10.0	-.041	-.034		1.478	-.051	-.050		1.546	-.025	-.056		1.149	-.030	-.058		1.312	-.041	-.061		1.204
11.0	-.032	-.038		1.490	-.040	-.052		1.550	-.015	-.063		1.177	-.021	-.063		1.339	-.029	-.069		1.183
12.0	-.026	-.040		1.505	-.034	-.055		1.557	-.010	-.071		1.212	-.015	-.071		1.367	-.021	-.076		1.210
14.0	-.017	-.044		1.535	-.022	-.055		1.576	.003	-.080		1.282	-.003	-.080		1.424	-.010	-.085		1.295
16.0	-.010	-.044		1.562	-.015	-.053		1.592	.007	-.090		1.339	.009	-.090		1.471	.008	-.095		1.359
18.0	-.003	-.043		1.583	-.007	-.050		1.604	.014	-.097		1.385	.016	-.099		1.508	.007	-.102		1.405
21.0	.007	-.039		1.614	-.001	-.045		1.625	.004	-.106		1.449	.002	-.106		1.561	-.006	-.112		1.464
24.0	-.007	-.026		1.644	-.013	-.017		1.647	-.005	-.111		1.514	-.006	-.111		1.611	-.011	-.116		1.513
27.0	-.020	-.034		1.669	-.018	-.026		1.658	-.001	-.104		1.559	.004	-.104		1.647	0	-.118		1.545
31.0	-.003	-.044		1.686	-.005	-.046		1.662	.007	-.107		1.583	.008	-.107		1.669	.003	-.118		1.560
35.0	-.026	-.054			-.028	-.056			-.020	-.125			-.020	-.123			-.024	-.129		
37.0				1.710				1.667				1.605				1.692				1.581
40.0	-.010	-.049			-.012	-.050			-.002	-.109			-.002	-.097			-.005	-.101		
45.0	-.009	-.045			-.012	-.046			-.003	-.106			.006	-.093			-.010	-.096		

Station	Circumferential distribution of C_p																			
	Outer shell, external				Outer shell, external				Outer shell, external				Outer shell, external				Outer shell, external			
$\theta \rightarrow$	198°	216°	234°	252°	198°	216°	234°	252°	198°	216°	234°	252°	198°	216°	234°	252°	198°	216°	234°	252°
0.5	-0.078	-0.052	-0.016	0.033	-0.248	-0.231	-0.207	-0.173	0.013	0.064	0.129	0.207	-0.042	-0.007	0.067	0.172	-0.137	-0.107	-0.058	0.018
14.0	-.022	-.034	-.003	-.047	-.029	-.040	-.003	-.058	-.012	-.045	-.006	-.105	-.019	-.045	-.005	.019	-.025	-.053	-.007	-.113
43.0	-.017	-.022	-.026	.009	-.017	-.023	-.028	.007	-.025	-.049	-.046	.007	-.028	-.049	-.046	.007	-.031	-.050	-.048	.004

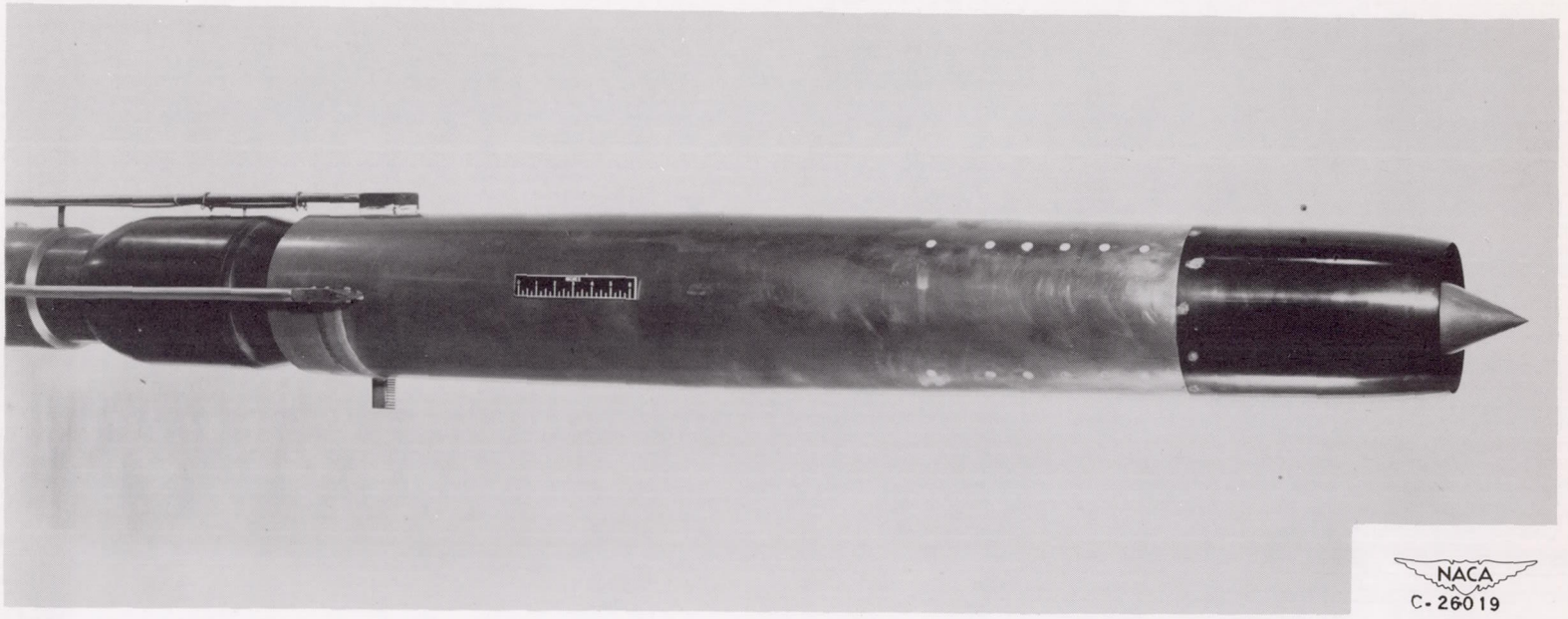
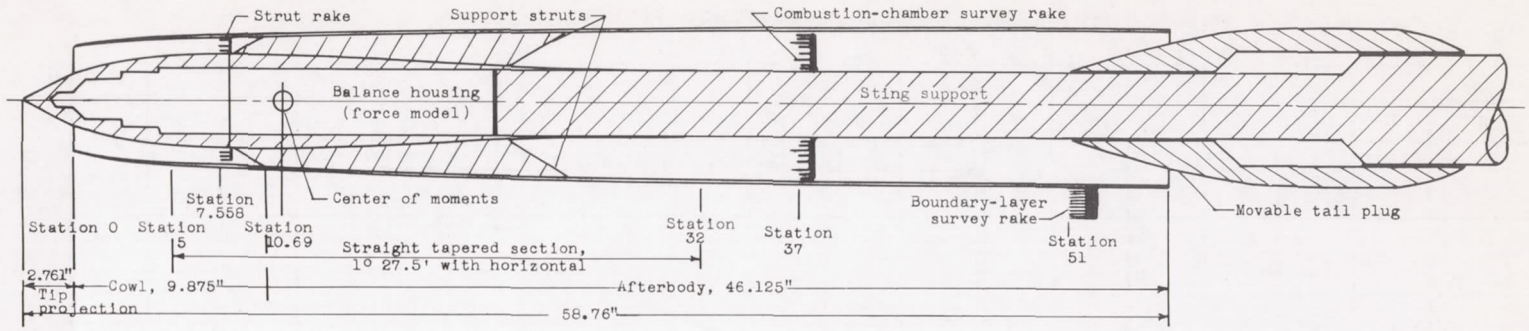
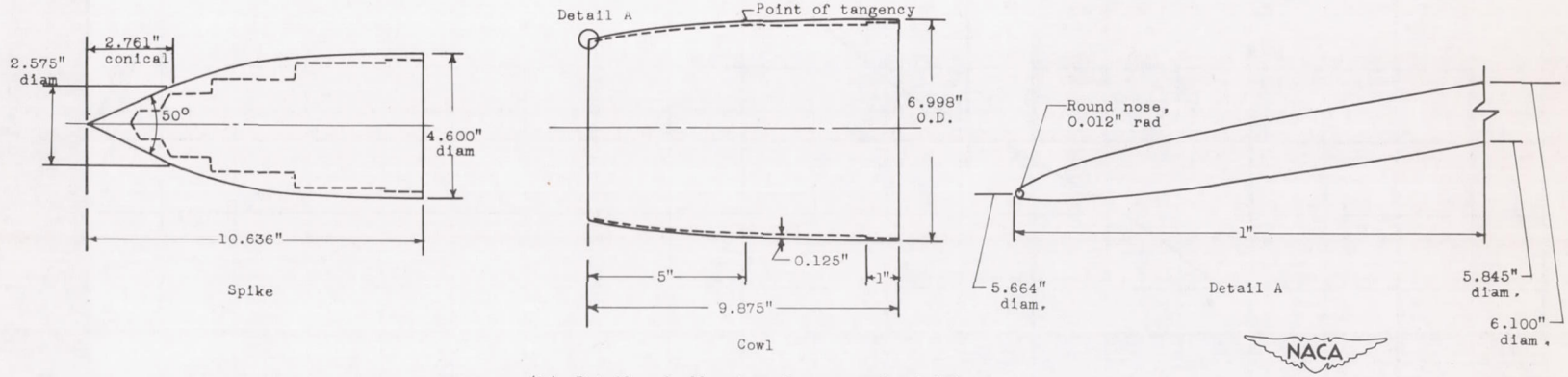


Figure 1. - Pressure model of NACA 8-inch ram-jet configuration.



(a) NACA 8-inch ram-jet configuration.



(b) Details of all-external compression inlet.

Figure 2. - Schematic diagram of NACA 8-inch ram-jet configuration showing principal dimensions of model and details of all-external compression inlet.

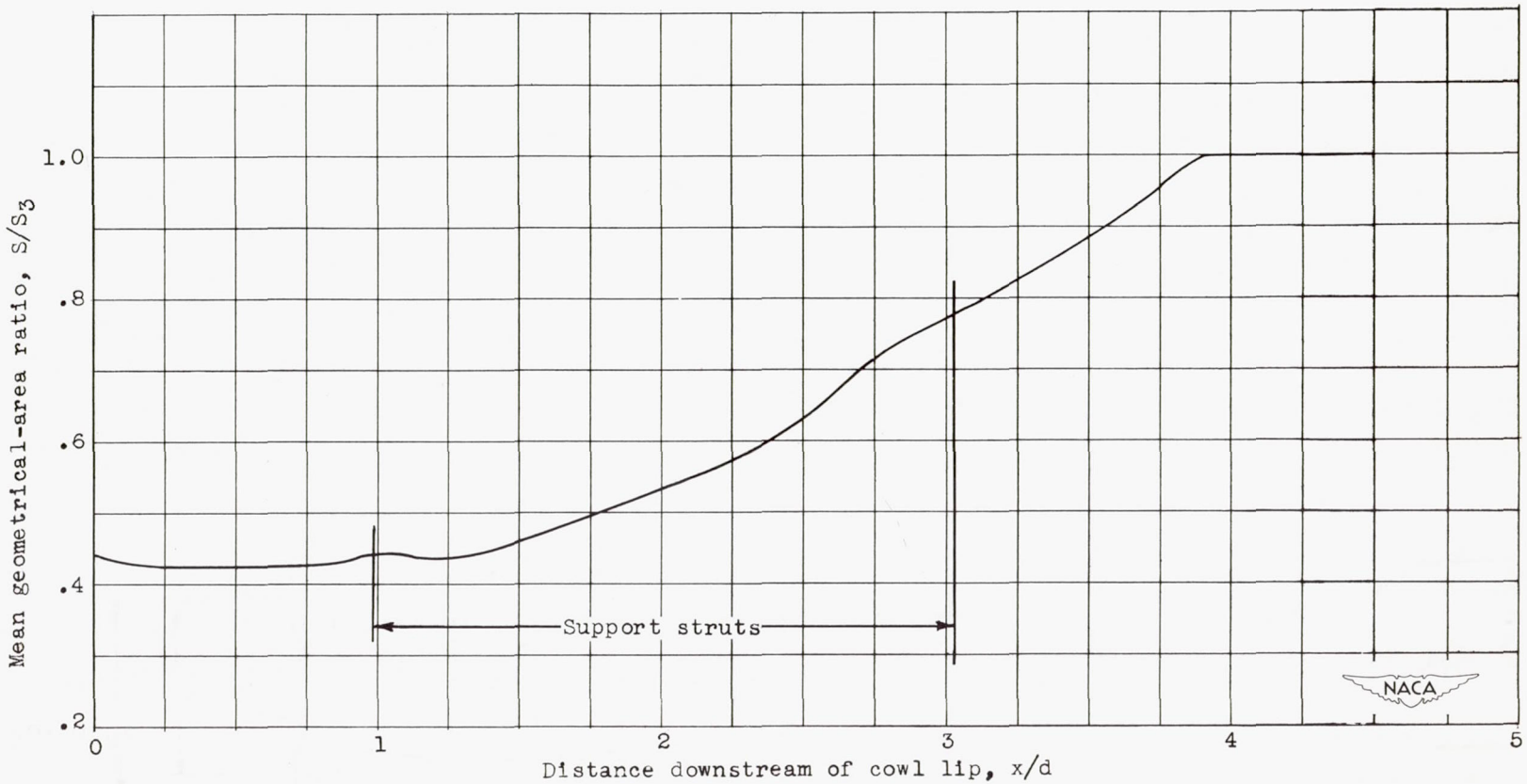
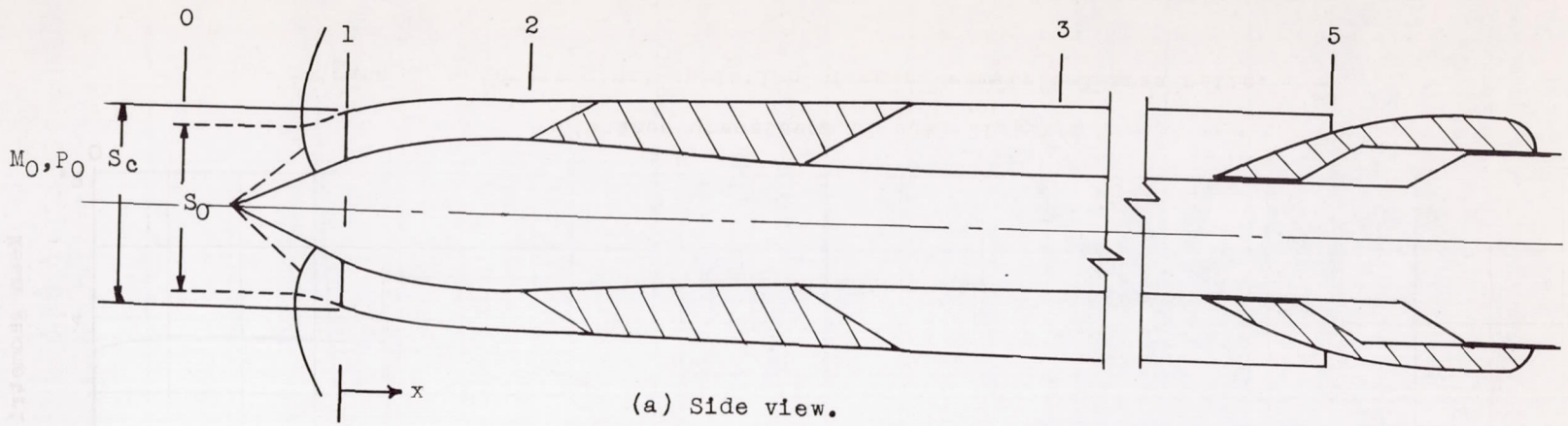
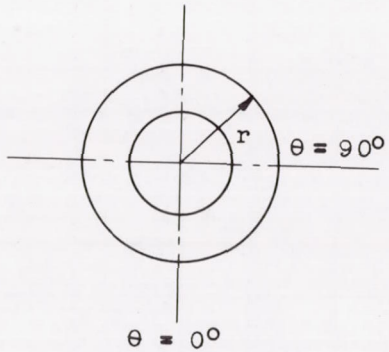


Figure 3. - Longitudinal variation of mean geometrical-area ratio.



(a) Side view.



(b) Front view.

Figure 4. - Notation for 8-inch ram-jet configuration.

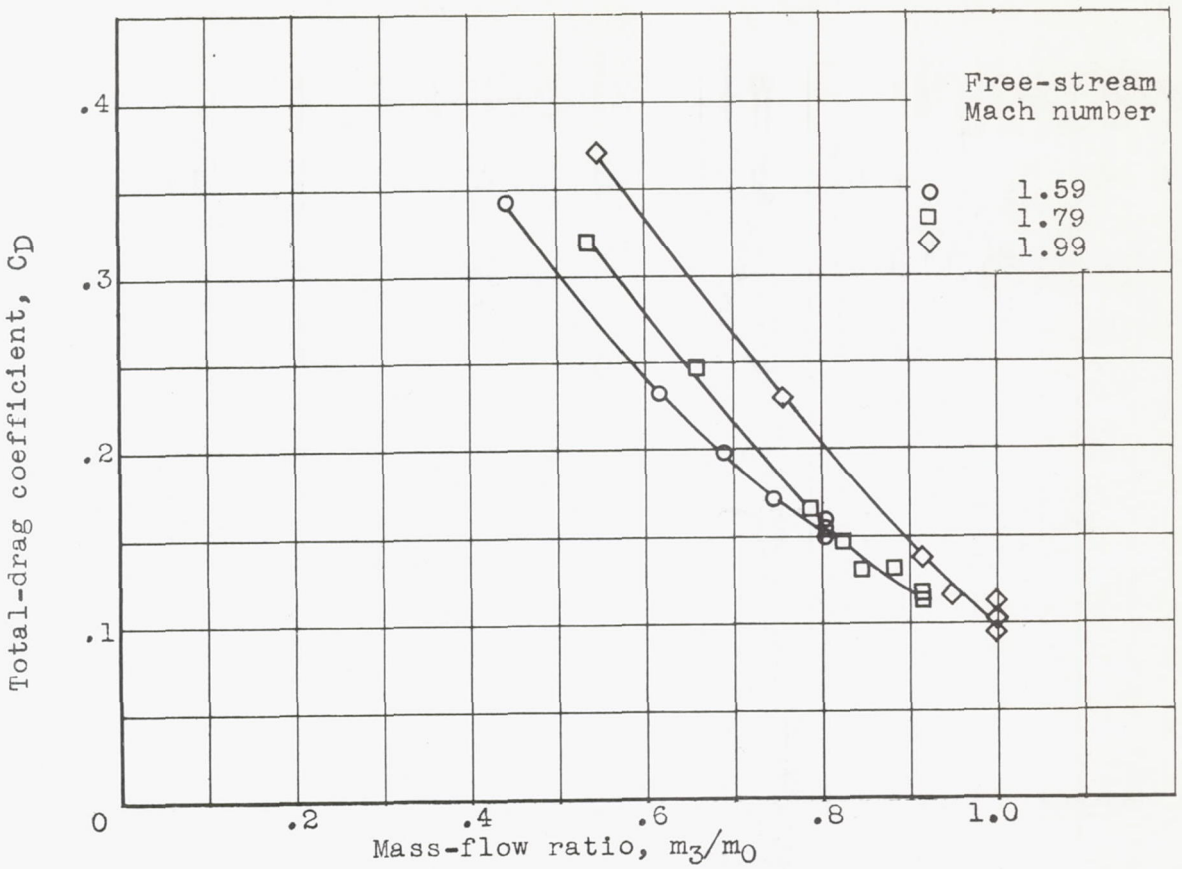


Figure 5. - Variation of total-drag coefficient with mass flow at zero angle of attack for three Mach numbers.

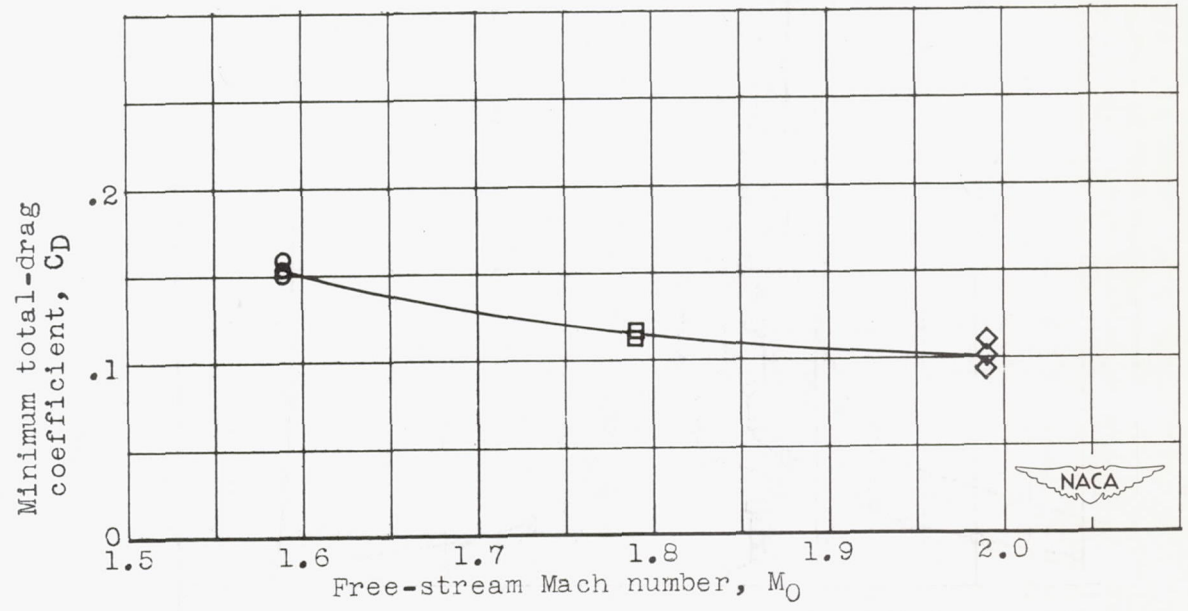
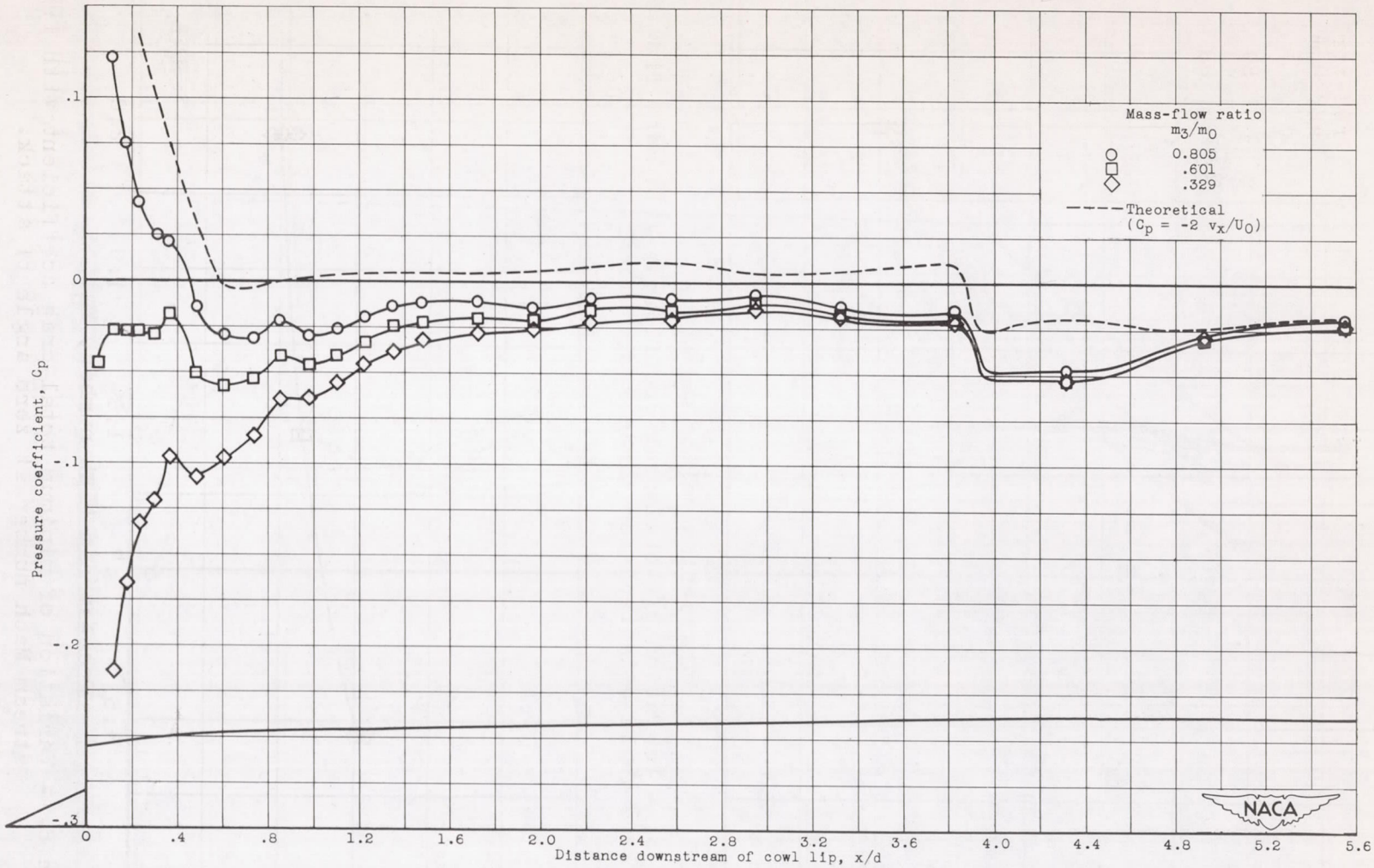


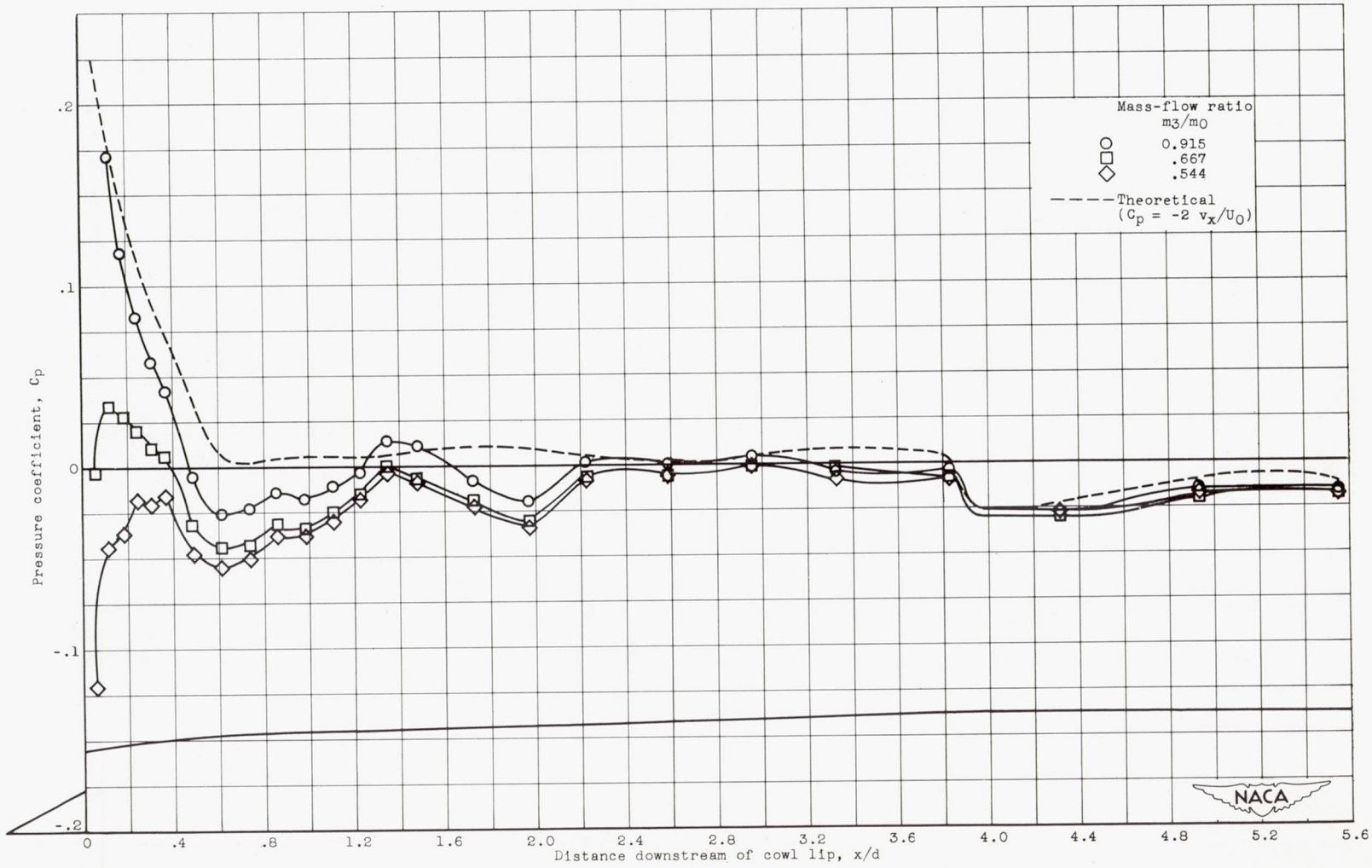
Figure 6. - Variation of minimum total-drag coefficient with free-stream Mach number at zero angle of attack.

2034



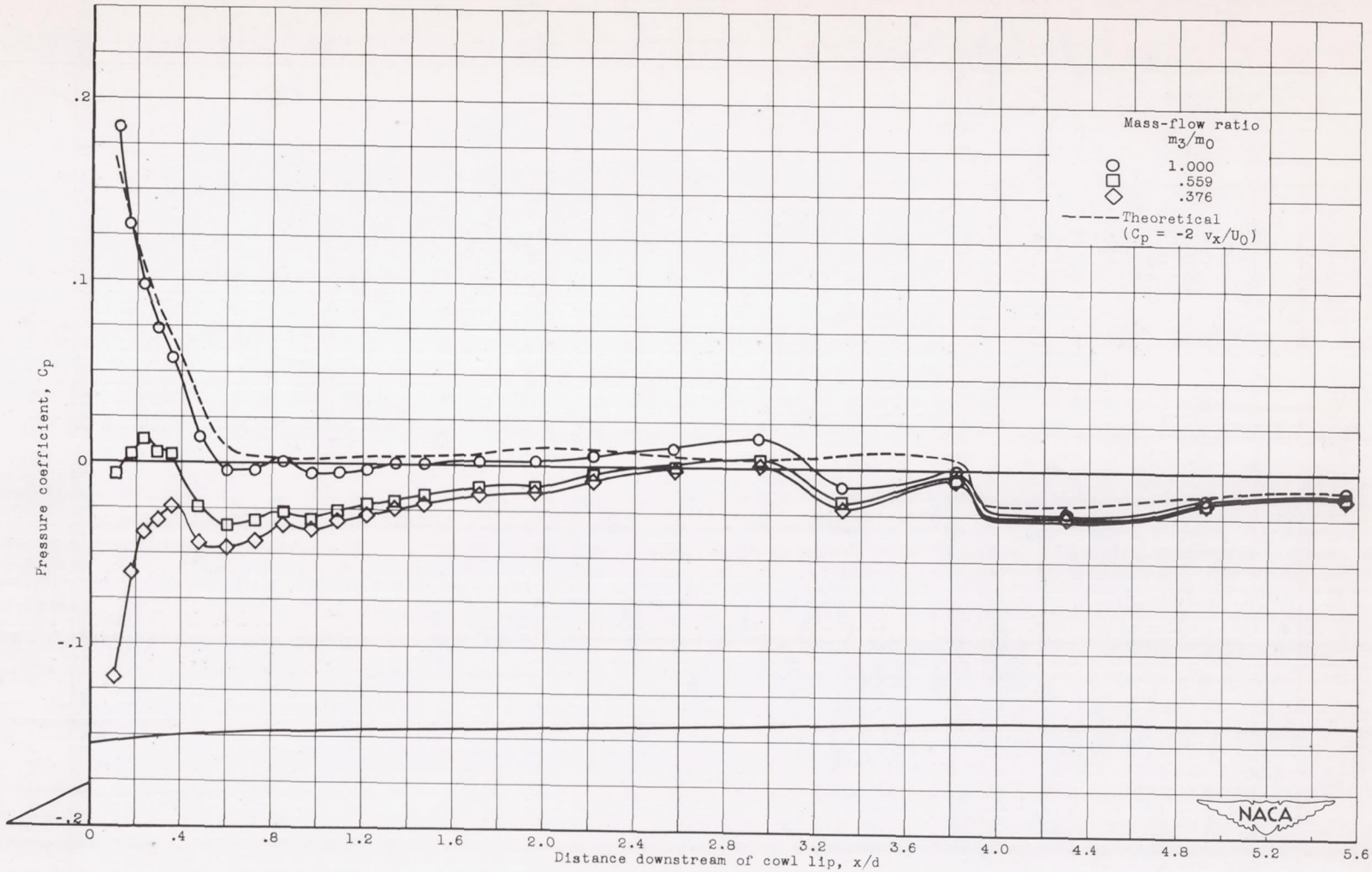
(a) Free-stream Mach number, 1.59.

Figure 7. - Longitudinal variation of external pressure coefficient at zero angle of attack for range of mass flows at three Mach numbers. Cylindrical coordinate θ, 180°.



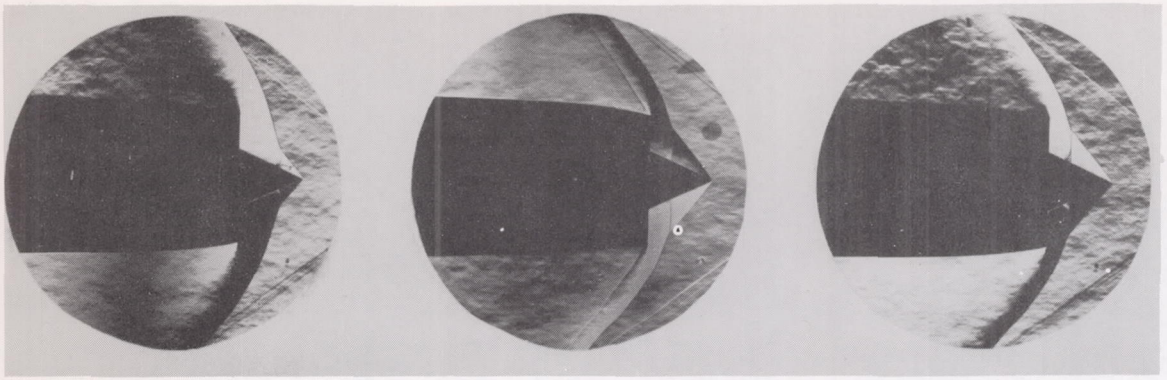
(b) Free-stream Mach number, 1.79.

Figure 7. - Continued. Longitudinal variation of external pressure coefficient at zero angle of attack for range of mass flows at three Mach numbers. Cylindrical coordinate θ, 180°.



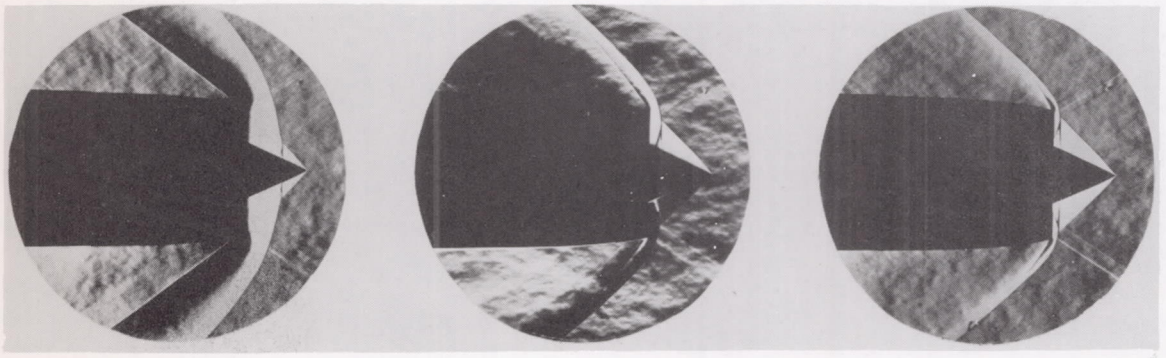
(c) Free-stream Mach number, 1.99.

Figure 7. - Concluded. Longitudinal variation of external pressure coefficient at zero angle of attack for range of mass flows at three Mach numbers. Cylindrical coordinate θ, 180°.



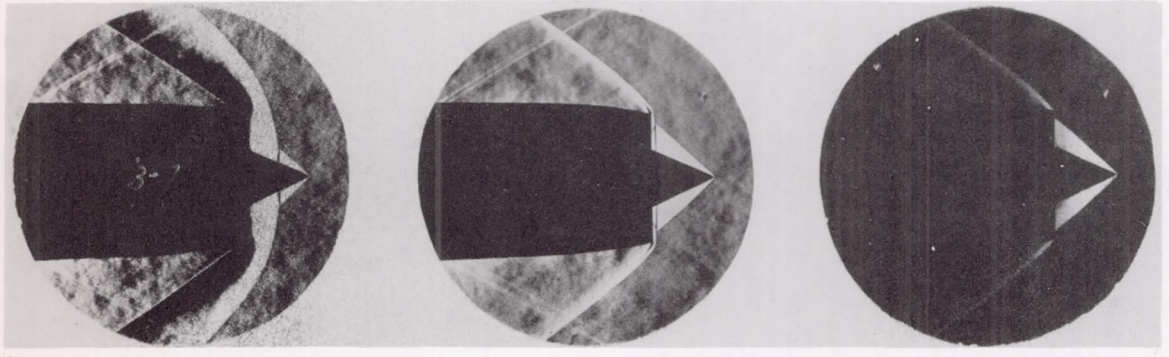
Mass-flow ratio 0.617 0.732 0.805

(a) Free-stream Mach number, 1.59.



Mass-flow ratio 0.544 0.870 0.915

(b) Free-stream Mach number, 1.79.



Mass-flow ratio 0.559 0.996 1.00

(c) Free-stream Mach number, 1.99.

NACA C-26039

Figure 8. - Typical schlieren photographs at zero angle of attack for three Mach numbers.

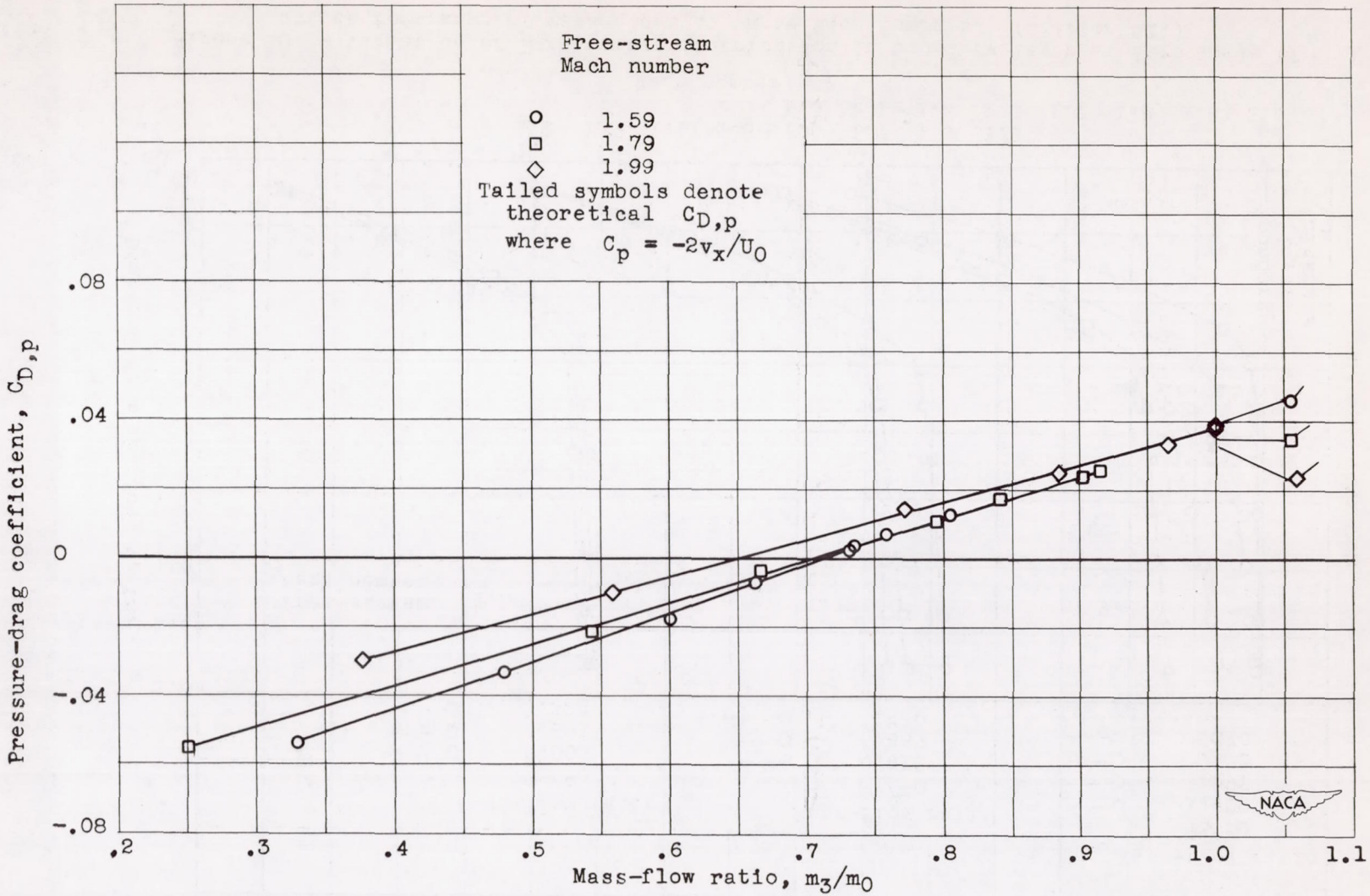


Figure 9. - Variation of pressure-drag coefficient with mass flow at zero angle of attack for three Mach numbers.

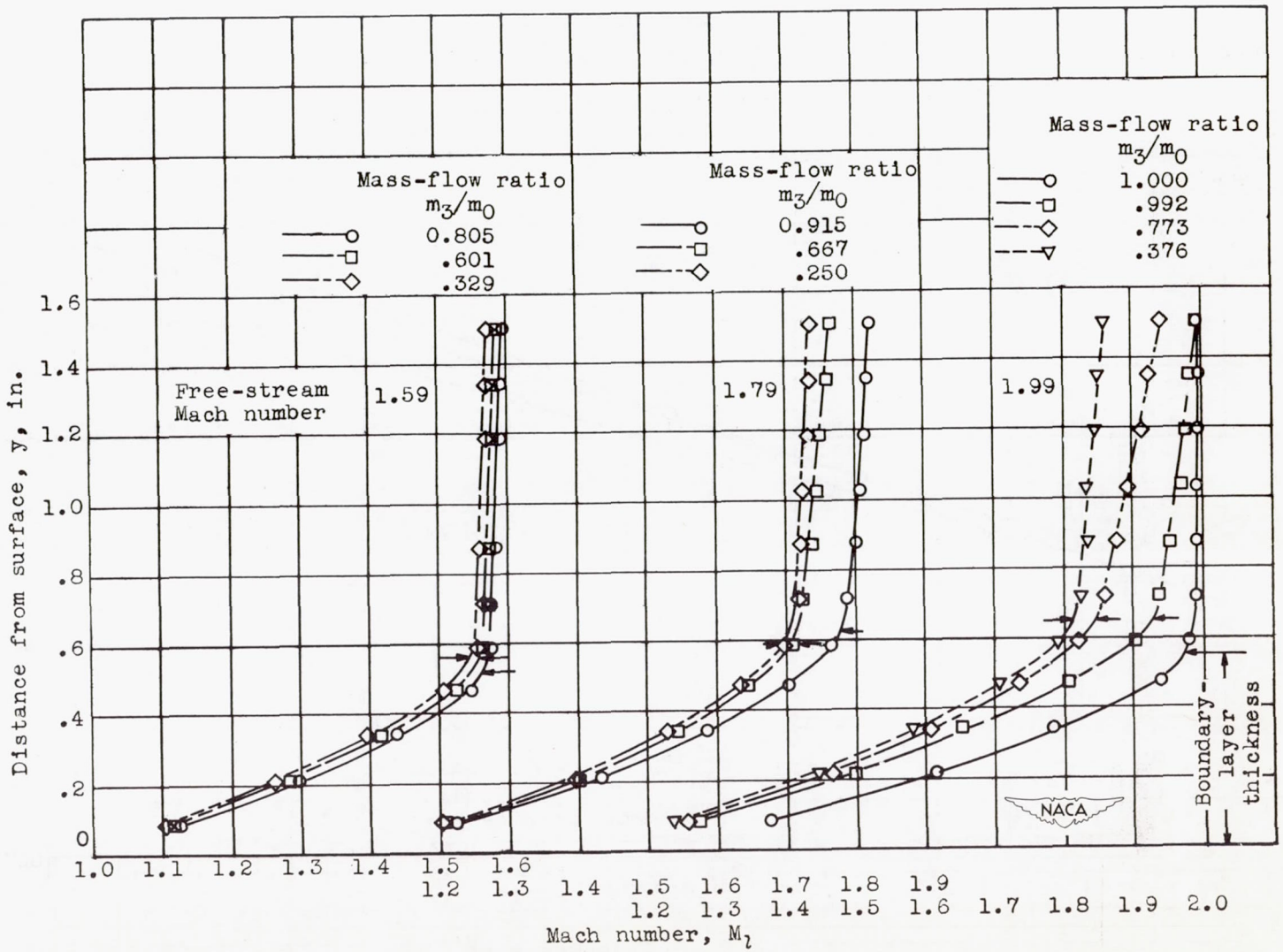


Figure 10. - Variation of Mach number distribution in boundary layer at zero angle of attack for range of mass flows at three Mach numbers. (Station 51.)

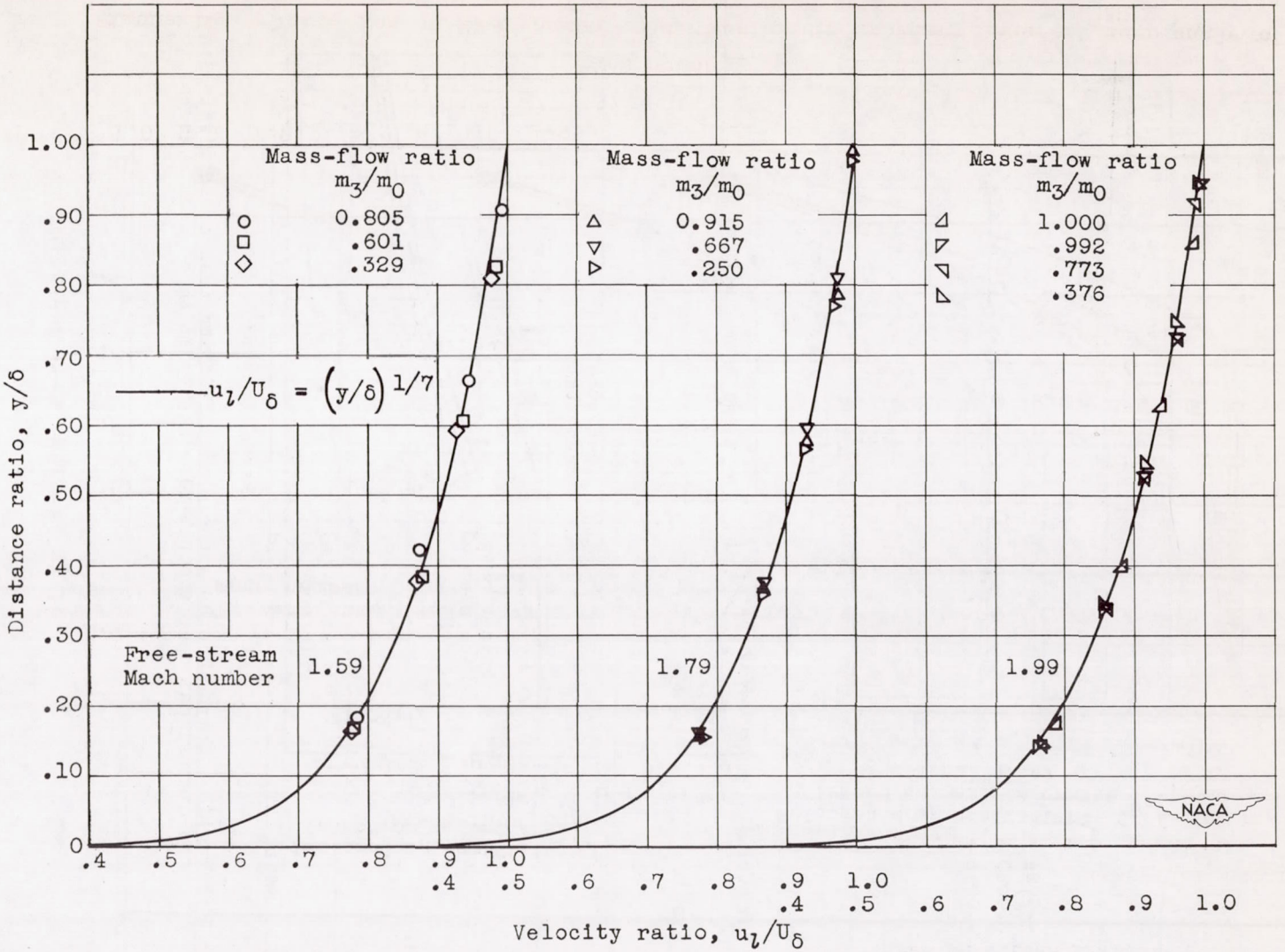


Figure 11. - Comparison of experimental and theoretical boundary-layer profiles at zero angle of attack for range of mass flows and three free-stream Mach numbers.

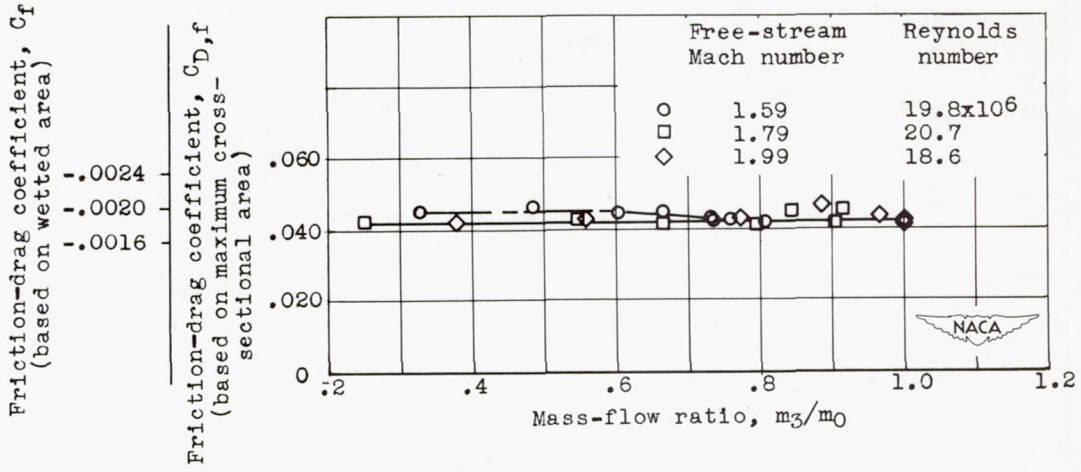


Figure 12. - Variation of friction-drag coefficient with mass flow at zero angle of attack for three Mach numbers.

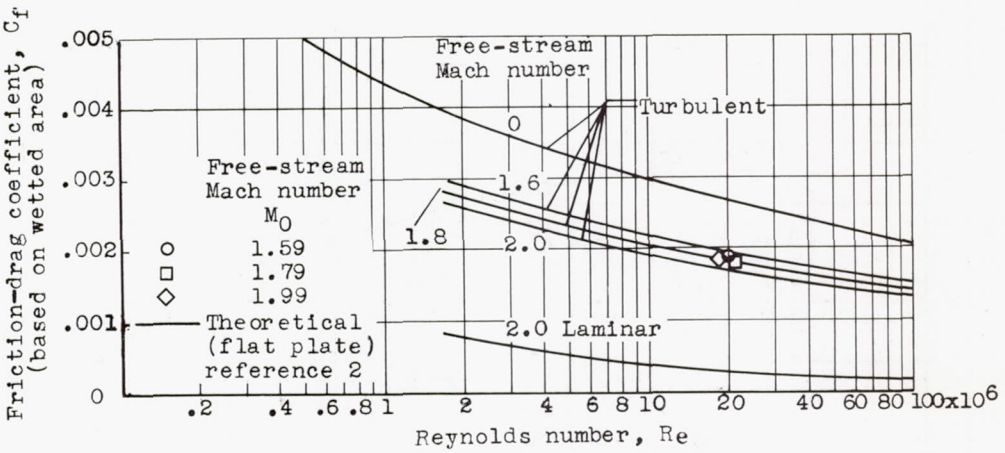


Figure 13. - Comparison of experimental friction-drag coefficient with two-dimensional compressible-flow theory at three Mach numbers.

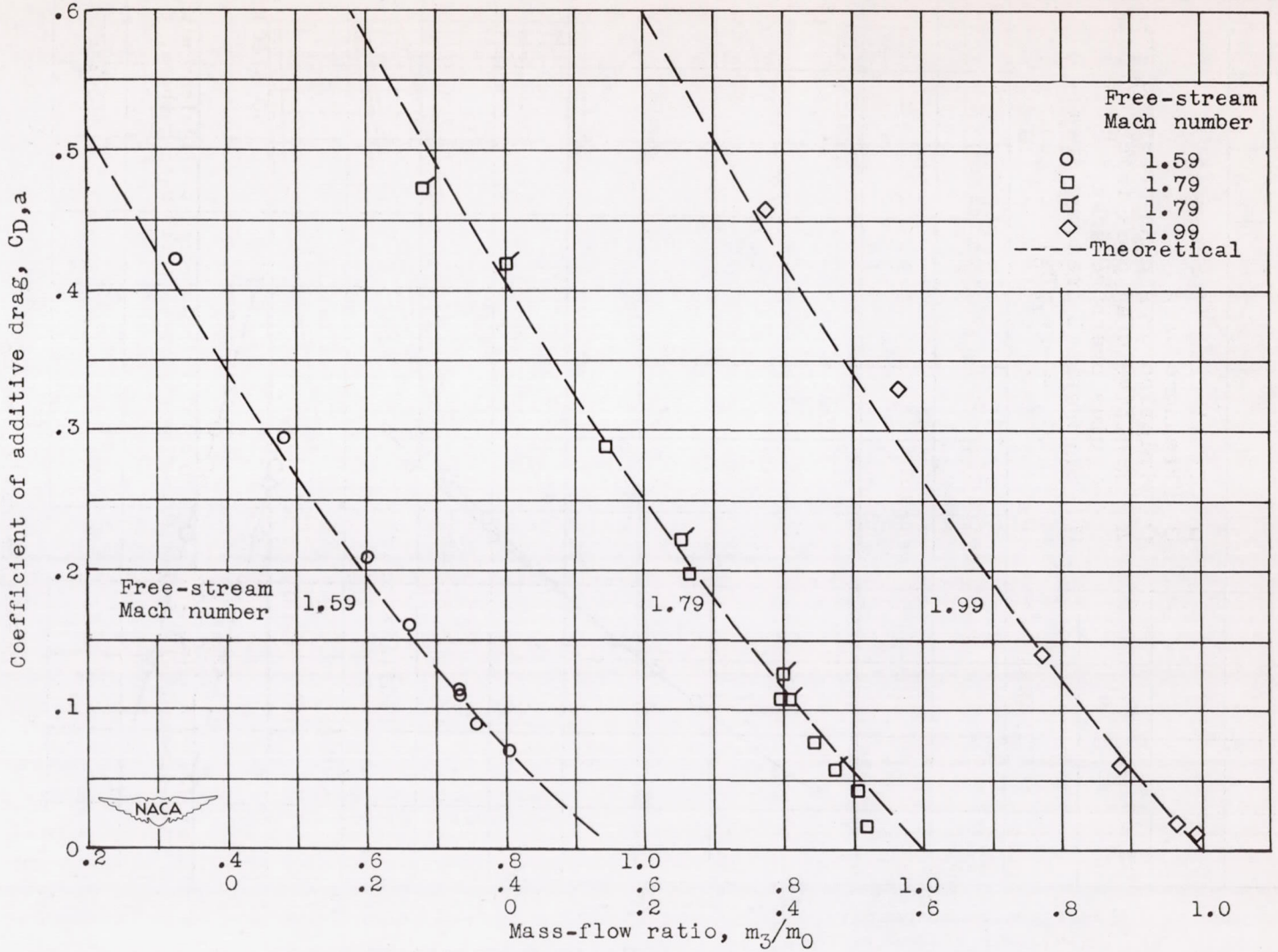
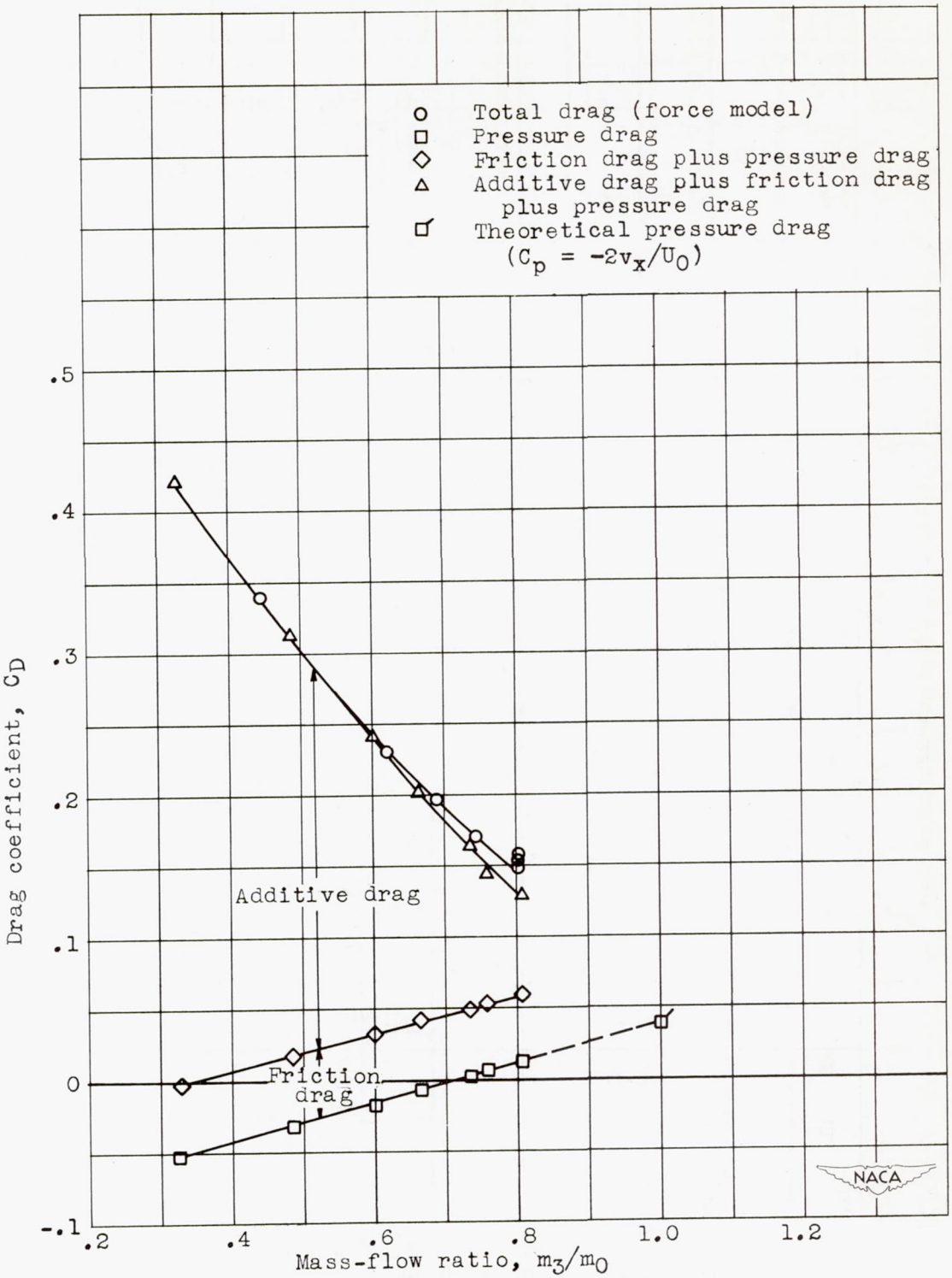
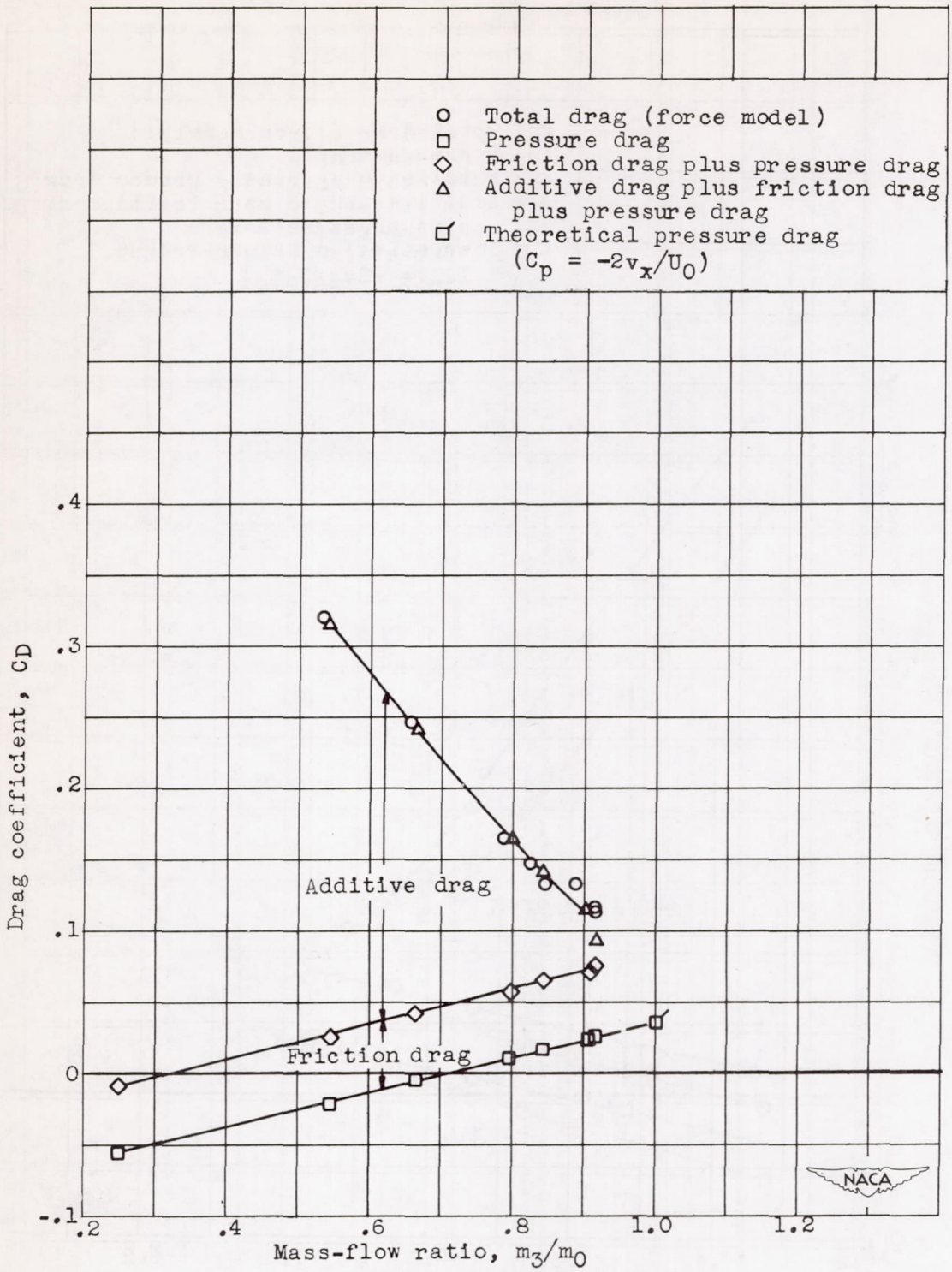


Figure 14. - Comparison of experimental additive-drag coefficient with one-dimensional theory for range of mass flows at three Mach numbers.



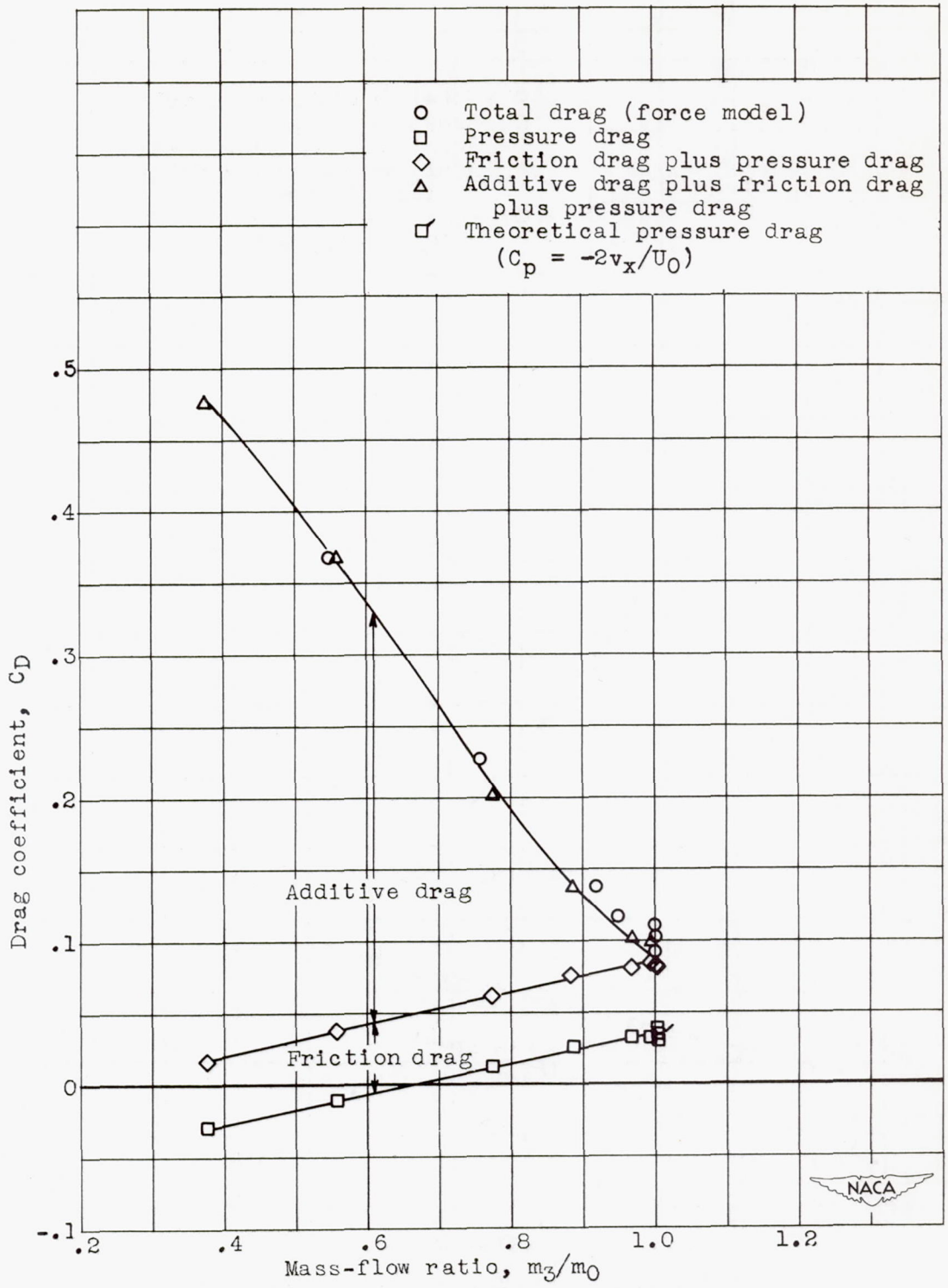
(a) Free-stream Mach number, 1.59.

Figure 15. - Variation of components of total-drag coefficient with mass flow at zero angle of attack for three Mach numbers.



(b) Free-stream Mach number, 1.79.

Figure 15. - Continued. Variation of components of total-drag coefficient with mass flow at zero angle of attack for three Mach numbers.



(c) Free-stream Mach number, 1.99.

Figure 15. - Concluded. Variation of components of total-drag coefficient with mass flow at zero angle of attack for three Mach numbers.

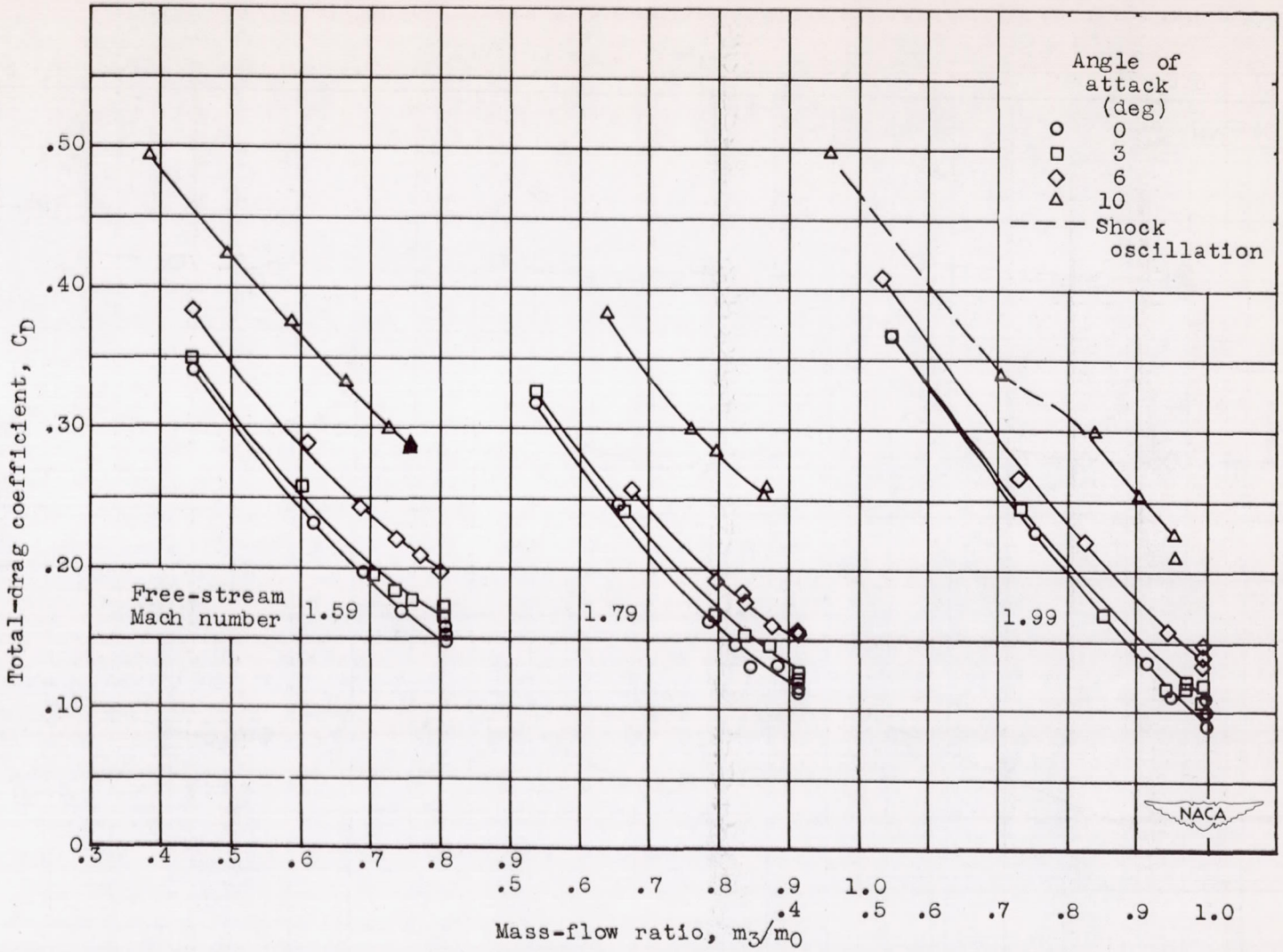


Figure 16. - Variation of total-drag coefficient with mass flow at four angles of attack for three Mach numbers.

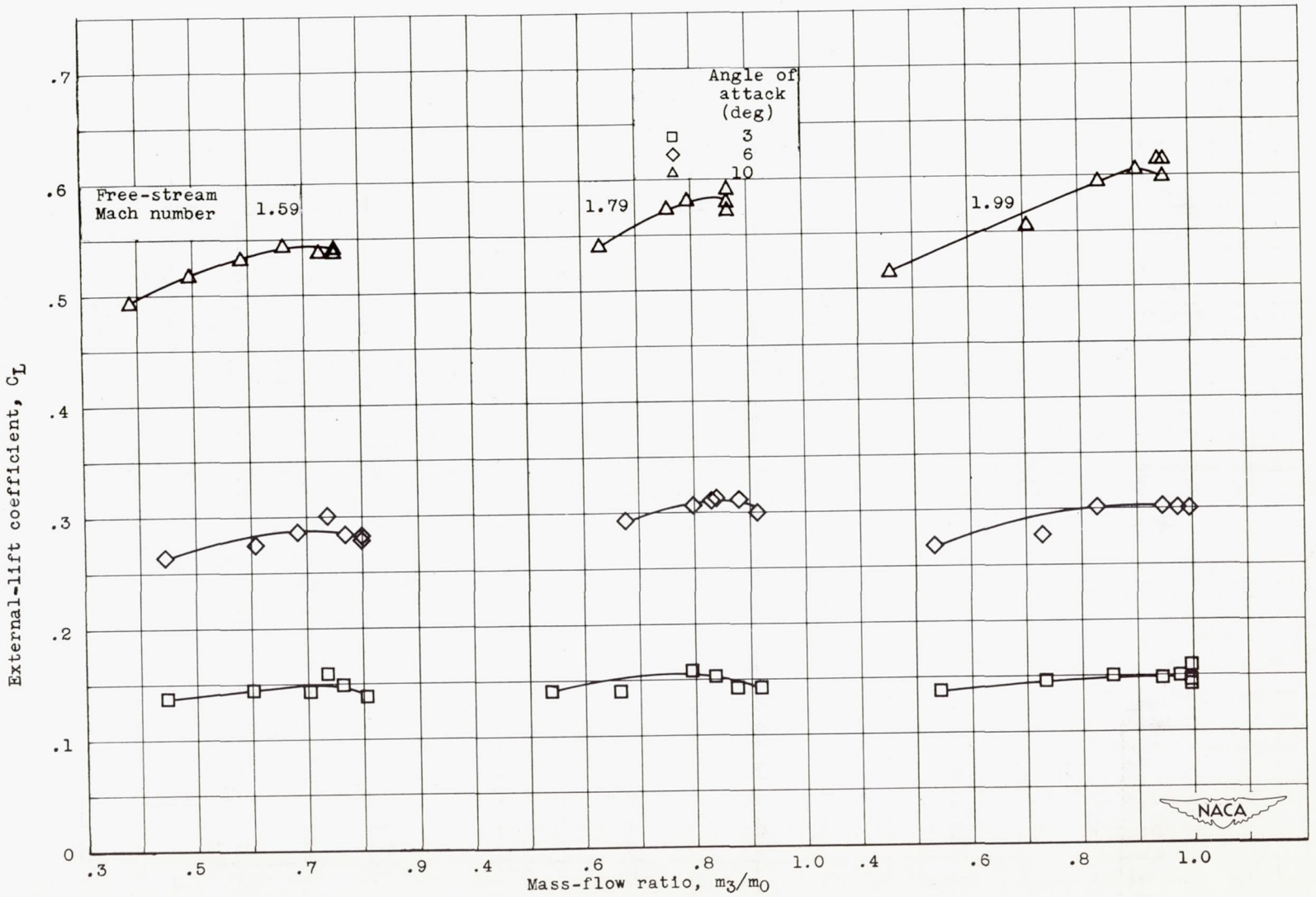


Figure 17. - Variation of external-lift coefficient with mass flow at three angles of attack for three Mach numbers.

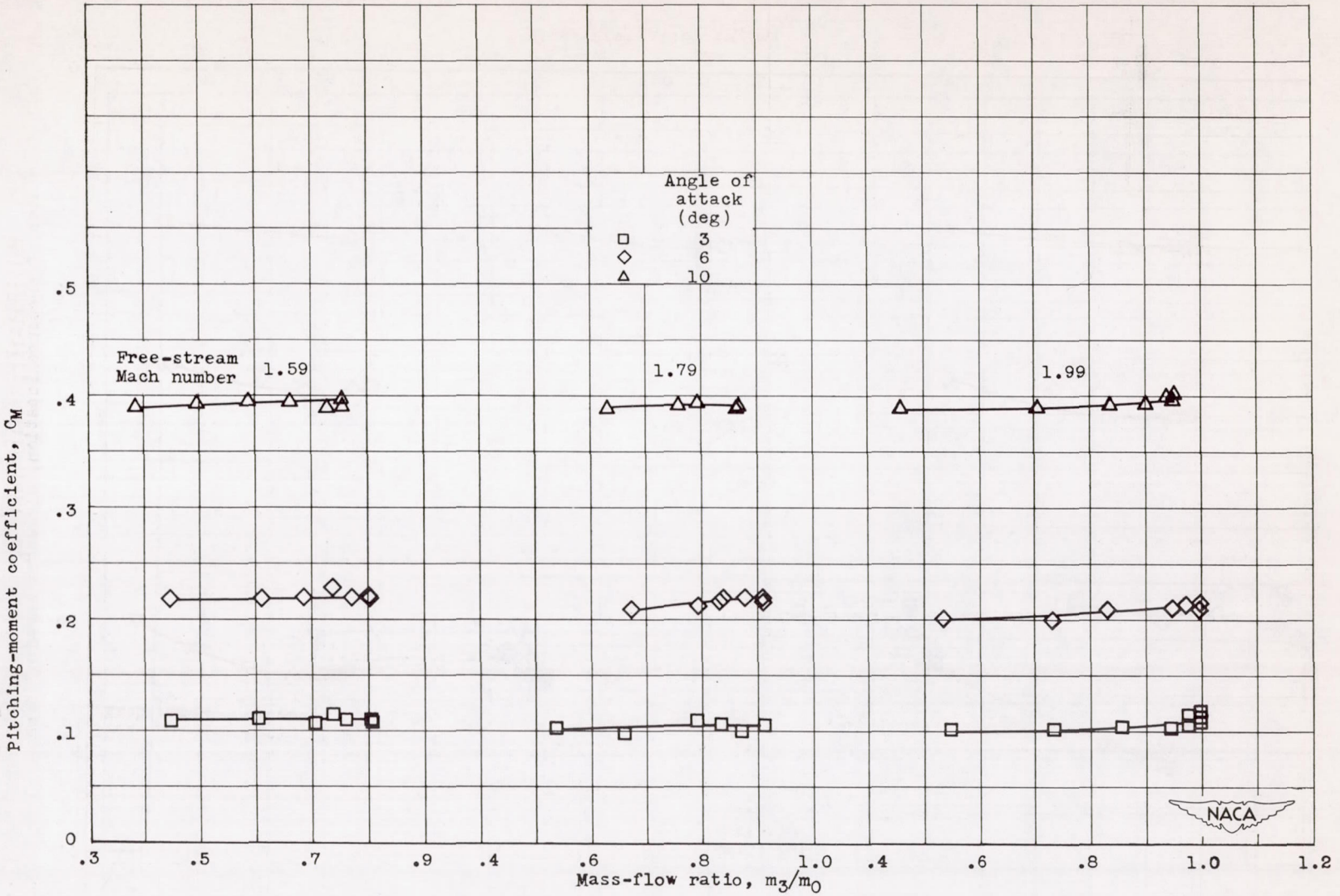


Figure 18. - Variation of external pitching-moment coefficient about base of model with mass flow at three angles of attack for three Mach numbers.

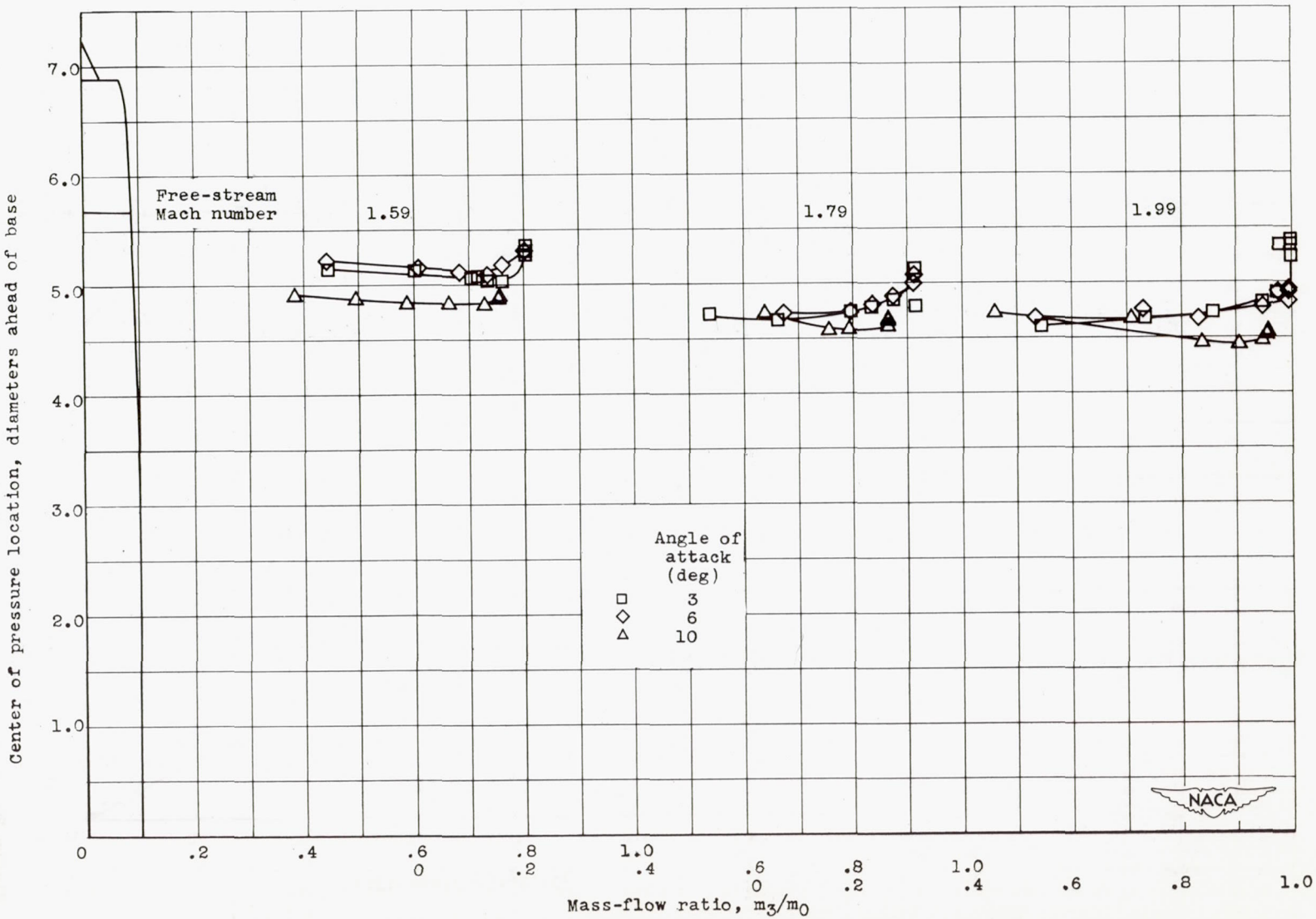


Figure 19. - Variation of center of pressure location with mass flow at three angles of attack for three Mach numbers.

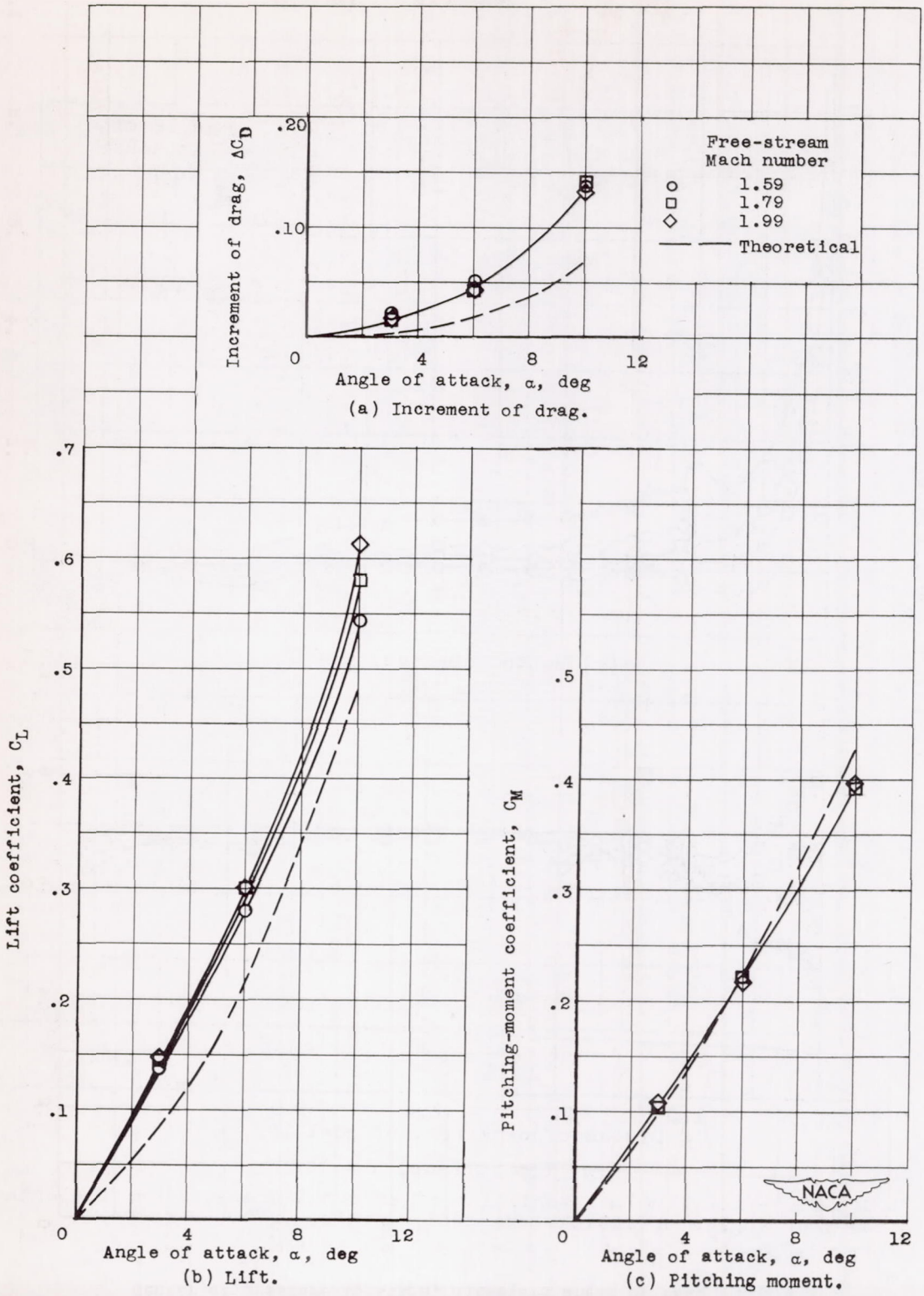


Figure 20. - Variation of external drag increment, lift and pitching-moment coefficients with angle of attack at critical mass flow for three Mach numbers.

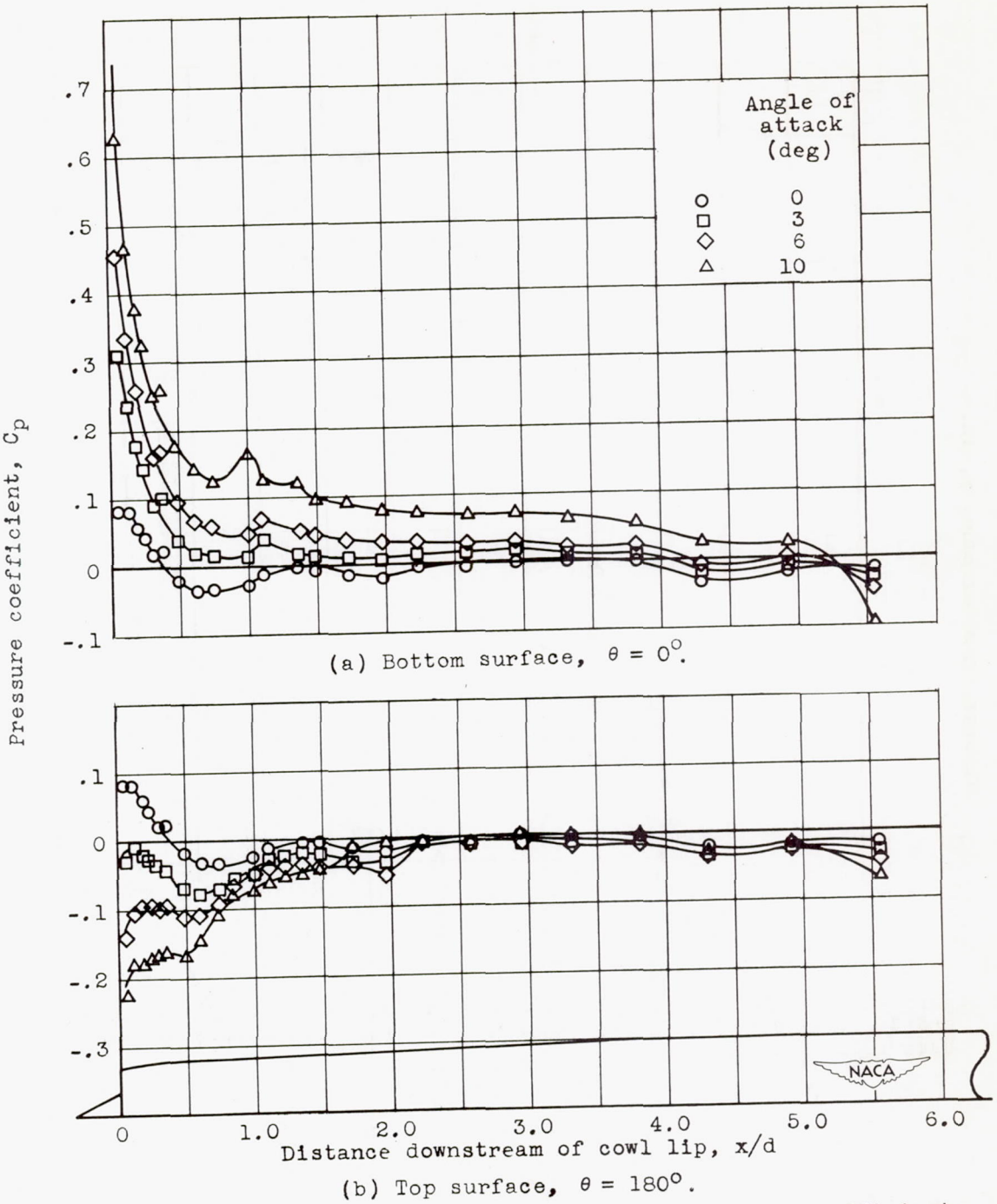
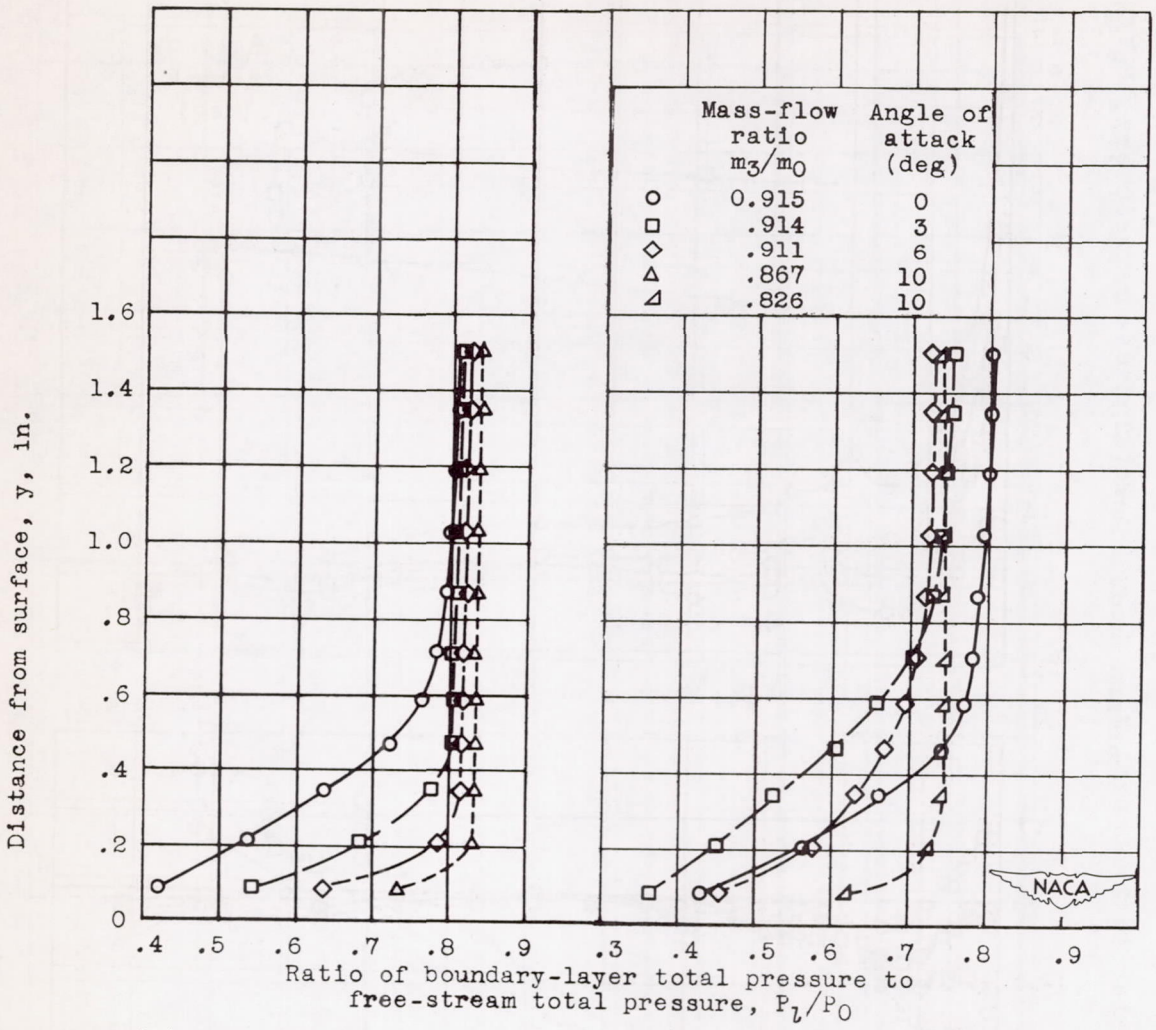


Figure 21. - Longitudinal variation of external-pressure coefficients for four angles of attack. Mass-flow ratio, 0.750; Mach number, 1.79.



(a) Bottom surface, $\theta = 0^\circ$. (b) Top surface, $\theta = 180^\circ$.

Figure 22. - Variation of total pressure in boundary layer over upper and lower surfaces of model at station 51 for four angles of attack. Mach number, 1.79.

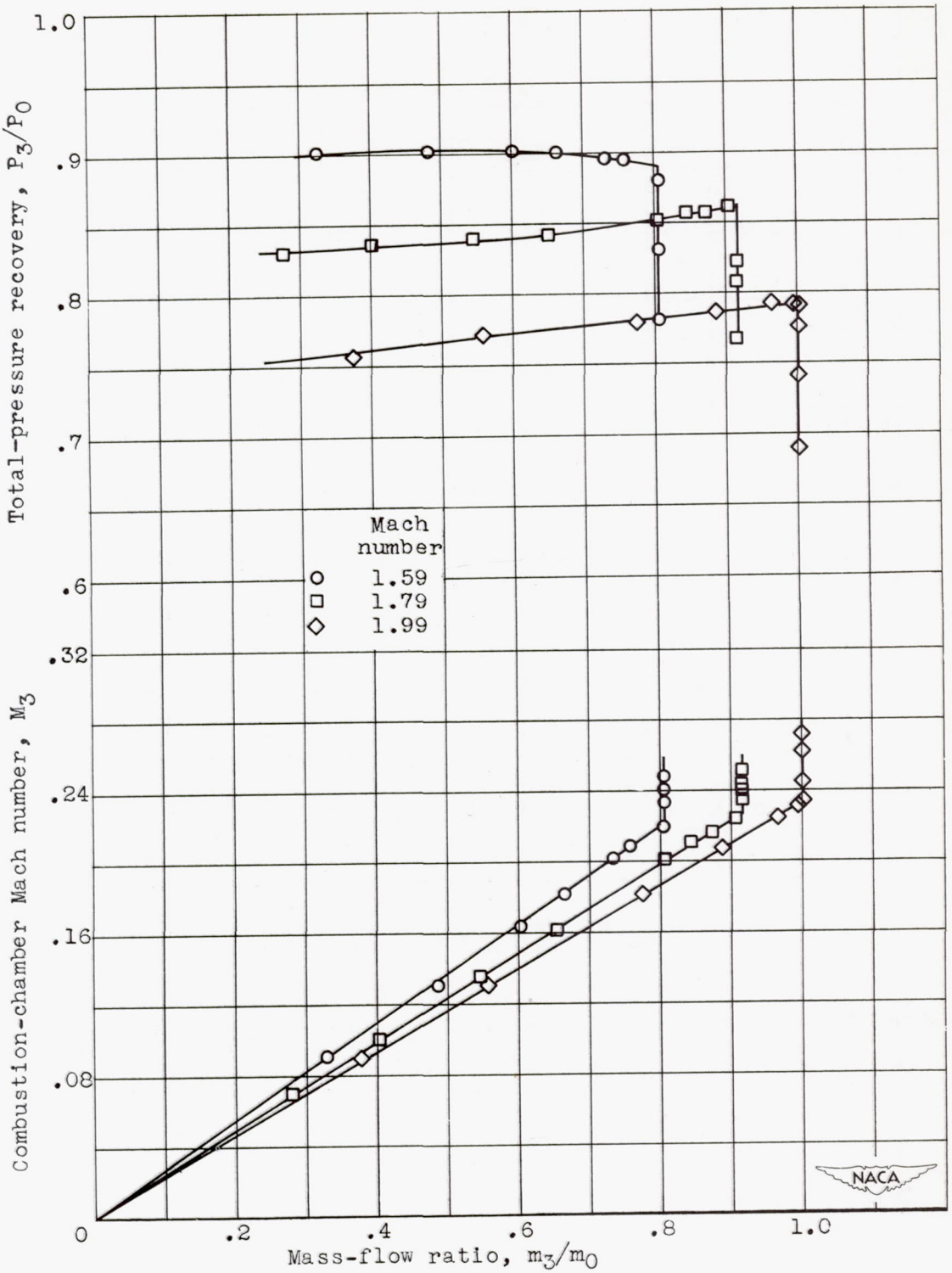


Figure 23. - Variation of total-pressure recovery and combustion-chamber Mach number with mass flow at zero angle of attack for three Mach numbers.

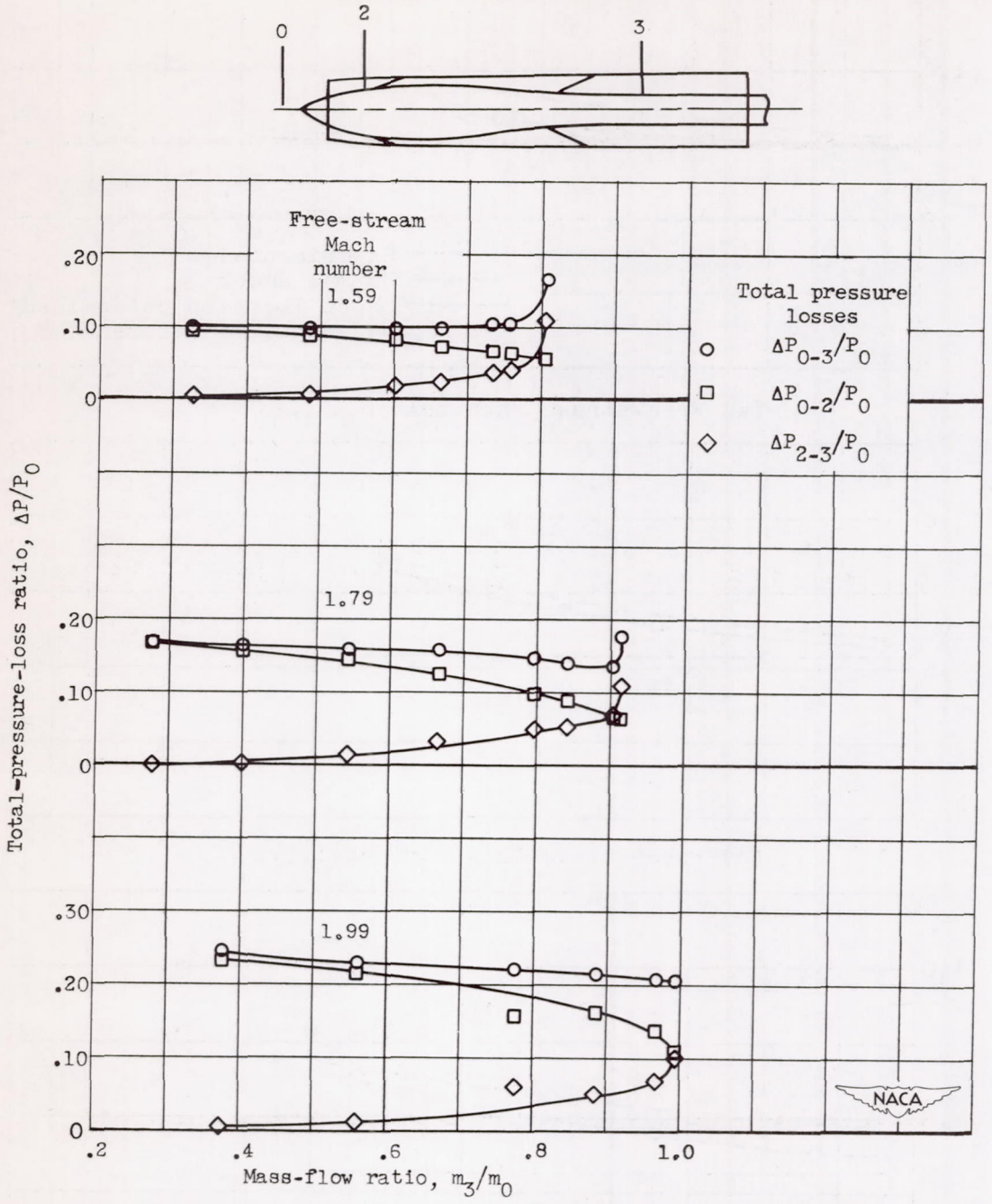
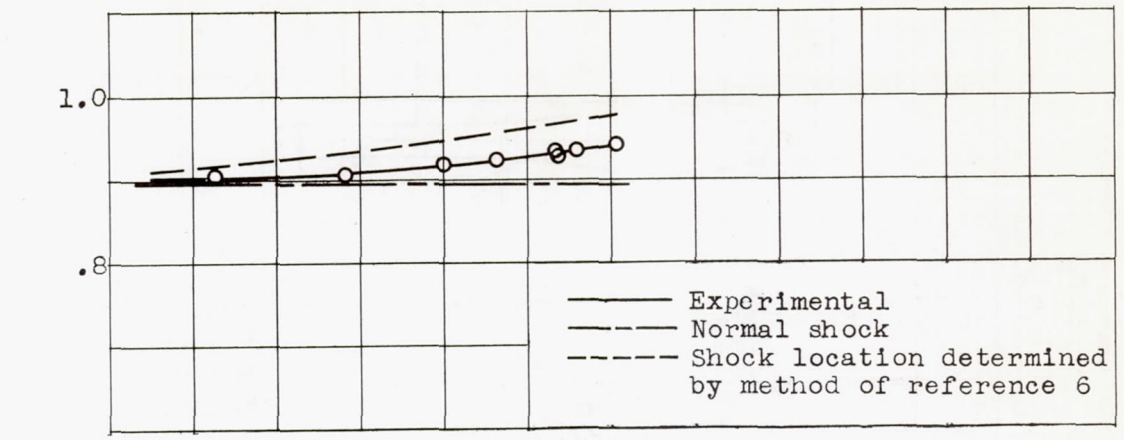
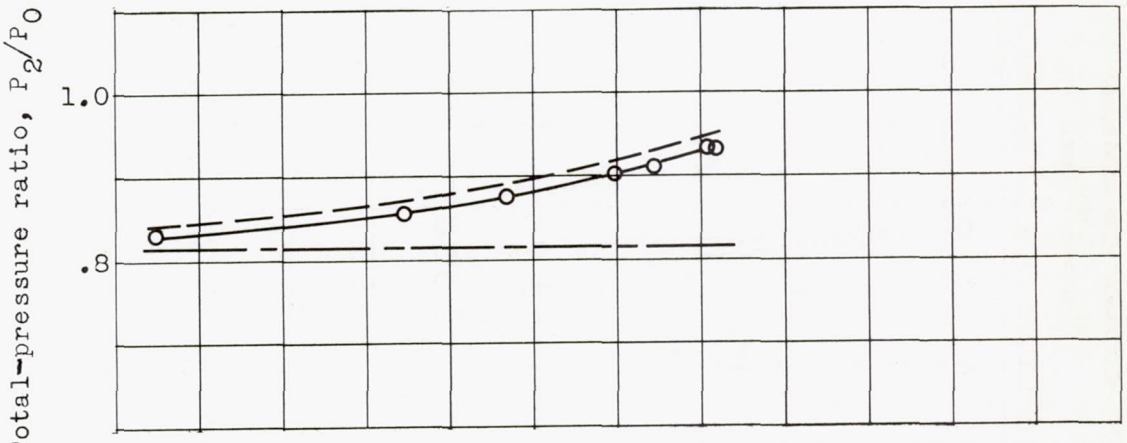


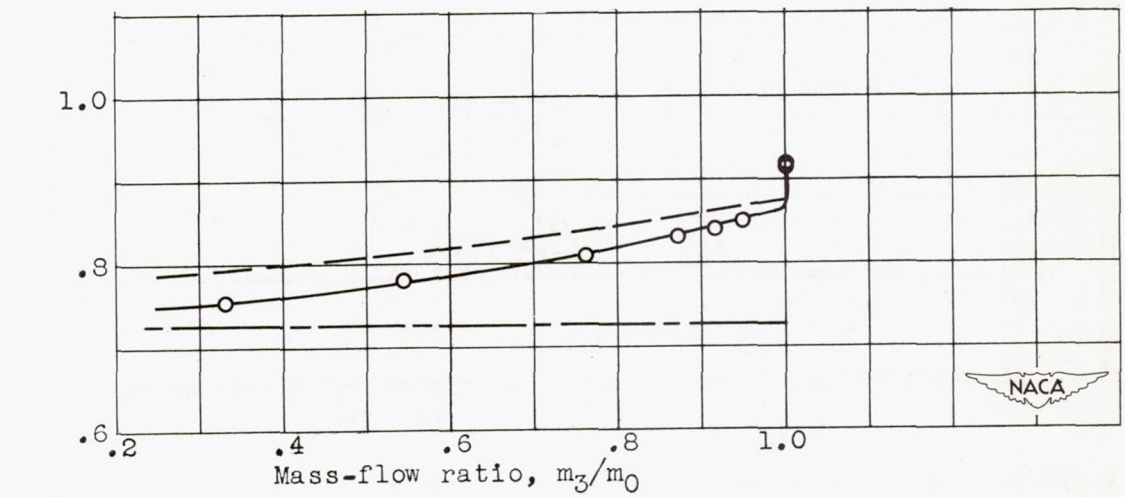
Figure 24. - Components of total-pressure loss at zero angle of attack for range of mass flows at three Mach numbers.



(a) Free-stream Mach number, 1.59.



(b) Free-stream Mach number, 1.79.



(c) Free-stream Mach number, 1.99.

Figure 25. - Comparison of experimental inlet losses with theory at zero angle of attack for range of mass flows at three Mach numbers.

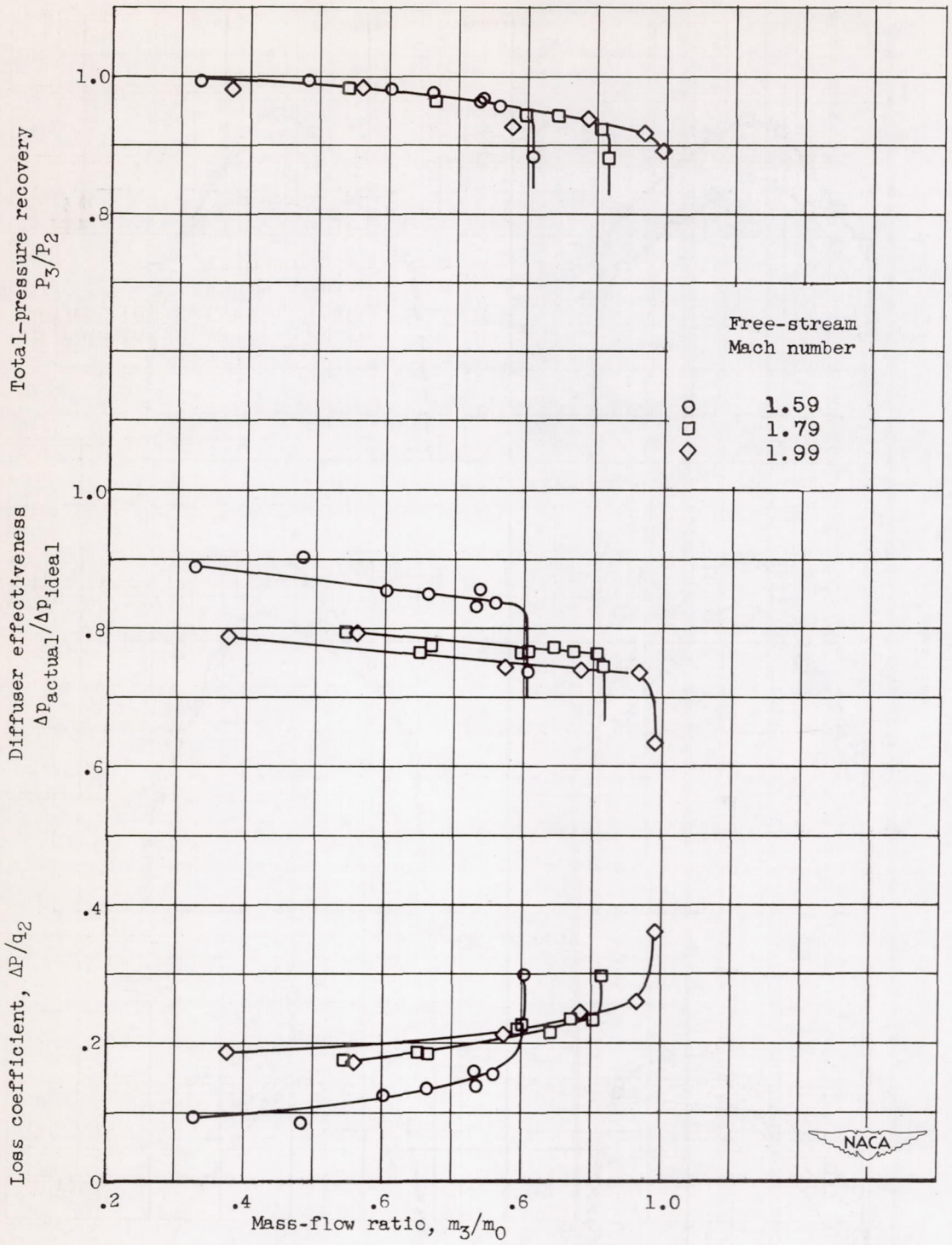


Figure 26. - Subsonic diffuser characteristics at zero angle of attack for range of mass flows at three Mach numbers.

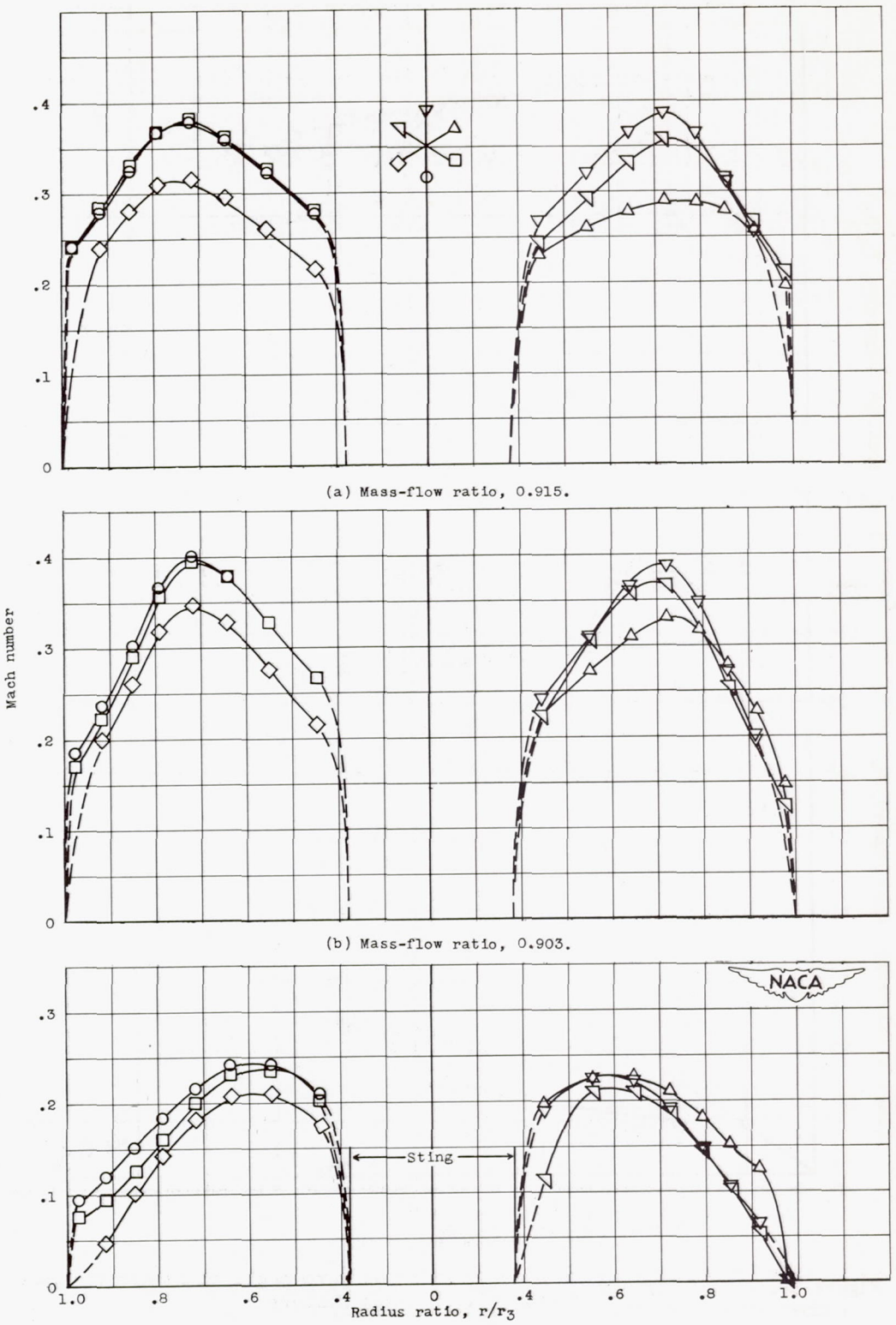
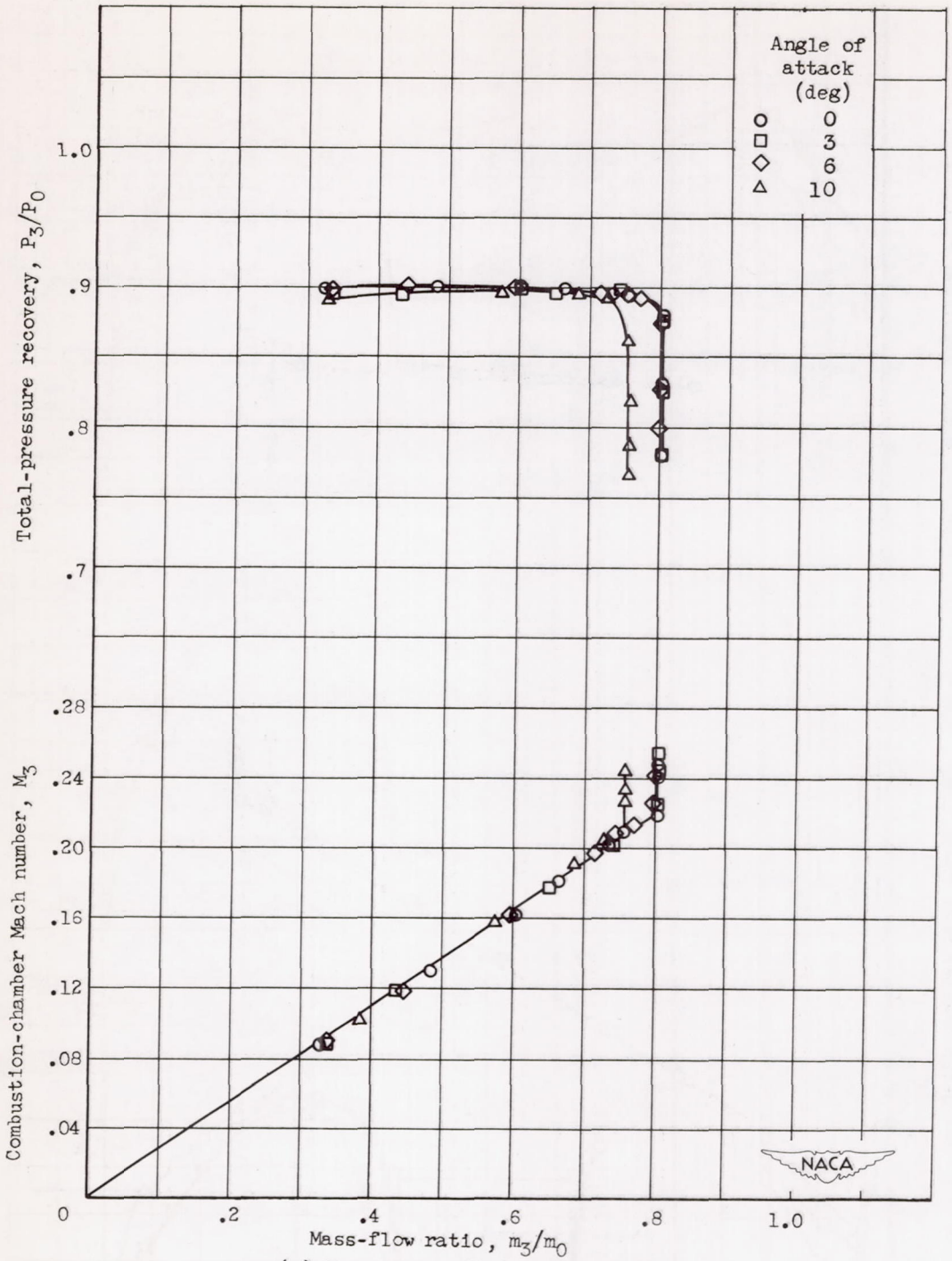
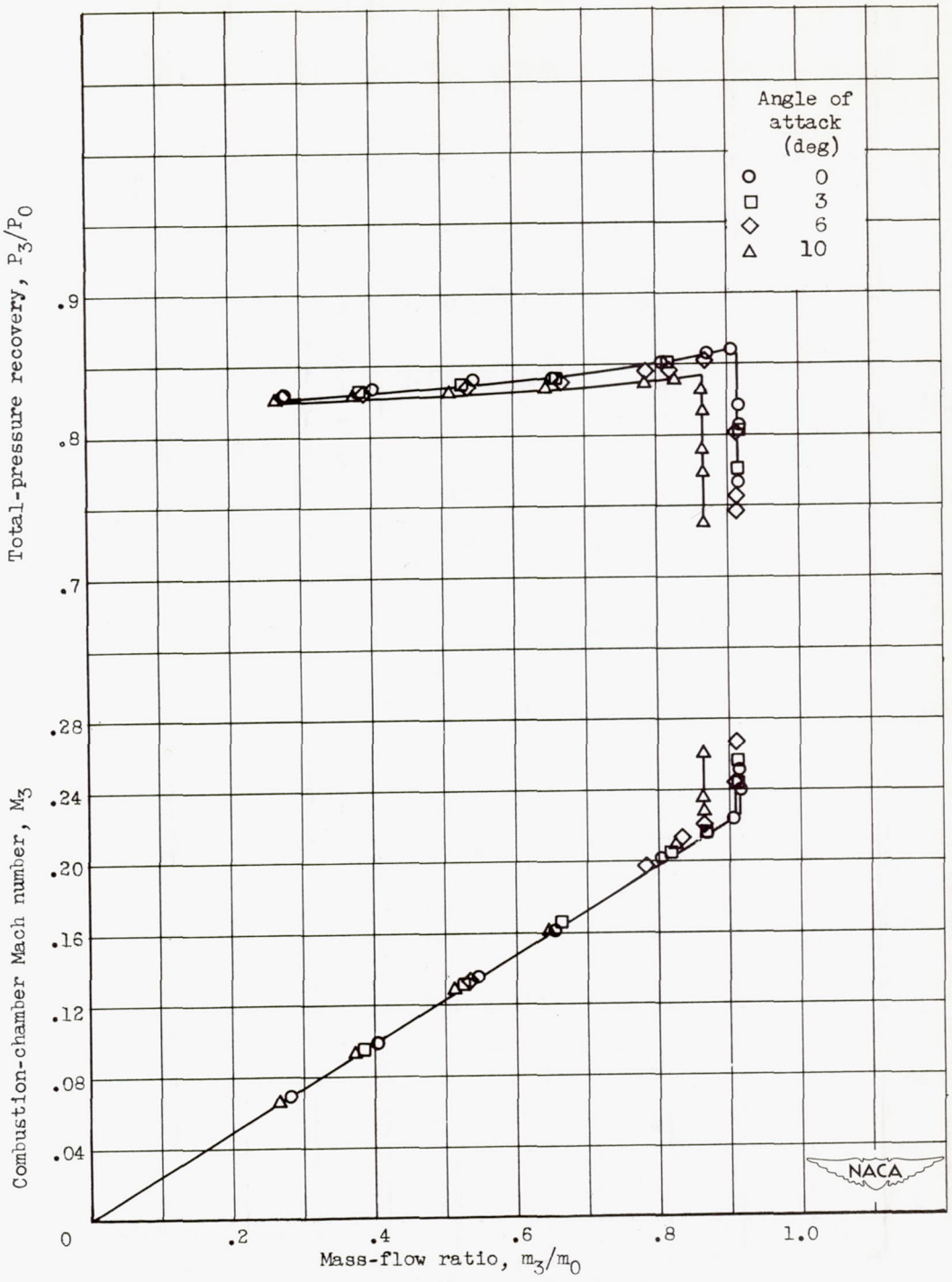


Figure 27. - Variation of Mach number distribution at entrance to combustion chamber for several mass flows at zero angle of attack. Mach number, 1.79.



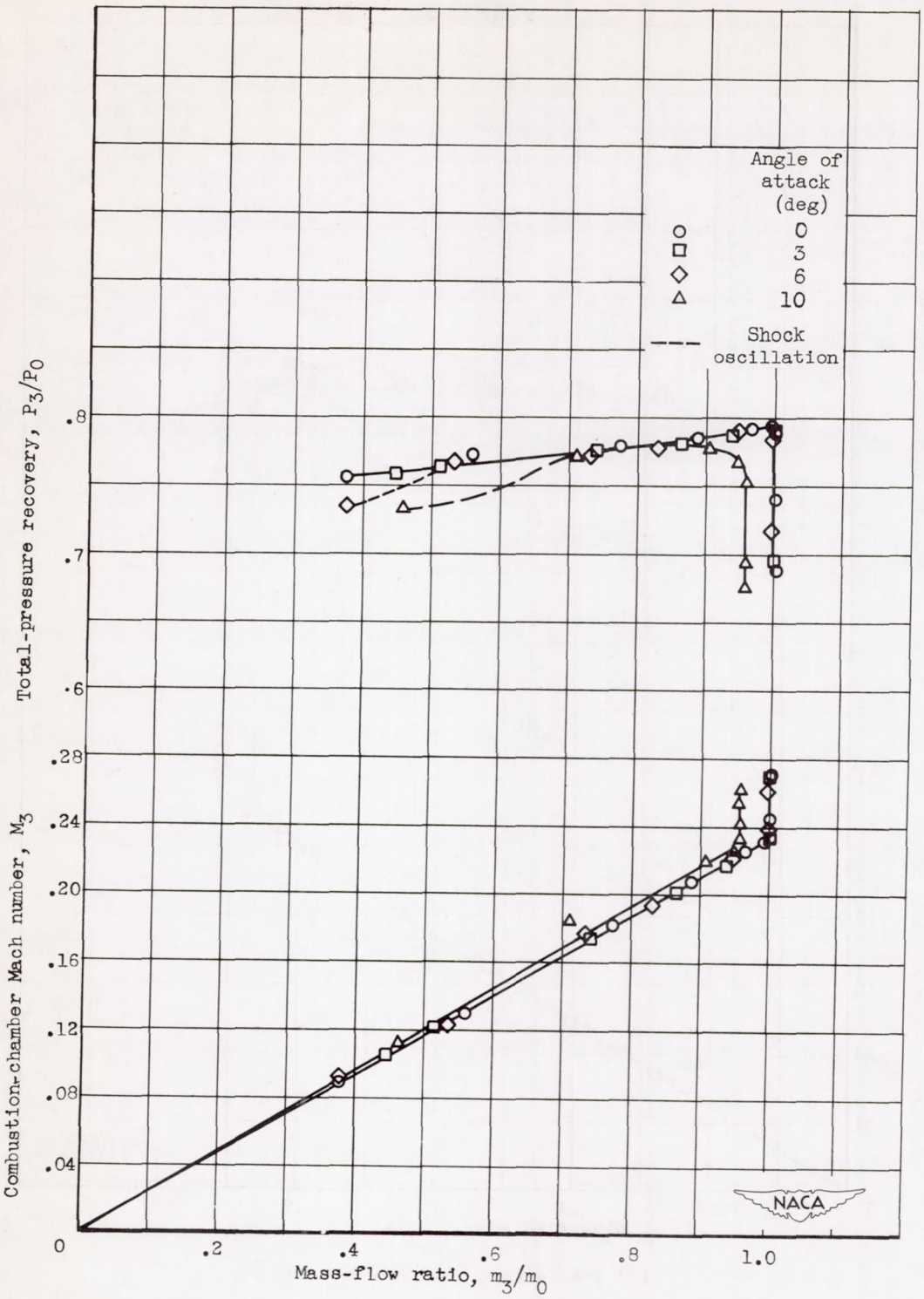
(a) Free-stream Mach number, 1.59.

Figure 28. - Variation of total-pressure recovery and combustion-chamber Mach number with mass flow at four angles of attack for three Mach numbers.



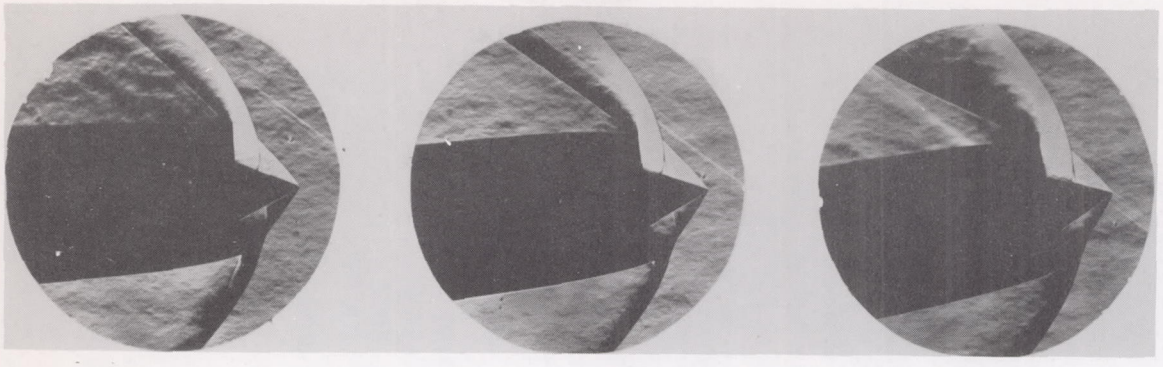
(b) Free-stream Mach number 1.79.

Figure 28. - Continued. Variation of total-pressure recovery and combustion-chamber Mach number with mass flow at four angles of attack for three Mach numbers.



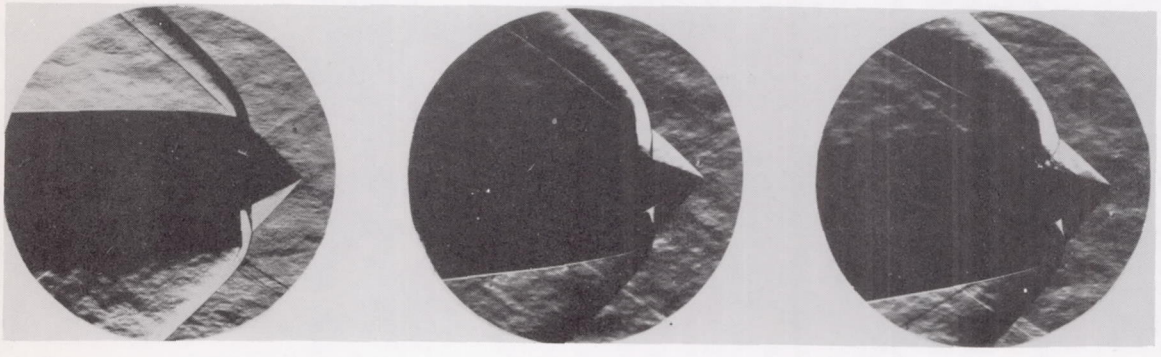
(c) Free-stream Mach number, 1.99.

Figure 28. - Concluded. Variation of total-pressure recovery and combustion-chamber Mach number with mass flow at four angles of attack for three Mach numbers.



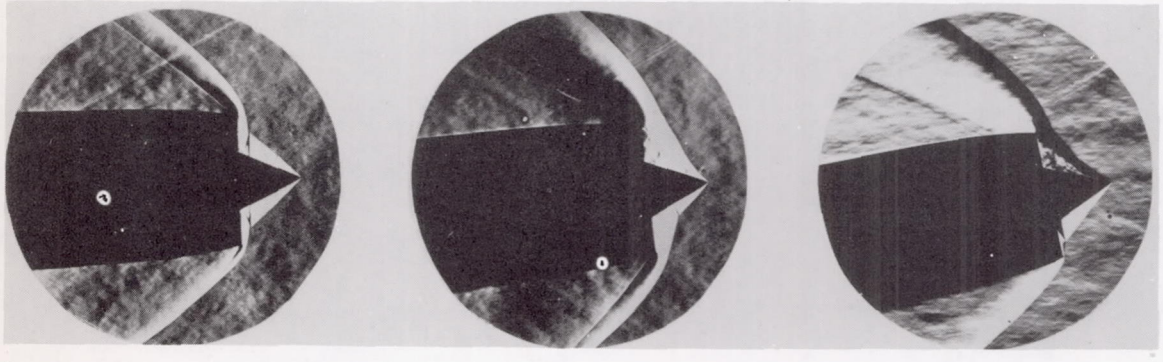
Angle of attack	3°	6°	10°
Mass-flow ratio	0.740	0.754	0.729

(a) Free-stream Mach number, 1.59



Angle of attack	3°	6°	10°
Mass-flow ratio	0.869	0.869	0.826

(b) Free-stream Mach number, 1.79



Angle of attack	3°	6°	10°
Mass-flow ratio	0.861	0.733	0.708

(c) Free-stream Mach number, 1.99.

NACA
C-26040

Figure 29. - Typical schlieren photographs at angles of attack for three Mach numbers.

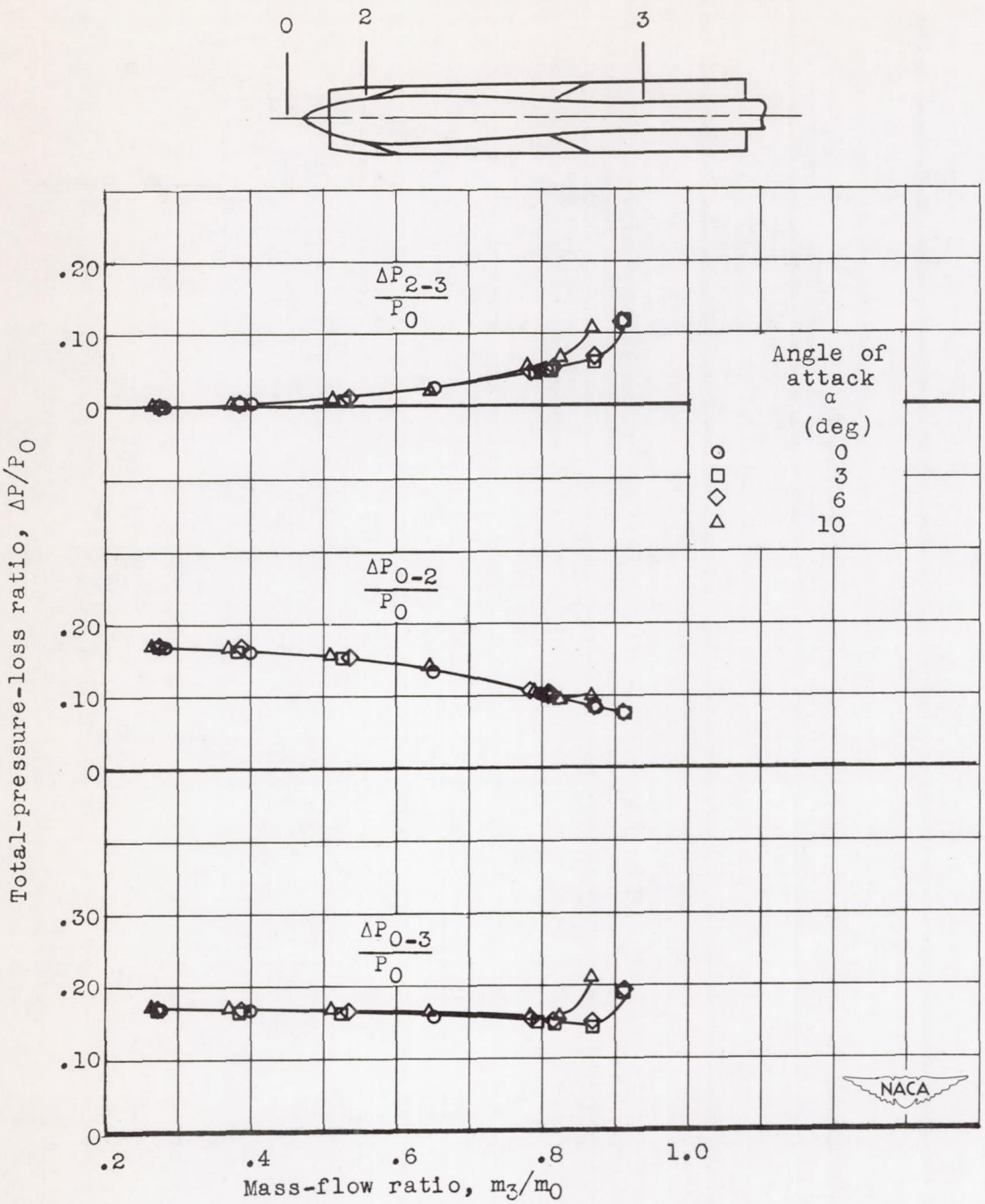


Figure 30. - Variation of inlet and subsonic diffuser losses with mass flow at four angles of attack. Mach number, 1.79.

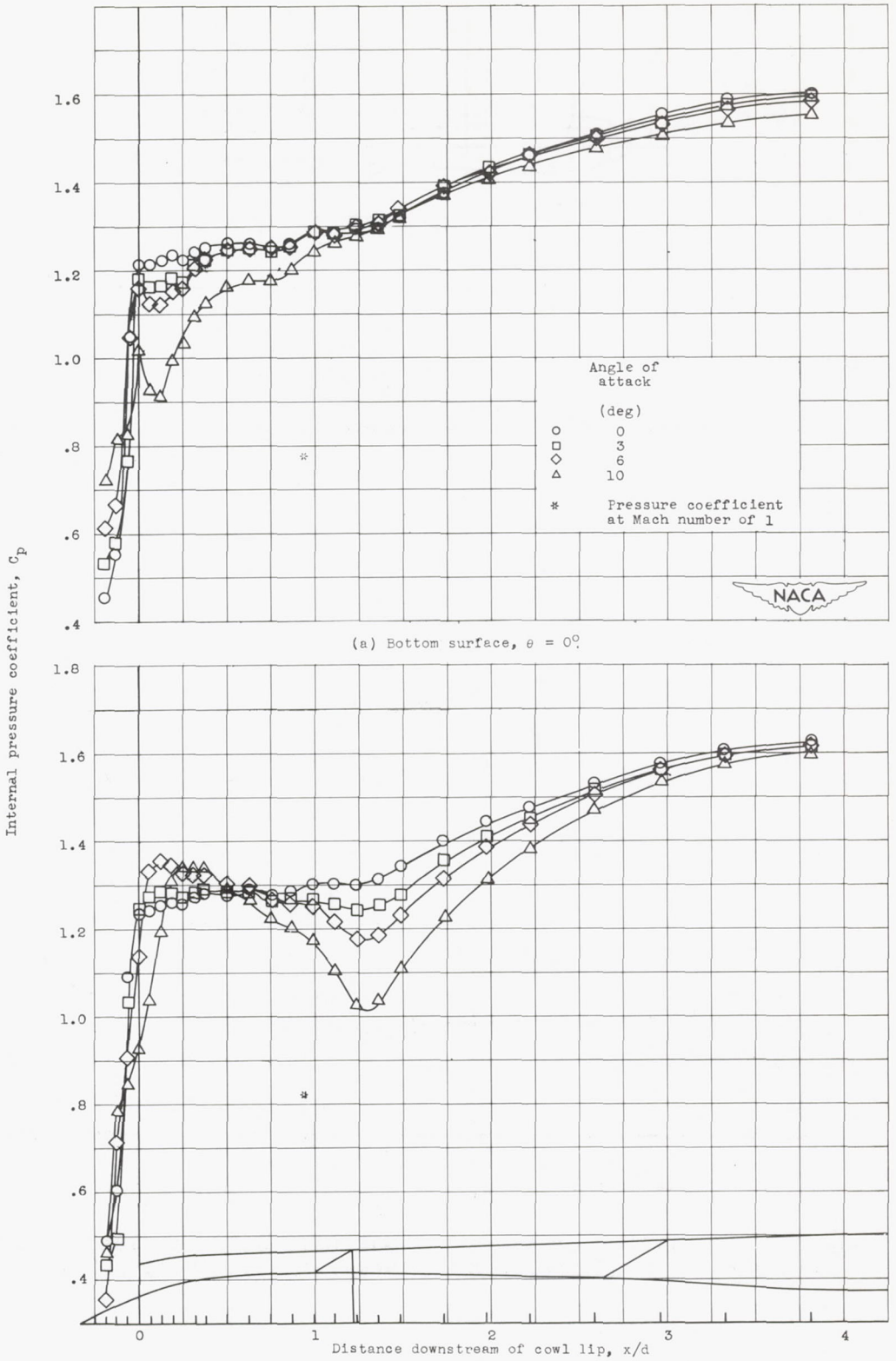
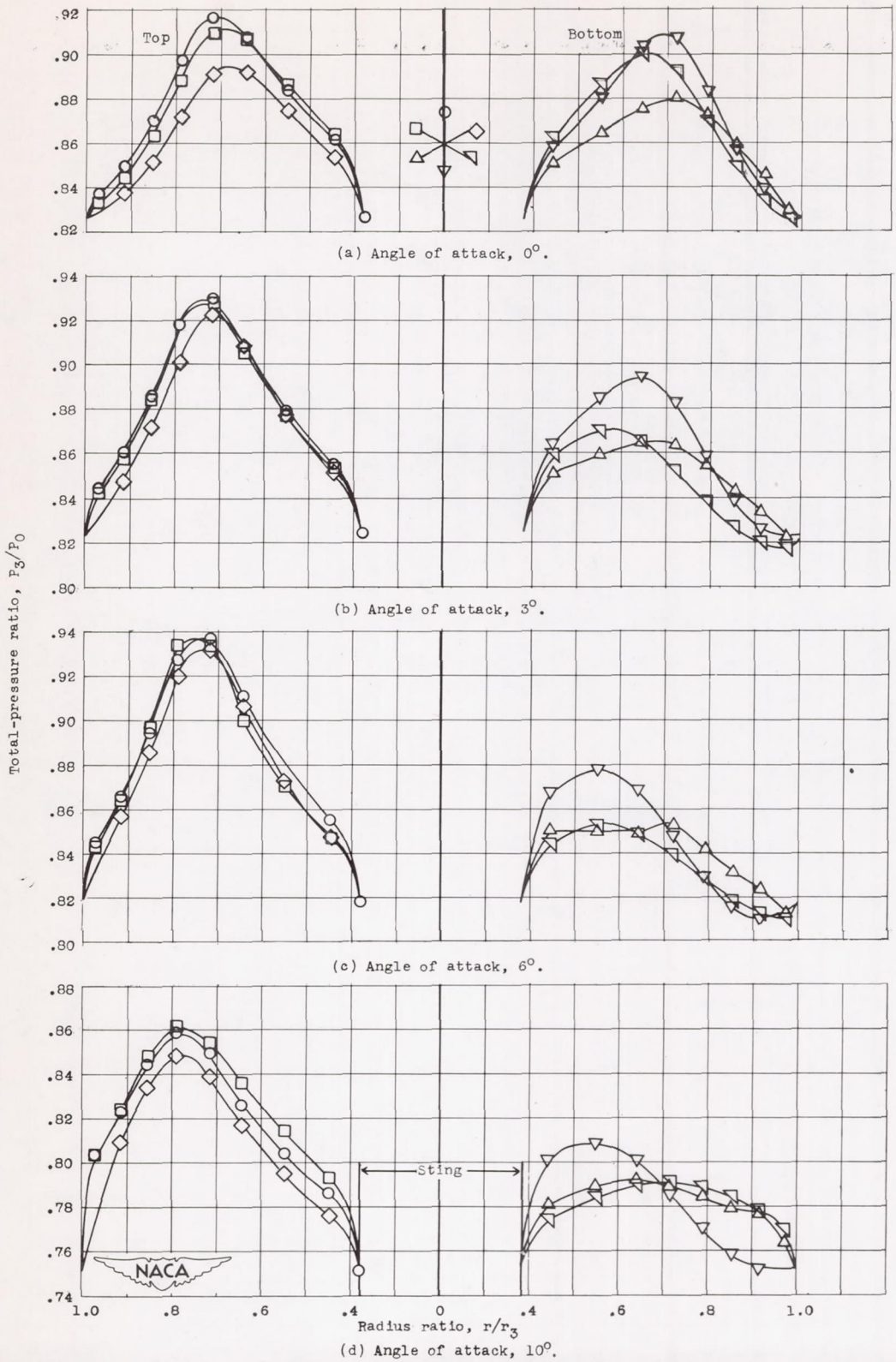


Figure 31. - Longitudinal variation of internal pressure coefficients at constant mass flow for four angles of attack. Mach number, 1.79; mass flow, 0.784.



(a) Angle of attack, 0°.

(b) Angle of attack, 3°.

(c) Angle of attack, 6°.

(d) Angle of attack, 10°.

Figure 32. - Variation of total-pressure distribution at entrance to combustion chamber for constant mass flow at four angles of attack. Mach number, 1.79; mass-flow ratio, 0.869.